

## BADGER Test Campaign at Grand Gulf Nuclear Station

Prepared by:  
Northeast Technology Corp.  
108 North Front Street  
UPO Box 4178  
Kingston, New York 12402

Prepared for:  
Entergy Nuclear Operations, Inc.  
under  
Contract No. 10157456

Rev:	Date:	Prepared by:	Reviewed by:	Approved by:
0	2/8/08	Matthew C. Harris	[Signature]	L.P. Mariani
1	10/1/10	[Signature]	M. C. Harris	L.P. Mariani

## Abstract

Boraflex is a neutron absorber material used for criticality control in some spent fuel racks. Premature deterioration of this material, via slow dissolution of the residual matrix, has been observed in some racks. The Boron-10 Areal Density Gage for Evaluating Racks (BADGER) was developed by Northeast Technology Corp. (NETCO) for the Electric Power Research Institute (EPRI). BADGER is a device that allows the in-situ measurement of the boron-10 areal density of the neutron absorber material installed in spent fuel racks for the purpose of reactivity control. This report describes the BADGER test conducted at Entergy Nuclear Operation's (ENO) Grand Gulf Nuclear Station (GGNS) December 2 – December 12, 2007.

The following report provides: an overview of the BADGER system, the test data from the Grand Gulf Nuclear Station campaign, an evaluation of that data including the measured areal densities, NETCO's conclusions with respect to the condition of the Boraflex in the Grand Gulf Nuclear Station spent fuel racks, and comparisons with prior blackness tests. A RACKLIFE model, established prior to the beginning of the test, provides a means for forecasting the rate at which each panel of Boraflex accumulates gamma exposure. The model, combined with the results of this BADGER test, provides the means for evaluating and implementing rack management strategies in an attempt to mitigate the effects of Boraflex degradation.

## Table of Contents

ABSTRACT .....	II
TABLE OF CONTENTS .....	III
LIST OF TABLES .....	IV
LIST OF FIGURES .....	V
1.0 INTRODUCTION .....	1
2.0 OVERVIEW OF THE BADGER SYSTEM .....	2
2.1 BADGER Equipment Description .....	2
2.2 Typical Operation of BADGER .....	3
3.0 SCOPE OF THE TESTING AT GRAND GULF NUCLEAR STATION .....	7
3.1 Spent Fuel Rack Description .....	7
3.2 Boraflex Panels Selected for Testing .....	7
4.0 BADGER TEST RESULTS .....	15
4.1 Normalized Transmission Traces .....	15
4.2 Panel Average Areal Density .....	16
4.3 Gaps, Cracks, and Other Anomalies .....	17
4.4 Comparison with Prior Blackness Tests .....	19
5.0 CONCLUSIONS AND RECOMMENDATIONS .....	34
6.0 REFERENCES .....	36
 APPENDIX A: BADGER Transmission Traces for Tested Panels .....	 A-1
APPENDIX B: Axial Distributions of Local Dissolutions, Gaps and Other Anomalies for Tested Panels .....	 B-1

## List of Tables

<b>Table</b>		<b>Page</b>
Table 3-1	RACKLIFE-Computed Dose and B <sub>4</sub> C Loss to GGNS Boraflex Panels Tested .....	14
Table 4-1	GGNS Areal Density and Panel Boron Carbide Loss .....	25
Table 4-2	Comparison of BADGER Measured Gaps with Previous Blackness Test Measurements .....	33



## List of Figures

Figure	Page
Figure 2-1	Typical Axial Cross Section of the Source and Detector Heads in Fuel Rack Cells ..... 5
Figure 2-2	Lateral Cross Section of the Source and Detector Heads ..... 6
Figure 3-1	GGNS Spent Fuel Pool ..... 9
Figure 3-2	GGNS Storage Cell Elements ..... 10
Figure 3-3	Isometric View of a Cruciform Element..... 11
Figure 3-4	GGNS Storage Cells ..... 12
Figure 3-5	Distribution of Panel Dose in the GGNS Spent Fuel Pool. .... 13
Figure 4-1	Normalized Transmission Traces for Panel RRR-15 East..... 20
Figure 4-2	Normalized Transmission Traces for Panel PPP-15 West ..... 21
Figure 4-3	Normalized Transmission Traces for Panel CC-27 East. .... 22
Figure 4-4	Normalized Transmission Traces for Panel CC-27 North..... 23
Figure 4-5	Measured Boron-10 Areal Densities for the Panels versus RACKLIFE Predicted Panel Exposure ..... 24
Figure 4-6	Axial Distribution of Dissolution in Panels Tested..... 26
Figure 4-7	Axial Distribution of Gaps in Panels Tested..... 27
Figure 4-8	Axial Distribution of Average Co-Planar Gapping in Panels Tested .. 28
Figure 4-9	Frequency Distribution of Total Dissolution Along the Panels Tested 29
Figure 4-10	Frequency Distribution of Number of Gaps in Panels Tested ..... 30
Figure 4-11	Frequency Distribution of Maximum Gap Size in Panels Tested ..... 31
Figure 4-12	Frequency Distribution of Cumulative Gap Size in Panels Tested ..... 32

## 1.0 INTRODUCTION

Boraflex is a neutron absorber material used for criticality control in some spent fuel racks. Premature deterioration of this material, via slow dissolution of the residual matrix, has been observed in some racks.<sup>[1,2,3]</sup> The Boron-10 Areal Density Gauge for Evaluating Racks (BADGER) was developed by Northeast Technology Corp. (NETCO) for the Electric Power Research Institute (EPRI) under research project WO-3907-01.<sup>[4,5]</sup> BADGER is a device that allows the in-situ measurement of the boron-10 areal density ( $^{10}\text{B}$  density expressed as grams  $^{10}\text{B}/\text{cm}^2$ ) of the neutron absorber material installed in spent fuel racks for the purpose of reactivity control. The development of BADGER was prompted by the observed in-service deterioration of Boraflex, as noted above. This report describes the BADGER test conducted at Entergy Nuclear Operation's (ENO) Grand Gulf Nuclear Station (GGNS) from December 2 to December 12, 2007. The testing was performed according to Northeast Technology Corp. Special Engineering Procedures: SEP-287-01, Rev 0<sup>[6]</sup> and SEP-287-02, Rev 0<sup>[7]</sup>.

Prior to this campaign at GGNS, ENO created a RACKLIFE<sup>[8]</sup> model of the spent fuel pool racks. This model provided a means to identify those storage cells and specific Boraflex panels that had been subjected to the most severe service histories in terms of integrated gamma exposure and, potentially, boron carbide loss. A sample population of panels was selected, which included some of the highest exposed panels ( $3.8 \times 10^{10}$  rads gamma), as well as a series of panels which had accumulated a spectrum of exposures and service histories over a range of 0.0 rads up to the highest dose panels. Also, several panels tested during previous blackness tests were selected to ascertain any increases in gap size due to shrinkage or dissolution. This allows an assessment of the condition of the Boraflex as a function of service history.

The following sections of this report provide an overview of the BADGER system, the test data from the GGNS campaign, an evaluation of that data, including the measured areal densities, and NETCO's conclusions with respect to the condition of the Boraflex in the GGNS spent fuel racks. The RACKLIFE model provides a means for forecasting the rate at which each panel of Boraflex accumulates gamma exposure, and therefore provides the means for evaluating and implementing rack management strategies and to mitigate the effects of Boraflex degradation.

## 2.0 OVERVIEW OF THE BADGER SYSTEM

### 2.1 *BADGER Equipment Description*

Figure 2-1 schematically depicts the deployment of the BADGER system. When in use, the system is suspended from the refueling bridge auxiliary crane. The bridge and crane are used to position the equipment in the horizontal plane for the purpose of moving BADGER over specific storage cells for testing. The areal density gage is lowered into and withdrawn from a specific cell via the BADGER drive system. The drive system is comprised of a stepper motor, gearbox and winch assembly that remotely raises and lowers the BADGER hardware. Also included on the drive platform are a shaft encoder, which provides a precise measure of the axial elevation of the BADGER hardware, and a load sensor, which trips the drive motor should the hardware hang up in a cell.

The BADGER hardware consists of a set of aluminum suspension poles and the aluminum source and detector heads that are suspended by the poles. Figure 2-1 also shows an axial cross-section of the source and detector heads positioned in two adjacent storage cells. The source and detector heads consist of aluminum boxes with tapered lead-ins on the bottom surface. The tapered lead-ins guide the device as it is inserted into the storage racks.

Figure 2-2 shows a lateral cross-section of the source and detector head. The detector head contains an aluminum block mounted on one inside face of the head that houses four two-inch high  $\text{BF}_3$  detectors. The aluminum block is shielded on all sides except for a two-inch window aligned with the detectors facing the source head. The detectors are encapsulated in watertight enclosures that are sealed to the waterproof detector cables. The source head contains a watertight aluminum tube that houses a  $^{252}\text{Cf}$  source when the equipment is in use.

The principle of BADGER operation is based on the attenuation of neutrons through the Boraflex panel between the source and detectors. Pool water in the source head thermalizes a portion of the fission neutrons produced by the  $^{252}\text{Cf}$  source. The number of thermal neutrons reaching the neutron detectors is a function of the number of boron-10 atoms ( $^{10}\text{B}$  areal density) in the Boraflex panel between the source and detectors. The magnitudes of the detector signals, in turn, are a function of the  $^{10}\text{B}$  areal density in the Boraflex panels. For panels with high areal density, the detector signals are low, whereas for low areal densities, the signals are high. BADGER is calibrated by passing the source and detector heads through a calibration cell containing sections of Boraflex with known  $^{10}\text{B}$  areal densities.

The detector signals are fed to four pre-amplifiers that are mounted on the drive assembly. Shielded cables connect the preamplifiers to four amplifiers in an electronics console positioned alongside the pool. The electronics console also houses a power

supply used by the amplifier, pre-amps, and detectors. The amplified detector signals are fed to a special counter board in a laptop computer for counting and recording. The computer serves as a data-logger and as a control unit for the stepper motor and positioning encoder.

## **2.2 Typical Operation of BADGER**

The BADGER system is applied to measure the  $^{10}\text{B}$  areal density in spent fuel racks in the following sequence. First, a special calibration cell is lowered into the pool, typically near the racks to be measured. After the equipment has been assembled poolside and suspended from the auxiliary crane, the source and detectors are submerged in the pool, so that the top of the source tube is just above the pool surface. At this point, the  $^{252}\text{Cf}$  source is transferred into the source tube, a seal plug is installed, and the BADGER probe (source and detector head) is lowered into the pool.

The BWR calibration cell has a sequence of Boraflex standards of varying known areal densities arranged axially, as well as some gaps of known size. At the beginning of a test campaign, the BADGER probe is lowered into the calibration cell and both sides are scanned. The bottom of the calibration cell establishes a reference elevation datum during calibration. After scanning the calibration cell, BADGER is ready for test operations. No further calibration is required during the campaign, unless excessive drift in the electronics occurs.

The areal density of a Boraflex panel is determined by comparing the detector count rate through the panel to the count rates through panels of known areal density in the calibration cell. In a Boraflex panel that has thinned due to dissolution of the residual Boraflex matrix, a higher detector count rate is recorded. The amount of thinning is determined by comparison with a fit of the standards in the calibration cell. To quantify the actual areal density of an irradiated panel in the racks that has undergone some dissolution, usually a relatively intact (e.g., unirradiated or low dose) panel in the racks of known areal density must be available to measure and compare against. This is to account for small but often significant differences between the calibration cell and the actual racks.

The absolute areal density in a panel is determined by constructing a fit of the form:

$$B-10 = m(\ln T) + b$$

where:       $T$  = neutron transmission  
                $B-10$  = boron 10 areal density  
                $m$  = slope  
                $b$  = intercept with the ordinate

The slope of the curve in the above equation is determined by measuring the transmitted neutrons in the calibration cell over areas of known areal density. The

constant  $b$  is determined by measuring  $T$  in an actual rack cell that has not sustained boron carbide loss (low or zero dose panel). This procedure is used because the calibration cell is not universal for all racks. Differences such as stainless steel structure/ wrapper thickness, distances between the source and the detectors, etc. exist between the actual racks and the calibration cell.

A Boraflex panel is tested in the following sequence. The probe is placed into two specific cells on either side of the Boraflex panel of interest and lowered to the bottom of the cell. A load sensor on the lift assembly provides indication of when the probe is fully inserted. The reference elevation datum is established at the bottom of the cell and all measurements of probe elevation are relative to this datum. (When analyzing the data, the elevation is subsequently adjusted to be relative to the bottom of the Boraflex panel according to as-built manufacturing drawings.)

The entire panel is scanned with the heads being moved in two-inch increments from the bottom of the cell to the top. The active portion of the detectors is two inches, so a scan measurement represents complete axial coverage of the panel. At each elevation, the counts of each detector are measured for a period of 10 seconds, and are recorded by the data-logging computer. As the scan proceeds, the test equipment operator monitors the computer as the counts are plotted on the screen as a function of axial elevation. The operator monitors the elevation data, where high count rates could be indicative of low boron-10 areal densities or gaps in the Boraflex panel. Measuring the BADGER elevation here provides an additional datum to measure elevation in the cell. After the elevation measurement is complete, the probes are moved out of the tested cells and to a new location for subsequent testing.

The process is repeated for subsequent panels scheduled for testing. The total time required for a scanning measurement is typically about one half hour per panel. As data is recorded by the data logging computer, data files containing detector count rates versus axial elevation in the cells are created on the hard drive which serves as a permanent record of the measurements.

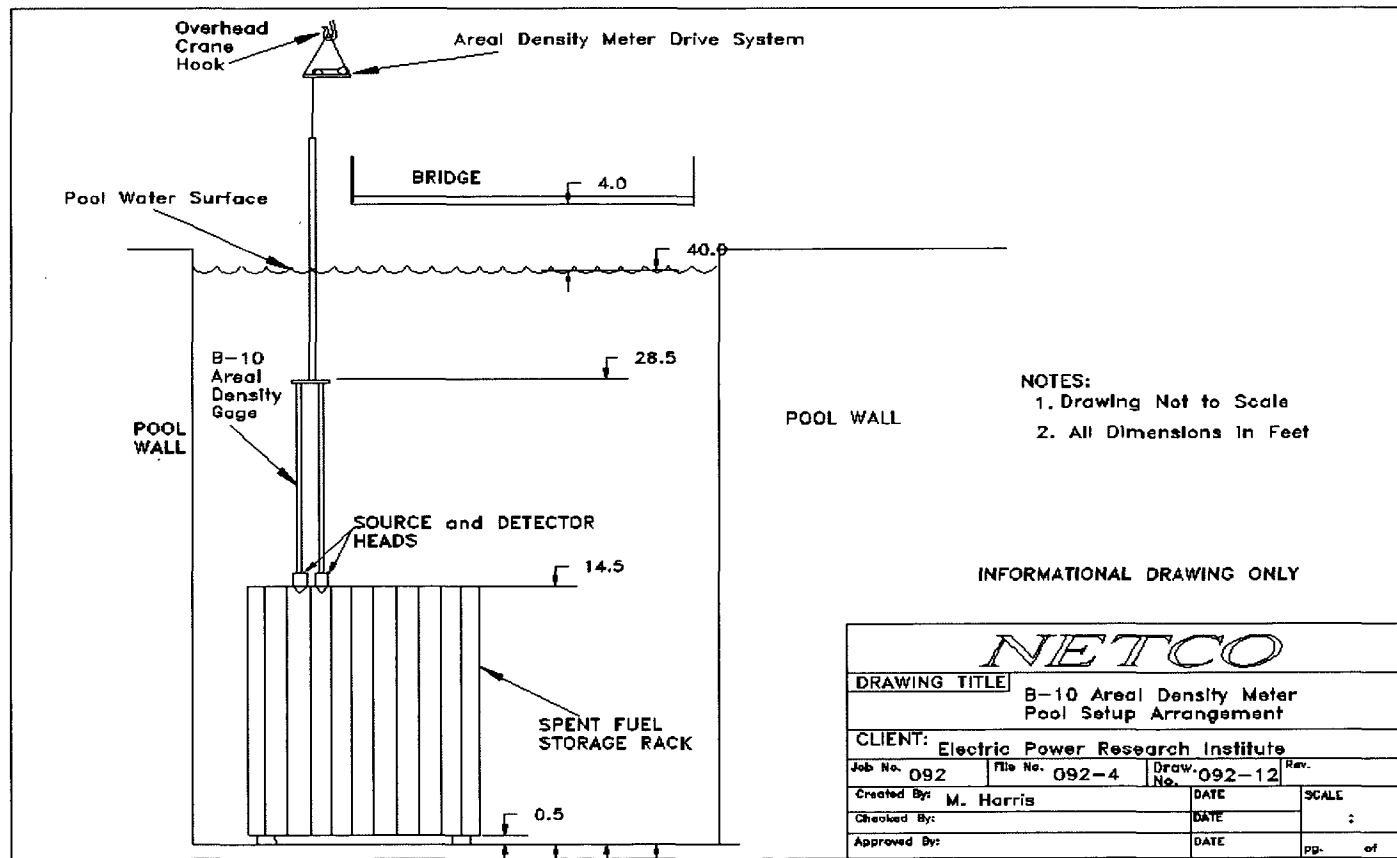


Figure 2-1  
Typical Axial Cross Section of the Source and Detector Heads in Fuel Rack Cells

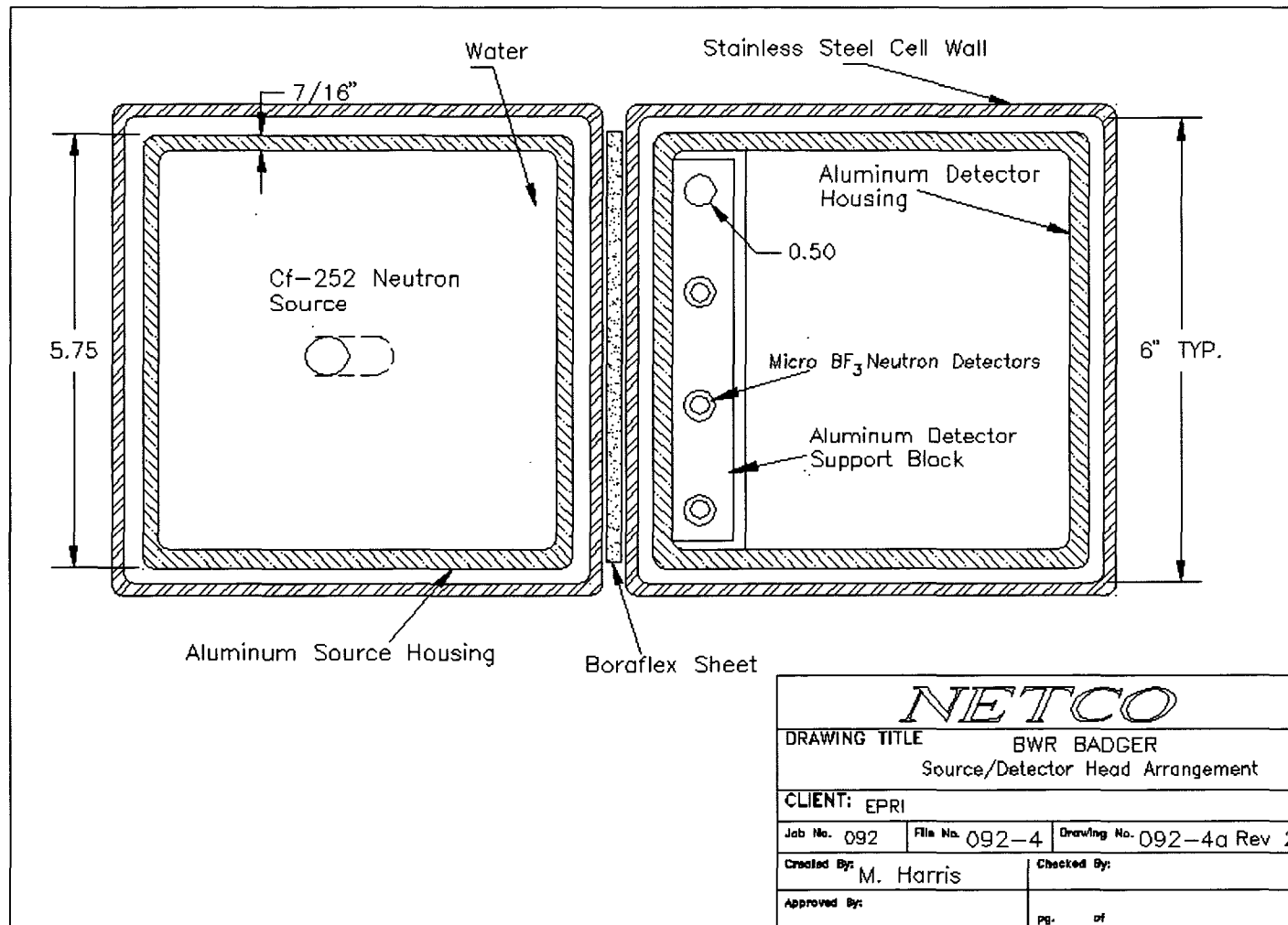


Figure 2-2  
Lateral Cross Section of the Source and Detector Heads

### **3.0 SCOPE OF THE TESTING AT GRAND GULF NUCLEAR STATION**

#### **3.1 *Spent Fuel Rack Description***

The spent fuel racks at GGNS are shown in Figure 3-1<sup>[9]</sup>. The racks consist of 16 modules of varying size for a total capacity of 4393 storage cells. Module 16 is unpoisoned and therefore not subject to BADGER inspection. The remaining modules utilize Boraflex as a poison and contain the panels selected for testing.

The design of these racks is such that one sheet of Boraflex separates the opposing faces of each fuel assembly. The individual storage cells are formed by creating a configuration of cruciform, "TEE" and "ELL" shaped elements, as shown in Figures 3-2 and 3-3. The resultant basic structure of this storage array is a square stainless steel cell with a 6.068 inch inside dimension and 169 inches in length, fabricated using 0.063 inch stainless steel sheets. Each cell has one sheet of Boraflex 144 inches long, 5.63 inches wide, and 0.070 inches thick (nominal) juxtaposed between each of the four outside faces and the neighboring cells.

To complete the rack module assembly, the structural elements containing Boraflex are welded together as shown in Figure 3-4. This rack design reduces, to a large extent, contact of the Boraflex with the pool water, which in turn reduces the interaction between the Boraflex and pool water. Panel dissolution is therefore expected to be diminished.

#### **3.2 *Boraflex Panels Selected for Testing***

A RACKLIFE model of the GGNS racks and pool was created by ENO based on as-built drawings. This model was used to simulate the actual service history of each panel of Boraflex in the GGNS storage racks, including integrated gamma exposure and B<sub>4</sub>C loss, at the time of testing. Figure 3-5 shows the predicted RACKLIFE distribution of panel gamma dose for the GGNS racks.

According to the RACKLIFE model, there is a fairly uniform gamma dose distribution throughout the pool. However, the highest dose panels, as well as the widest spectrum of dose among local panels, have been calculated for module 6. This module and modules 11 and 5 were the modules selected for BADGER testing by ENO. The highest dose panel, according to the model, is panel CC-27 East in module 6 with an integrated gamma dose of  $3.83 \times 10^{10}$  rads.

A total of 45 panels were selected for testing by ENO and the basis of selection was reviewed by NETCO. The panels selected for testing are listed in Table 3-1 along with the RACKLIFE predicted dose and B<sub>4</sub>C loss. Panels exhibiting a spectrum of exposure



levels from zero dose to the highest dose have been tested. Panels listed in Table 3-1 marked with an asterisk were previously subjected to blackness testing. Plant operational requirements permitted BADGER testing of 32 of the 45 panels selected. The panels tested are listed in Table 4-1

Integrated absorbed gamma dose is a necessary but not a sufficient predictor of panel boron carbide loss. Panels that received a moderate dose many years ago, at the present time, may have undergone more dissolution than a panel that more recently received a higher exposure. In any event, once a critical dose has been received (about  $2 \times 10^9$  rads), Boraflex becomes susceptible to dissolution by the pool water. The dissolution reaction is an equilibrium reaction that is, in part, dependent upon the reactive silica concentration of the pool water in contact with the Boraflex. Dissolution is due to both the integrated dose above the critical value and to the interaction of the pool water with the high dose panel. Panel dissolution can, therefore, be strongly dependent upon panel cavity volume, pool currents and water exchange rates with the panel cavity. All of these factors can, in turn, influence the silica concentration of the pool water in contact with the Boraflex panels. The RACKLIFE code predicts the  $B_4C$  loss from Boraflex based on the chemical kinetics of silica dissolution and on the integrated absorbed dose. At the time of BADGER testing, the GGNS RACKLIFE model predicted a 5.9% peak boron carbide loss from the racks.

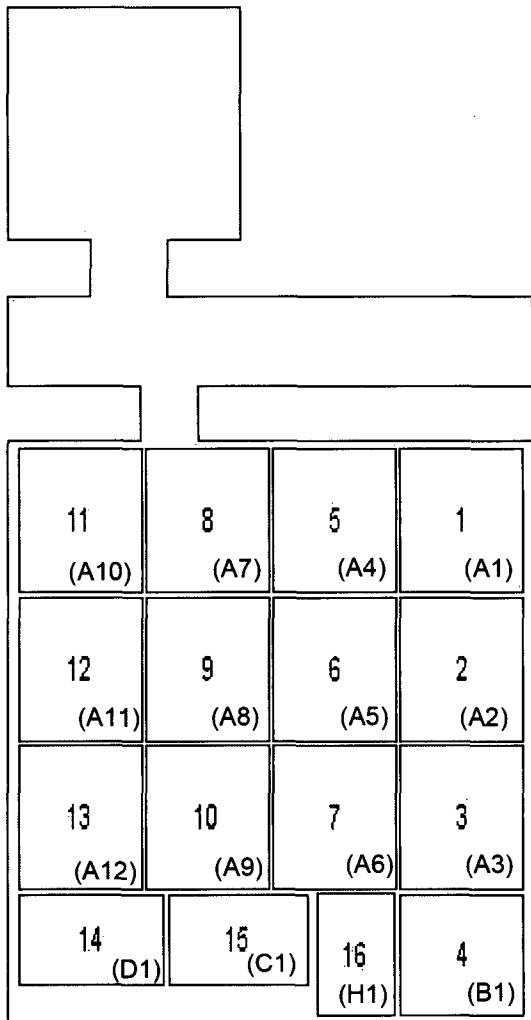


Figure 3-1  
GGNS Spent Fuel Pool  
(Labels in Parenthesis are Entergy Nuclear Operations Module Designations.)

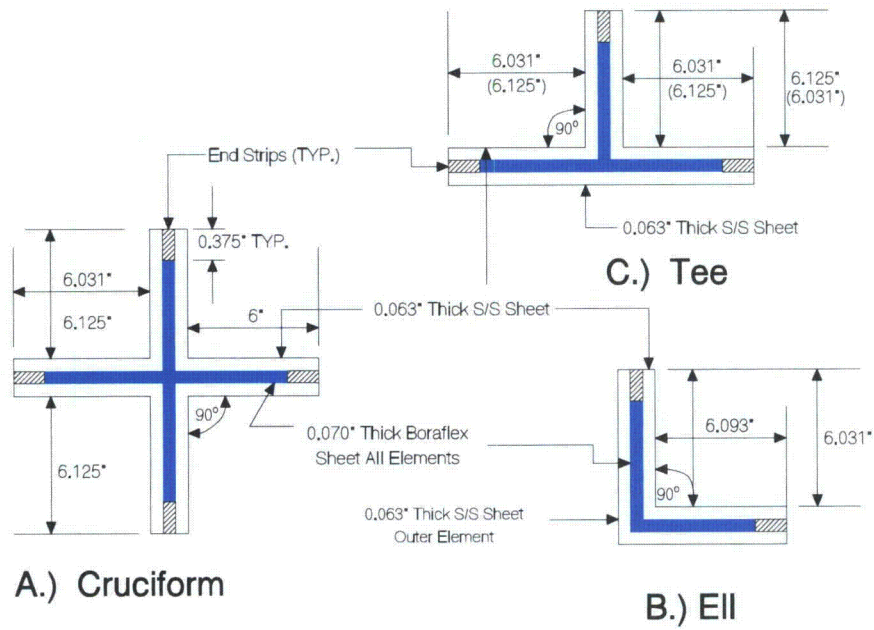
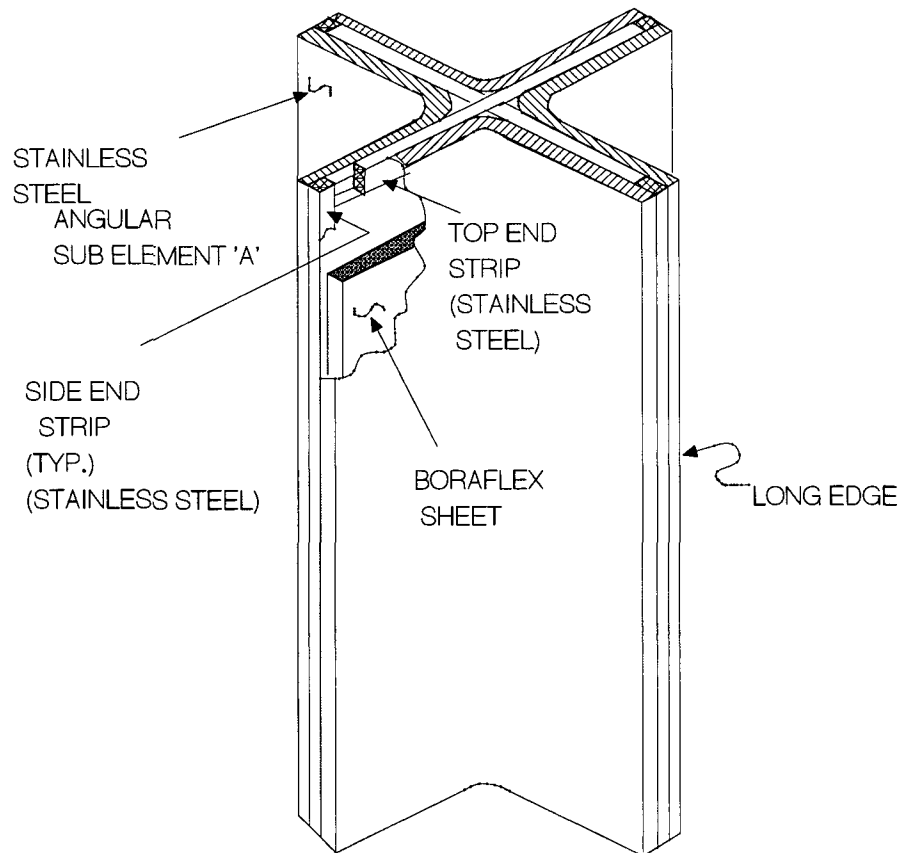


Figure 3-2  
GGNS Storage Cell Elements



**Figure 3-3**  
**Isometric View of a Cruciform Element**

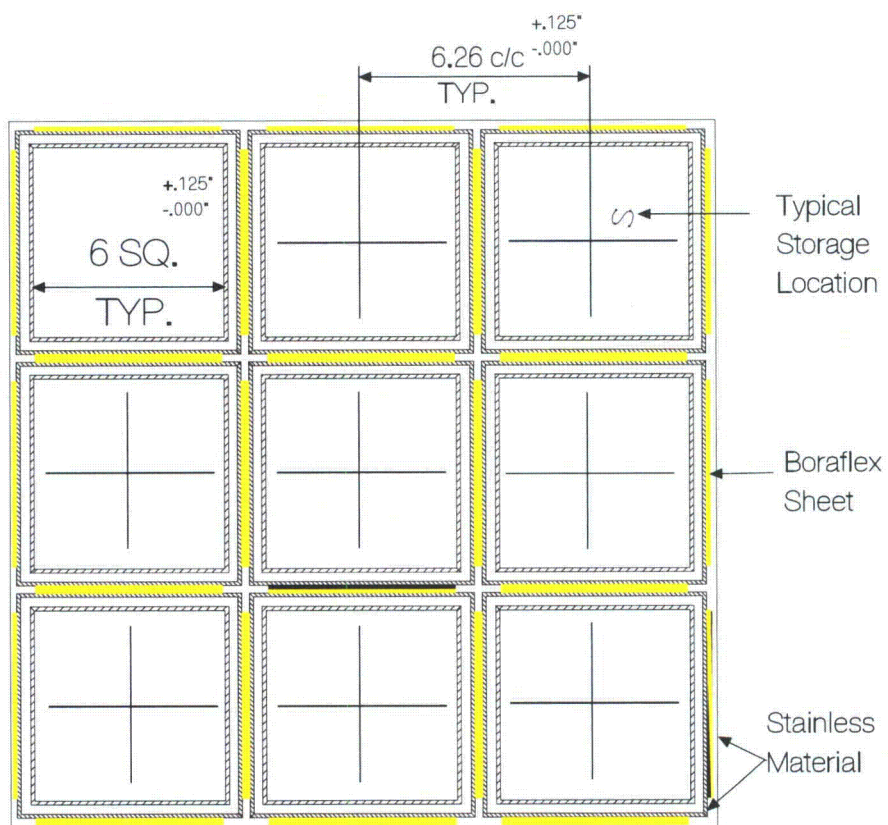


Figure 3-4  
GGNS Storage Cells

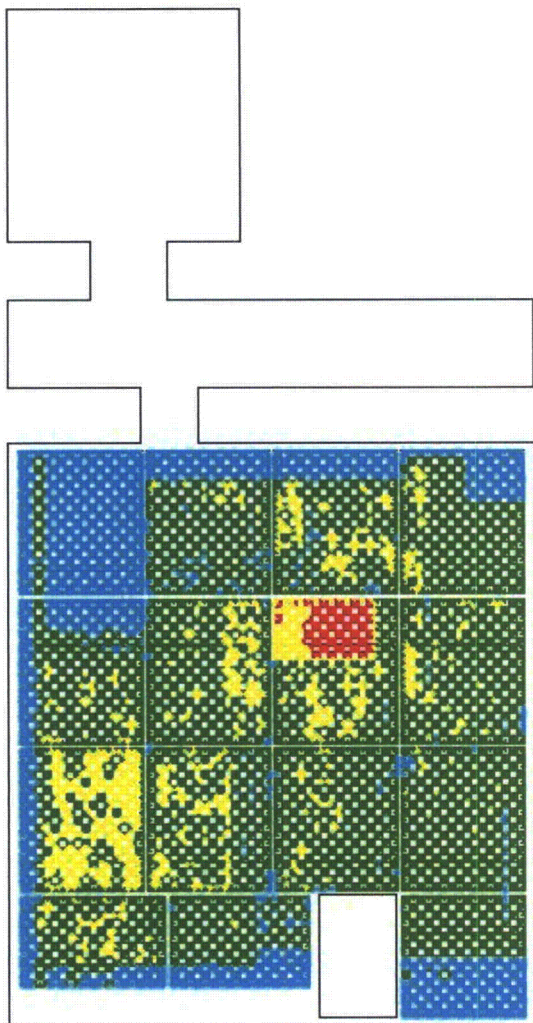


Figure 3-5  
Distribution of Panel Dose in the GGNS Spent Fuel Pool.

Red is  $\geq 3.0 \cdot 10^{10}$  rads  
Yellow is  $\geq 1.0 \cdot 10^{10}$  rads  
Green is  $\geq 2.0 \cdot 10^9$  rads  
Blue is  $< 2.0 \cdot 10^9$  rads

Module	Panel	Absorbed Dose (Rads)	Predicted B <sub>4</sub> C Loss (%)
6	CC-27 East*	3.8E+10	5.9
6	CC-27 West*	3.3E+10	5.9
6	CC-27 North*	3.7E+10	5.9
6	CC-27 South*	2.2E+10	5.9
6	AA-27 North*	3.1E+10	5.9
6	AA-27 South	2.3E+10	5.9
6	AA-27 East*	3.5E+10	5.9
6	AA-27 West*	3.5E+10	5.9
6	EE-27 East*	2.9E+10	5.8
6	DD-26 South	3.0E+10	5.8
6	DD-28 North	1.6E+10	5.8
6	FF-28 South	2.7E+09	5.0
6	FF-30 North	7.3E+09	5.3
6	EE-29 West	7.4E+09	5.2
6	GG-29 East	6.8E+09	5.2
6	DD-28 South	4.6E+09	5.0
6	DD-30 North	8.3E+09	4.8
6	CC-29 West	8.1E+09	5.7
6	EE-29 East	8.9E+09	4.9
6	U-23 West	1.8E+10	5.9
6	V-24 East	1.9E+10	5.9
6	V-20 East	1.8E+10	5.9
6	HH-24 North*	3.0E+10	5.8
6	HH-24 South*	3.0E+10	5.8
6	HH-24 East*	3.0E+10	5.8
6	HH-22 North*	3.0E+10	5.8
6	HH-22 South*	3.0E+10	5.8
6	HH-22 East*	3.1E+10	5.8
1	P-7 North	1.8E+10	4.6
5	T-13 North	1.6E+10	4.6
5	T-13 South	1.6E+10	4.6
5	U-12 South	5.2E+09	4.3
5	U-14 North	5.8E+09	4.4
5	BB-13 North	2.3E+09	4.1
5	BB-11 South	5.2E+09	4.2
5	AA-12 West	1.1E+10	4.6
5	CC-12 East	1.8E+09	3.8
5	AA-12 South	1.8E+10	4.6
11	PPP-15 North	3.9E+09	3.7
11	PPP-15 South	5.1E+09	3.7
11	PPP-15 East	1.6E+09	3.4
11	PPP-15 West	1.3E+09	3.3
11	RRR-15 East	0.0E+00	3.1
11	QQQ-14 South	0.0E+00	3.1
11	QQQ-16 North	0.0E+00	3.1

Table 3-1  
RACKLIFE-Computed Dose and B<sub>4</sub>C Loss to GGNS Boraflex Panels Tested

(\* Panels previously subjected to Blackness Testing)

## 4.0 BADGER TEST RESULTS

### 4.1 *Normalized Transmission Traces*

The normalized transmission traces for all panels tested are contained in Appendix A. A normalized transmission is determined by calculating the average detector count rate in the Boraflex away from gaps and other anomalies, and plotting the deviation from this average. A normalized transmission trace shows deviations from a condition of uniform loss. Thus deviations from the zero line, represent a combination of counting statistics, shrinkage induced gaps, and local differences from a uniform panel boron carbide loss. A flat trace is not indicative of zero dissolution, only that the dissolution is uniform along the length of the panel. The salient features of a few of these traces are described below to aid the reader in interpreting the traces in the Appendices.

Figure 4-1 contains a plot of the four normalized transmission traces developed during a scan of panel RRR-15 East. This panel was chosen to be the reference standard against which the other panels would be measured. This panel, while not completely unirradiated, has accumulated only minimal dose and it shows a very uniform transmission trace. This suggests, as was predicted by RACKLIFE, minimal boron carbide loss. With the BADGER heads resting on the bottom of the cell, the detectors are slightly below the bottom of the Boraflex panel. As BADGER moves up the cell, the trace of the detectors is seen to rapidly fall to the zero (average transmission) line. A rapid fall within about two inches of the bottom of the Boraflex panel suggests that the panel bottom is relatively intact and has not shrunk significantly.

Figure 4-2 contains the normalized transmission trace for panel PPP-15 West. This trace indicates the presence of a gap at about 70" elevation that is about 1.4" in size. There is also a smaller gap at 20" elevation. Away from these gaps the Boraflex appears to be uniform.

With an absorbed dose of  $3.8 \cdot 10^9$  rads, panel CC-27 East is one of the higher dose panels tested. Figure 4-3 contains the normalized transmission traces for panel CC-27 East. There are seven areas designated as gaps. These areas also are characterized as showing local dissolution around the gap edges. They, therefore, are not typical gaps in the sense that they are not sharply defined. These seven gaps are evident at elevations of 64", 78", ~80", ~88", an extensive area between 116" and 126", ~132" and 140". The panel has some form of dissolution over most of its length as indicated by the elevated signals of detectors 1 and 2. The areas not characterized as 'Gaps' have been designated as areas of "Local Dissolution." "Local Dissolution" differentiates those areas so designated from panel areas that have experienced more uniform loss or "Thinning." In addition, the top half of the panel shows more severe dissolution than the bottom of the panel.



Figure 4-4 shows the trace of panel CC-27 North. This trace shows edge dissolution as indicated by detector 4. Panels CC-27 North and CC-27 East are adjacent and the alignment of the detectors is such that the panel edge traversed by detector 4 in Figure 4-4 is adjacent to the panel edge traversed by detector 1 in Figure 4-3. The edge dissolution of both panels indicates a likely flow path common to both panels resulting in increased edge dissolution.

## 4.2 Panel Average Areal Density

Based on a quantitative analysis of the BADGER data, the panel average boron-10 areal densities have been computed. Figure 4-5 contains a plot of measured areal density versus dose for the thirty-two panels tested. In addition to the areal density values, the measurement uncertainties are also shown. The error bars represent measurement uncertainty due to BADGER measurement uncertainty and statistical uncertainty associated with the areal density calculation for each panel. The BADGER measurement uncertainty is determined experimentally by scanning a given panel from both faces. The comparison between calculated areal density values for each scan gives a conservative estimate of the measurement uncertainty. The fractional deviation in areal densities,  $\kappa$ , is used, in combination with the statistical uncertainty,  $\sigma$ , to determine the total uncertainty in areal density ( $\delta\rho$ ):

$$\delta\rho = \kappa\rho + \sigma$$

The nominal as-built areal density of the GGNS Boraflex was 0.0204 gms B-10/cm<sup>2</sup> when the material was produced<sup>[9]</sup>. Panel to panel variations in as-built areal density of  $\pm 10\%$  are typical. The dashed curves in Figure 4-5 represent the nominal areal density and the  $\pm 10\%$  variation from the nominal corrected for densification of the Boraflex. The areal density of irradiated Boraflex actually increases up to a gamma dose of approximately  $1.0 \times 10^{10}$  rads due to an increase in actual density of the Boraflex from radiation induced shrinkage, assuming no dissolution. Also shown in Figure 4-5 is the minimum certified areal density (0.0175 gms B-10/cm<sup>2</sup>) and the minimum allowable areal density of 0.0170 gms B-10/cm<sup>2</sup>. The latter is established by the criticality analysis of record for the GGNS storage racks with degraded Boraflex. In comparing the measured data with the as-built panel areal density (corrected for densification), it appears that four of the panels (within one sigma) fall outside of the expected range of areal densities. It should be pointed out that those panels that exhibit the largest measured loss are not necessarily the panels with the highest predicted absorbed dose. As noted in Section 3.2, the time of exposure, amount of gamma exposure as well as the duration of exposure to the pool water are all factors that influence panel boron carbide loss. Thus, strict correlation with dose alone is not expected.

The average areal density of all panels measured is  $0.0191 \pm 0.0012$  grams B-10/cm<sup>2</sup>. This is slightly higher than the nominal "as-built" value of 0.0204 grams B-10/cm<sup>2</sup>. As noted subsequently, this is due to Boraflex densification. The lowest measured areal density value of the panels tested was 0.0166 grams B-10/cm<sup>2</sup>. This is slightly less

| 1  
| 1

than the areal density limit of 0.0171 B-10/cm<sup>2</sup> assumed in the current criticality analysis of record<sup>[9]</sup>.

Table 4-1 shows the measured areal density values for the panels tested. For each panel tested, this table also shows the number of gaps, the size of the largest gap, total amount of dissolution along each panel, and the RACKLIFE predicted boron carbide loss and absorbed dose. The RACKLIFE values are taken from Table 3-1.

The measured areal density data exhibited some variability due to variations in water exchange rate between the volume within the Boraflex enclosure and the bulk pool volume. The rate of Boraflex dissolution is a strong function of the reactive silica concentration within the panel enclosure, which in turn depends on the water volume exchange rate. The panel enclosure forms a tight stainless steel frame around the Boraflex, enclosing it within the structural elements of the rack (See Figures 3-2 and 3-3). This configuration provides for significant isolation of the Boraflex panels from the bulk pool water. The current RACKLIFE model uses an exchange rate of 0.5 panel-enclosure-fluid-volumes per day. Considering the already small panel volume, this suggests limited interaction of the bulk pool water volume with the panels. However, this interaction is sufficient to cause elevated pool silica levels. Dissolution, though small, is expected and has been seen during this analysis. Panel to panel variation in the enclosure fit can lead to variations in this dissolution. RACKLIFE uses an average value for the exchange rate and assumes that it is the same for all panels. Therefore, calculated boron carbide loss is for a panel with average exchange rate. On average, RACKLIFE projections have been shown to be quite accurate but variations in dissolution due to variability in enclosure fit and in exchange rate are not considered.

### **4.3 Gaps, Cracks, and Other Anomalies**

Boraflex is predisposed to forming gaps due to radiation-induced shrinkage. This shrinkage can be accentuated by the non-uniform nature of the gamma dose absorbed by a Boraflex panel in the spent fuel pool racks. Absorbed dose gradients along a panel will cause differential shrinkage, which leads to shear stresses. This process is enhanced by the tendency of Boraflex to swell and fully harden more rapidly where water from the aqueous pool environment can flow more rapidly into the panel cavity, such as between welds or where there are manufacturing anomalies that permit increased flow into the panel cavity. The result is shrinkage-induced gaps and/or cracks. The axial distributions of local dissolution, gaps and other anomalies for each panel tested are given in Appendix B.

A crack is a lateral anomaly that is smaller than 1/3 inch axially, the lower limit on BADGER's ability to detect gaps. This uncertainty ( $\pm 1/3$ ") has been determined experimentally. A crack may bisect the panel, like a gap. A crack may also just extend a short distance into a panel from the panel edge, often at an angle other than a perpendicular to the edge, which is indicative of local shear stresses. Because a crack is below BADGER's resolution, it is also possible that it is simply a region of local dissolution that does not fully penetrate the thickness of the panel. In characterizing

anomalies, it is up to the test engineer to distinguish between gaps and cracks when interpreting the test data.

Gap size is determined by utilizing a transmission ratio fit derived from calibration cell data. This fit calculates effective gap size for the anomaly selected. In interpreting test data, it is not uncommon to characterize features that have an effective size less than 1/3" as a gap. While such anomalies may in fact be a crack or a horizontal region of local dissolution, in this analysis all such anomalies have been characterized as gaps to provide consistency with prior panel blackness testing campaigns.

In addition to gaps and cracks, other anomalies were observed in the GGNS panels. These include small areas of end dissolution, typically along the bottom or edge of a panel. For example, edge dissolution along the top edge of the panel (see e.g. detector 4 signal) and sedimentation of lost boron carbide along the bottom of panel CC-27 South in Figure 4-4 is evident.

Figure 4-6 shows that the axial distribution of local dissolution among the panels is more pronounced in the middle and upper regions of the panels. The panel area above approximately 110" of elevation seems to be more susceptible to panel dissolution effects. This is likely due to the increased flow of pool water in the panel enclosure of the upper sections of the panel as a result of shrinkage induced gaps.

Figure 4-7 shows the fraction of panels tested that had a gap at a given elevation. The figure shows that a gap is more likely to form in the middle third of the panel and to a lesser extent in the upper third. This trend is particularly evident at approximately 86" and 132". As mentioned previously, the elevations at which gaps exist seem to be the points where dissolution is more likely to occur. Figure 4-8 shows the axial distribution of inches of gap per panel. In preparing the data for this figure, the sum of gap sizes centered around a given elevation is divided by the number of panels tested. This figure is meant to be a quantitative indication of the gap severity to be expected at a given elevation for all of the panels tested. The principle conclusion to be drawn from this figure is that if any 2 inch strip at a given elevation of the racks were to be examined, the maximum amount of average coplanar gap per panel would be less than ~0.45 inches in that 2 inch strip.

Figure 4-9 shows the frequency distribution of total inches of local dissolution along a given panel. Most of the panels show some amount of dissolution. However, as described previously, most of this dissolution is uniform over the entire panel and amounts to the equivalent of thinning in a localized area. Areal density values show that, on average, the panels are not significantly dissolved.

Figure 4-10 shows the distribution of the number of gaps per panel, and Figure 4-11 shows the distribution of the maximum individual gap size over all of the gaps in a panel. The largest single gap observed is seen to be ~9.6 inches. Figure 4-12 shows the distribution of cumulative gap size in all of the panels tested. The largest cumulative gap size is seen to be 20.1 inches.

#### **4.4 Comparison with Prior Blackness Tests**

Prior to this BADGER test campaign, GGNS had on several occasions performed blackness testing of the spent fuel pool storage racks.<sup>[9]</sup> Blackness testing provides the approximate elevation of gaps and an indication of gap size. It is not as precise as BADGER with respect to gap size and elevation and does not provide a quantitative measure of panel areal density. A comparison of BADGER test results with blackness testing results is provided in Table 4-2, which provides a qualitative comparison of the size and position of gaps observed. In general, the gaps elevations measured previously were in close agreement with the current BADGER measurements. In most cases gap sizes have noticeably increased since the last blackness test measurements. In several instances (e.g., AA-27 East, BB-27 East, HH-24 South), several new gaps have been detected by BADGER.

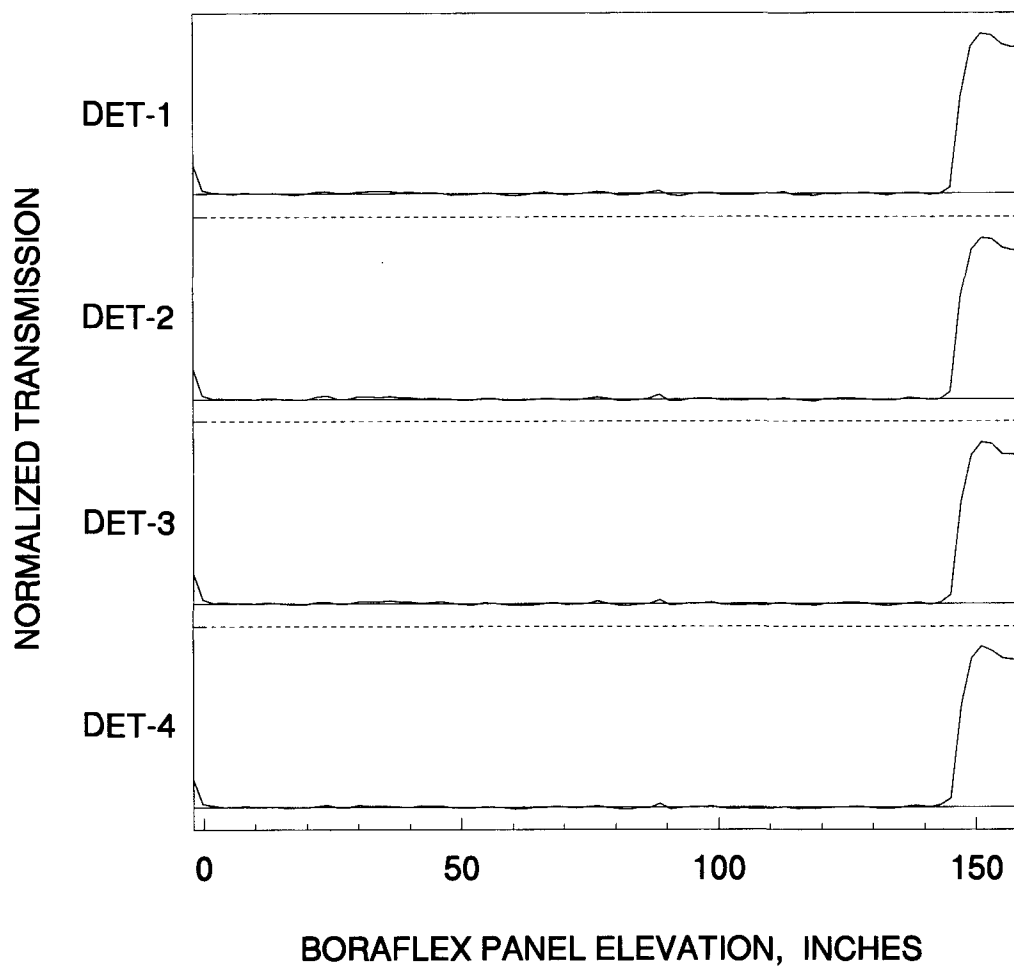


Figure 4-1  
Normalized Transmission Traces for Panel RRR-15 East

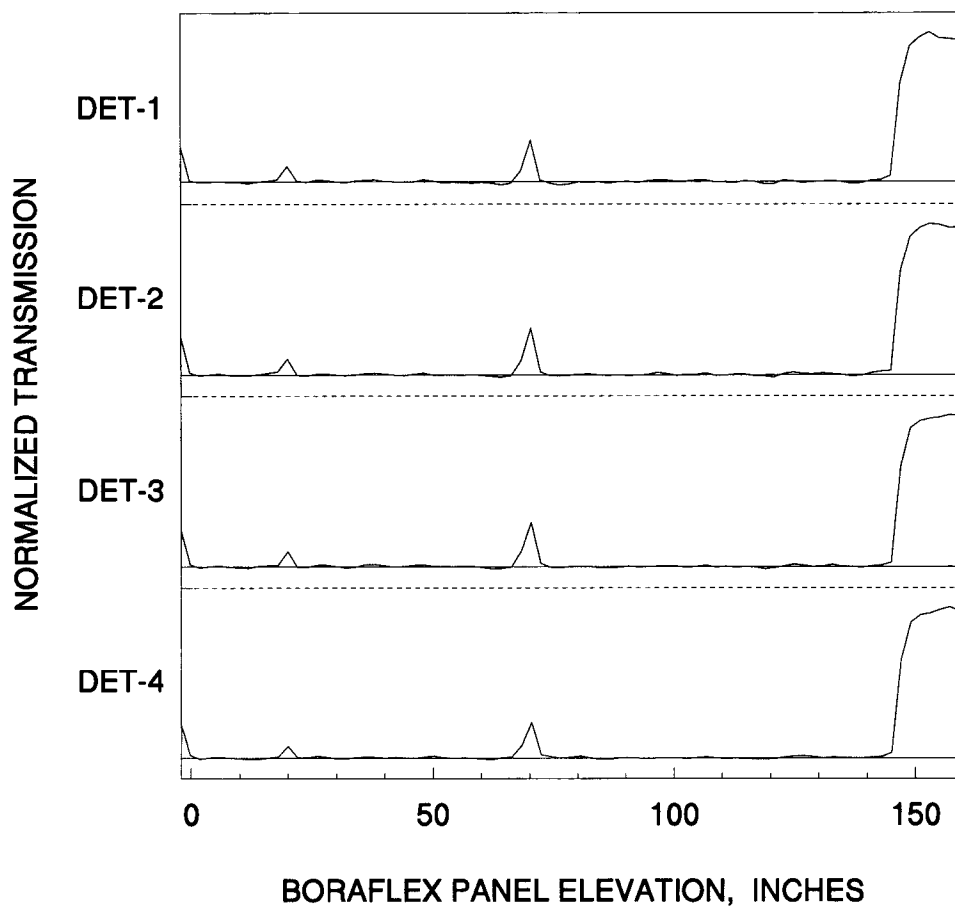


Figure 4-2  
Normalized Transmission Traces for Panel PPP-15 West

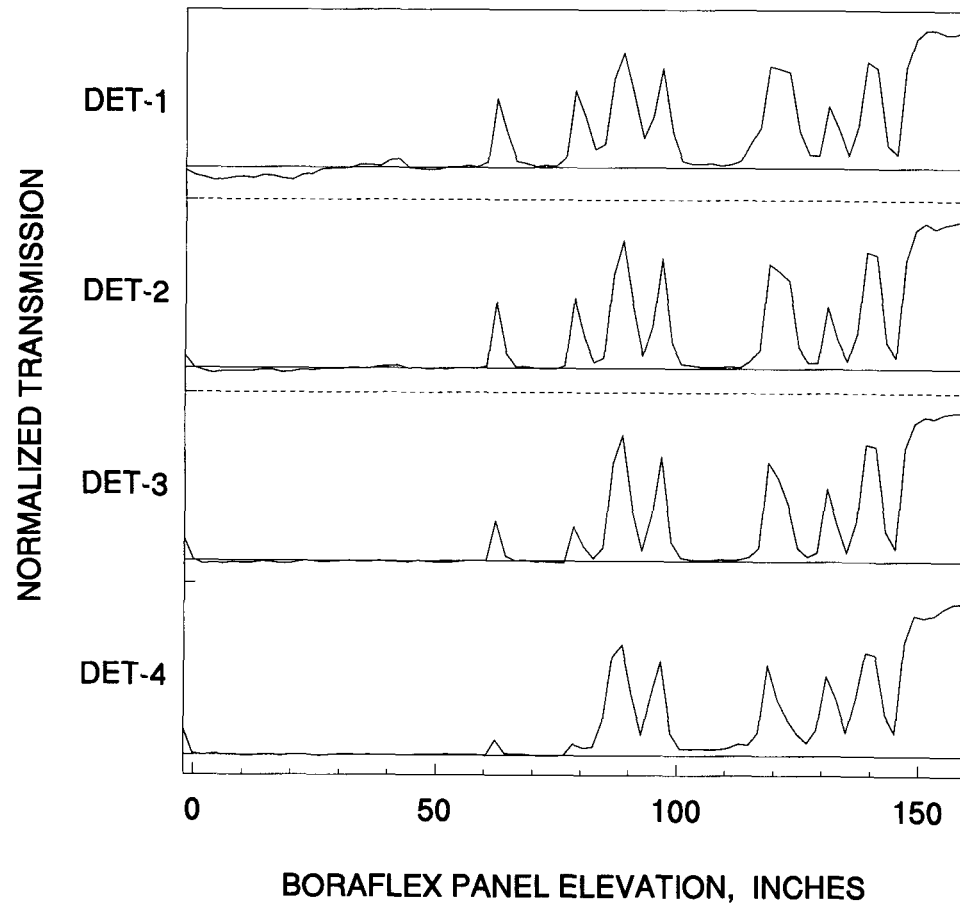


Figure 4-3  
Normalized Transmission Traces for Panel CC-27 East.

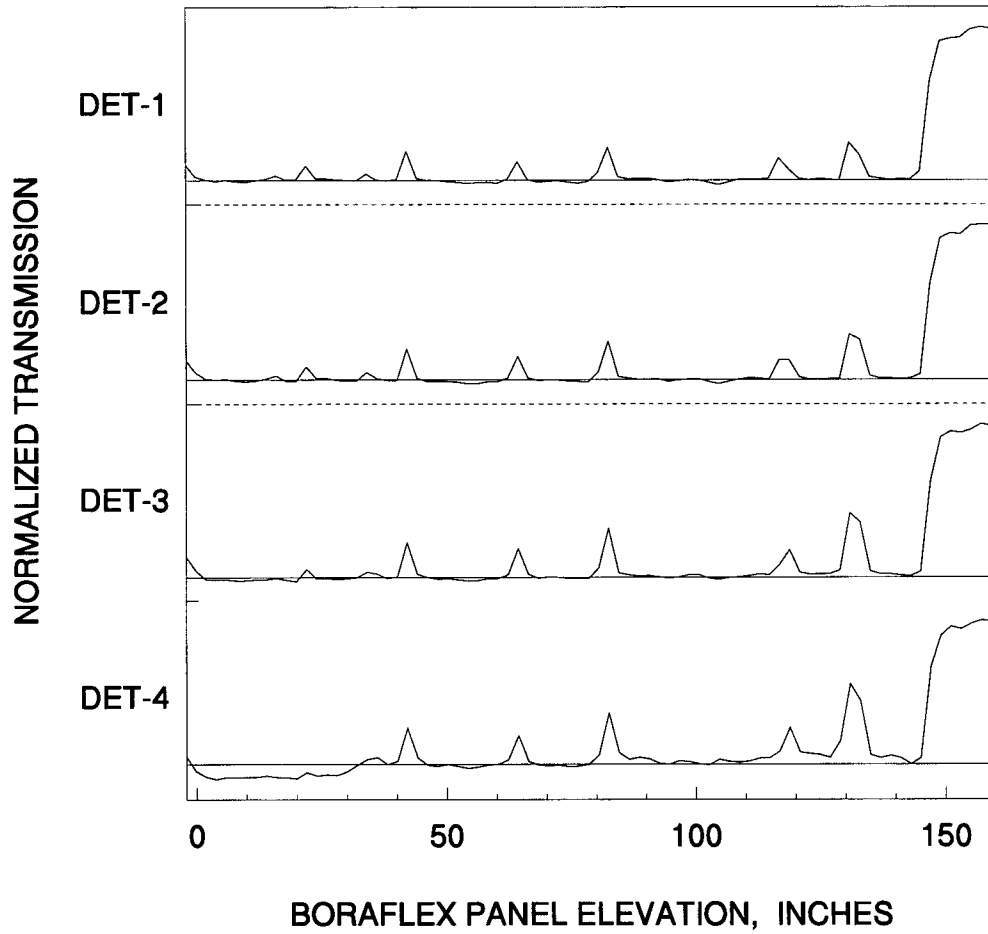


Figure 4-4  
Normalized Transmission Traces for Panel CC-27 North.



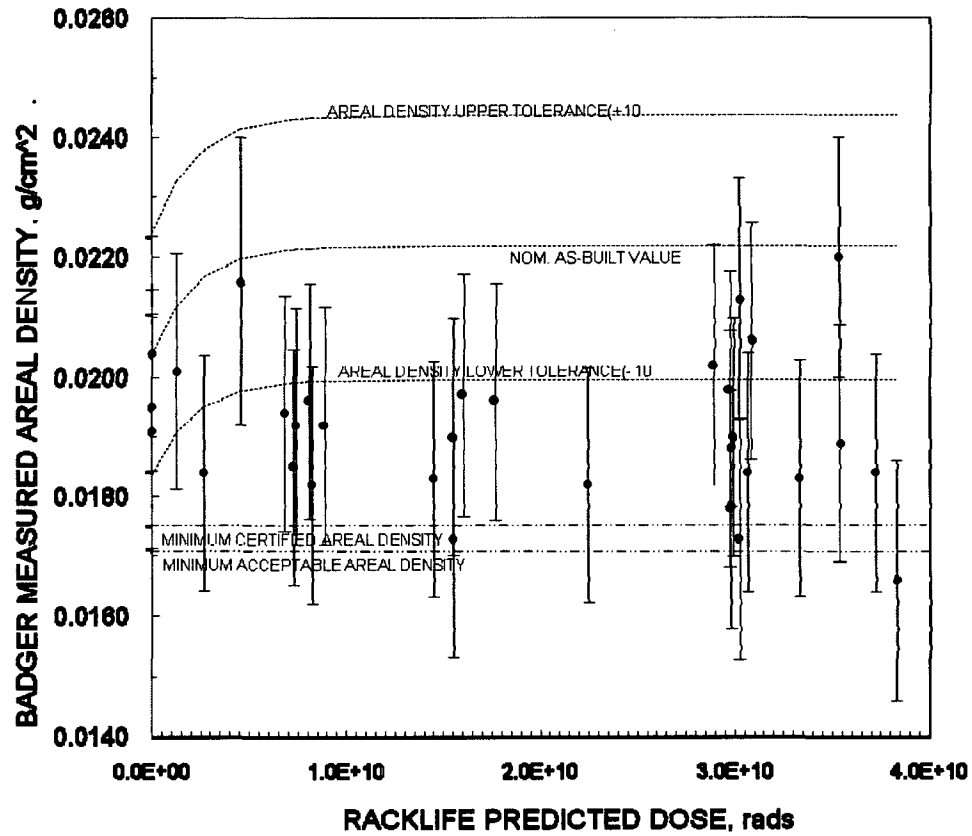


Figure 4-5  
Measured Boron-10 Areal Densities for the Panels versus RACKLIFE Predicted Panel Exposure

Panel	Absorbed Dose (Rads)	Predicted B4C Loss (%)	Areal Density (g/cm <sup>2</sup> )	% Deviation from Unirradiated Panels	Number of Gaps	Max Gap Size (in)	Total Inches of Dissolution
ZQ14 South	0.00E+00	3.14	0.0195	0.0%	3	0.63	22
ZQ16 North	0.00E+00	3.14	0.0191	-2.1%	3	0.67	20
ZR15 East	0.00E+00	0.00	0.0204	4.6%	0	0.00	8
ZP15 West	1.26E+09	3.34	0.0201	3.1%	2	1.37	2
FF28 South	2.68E+09	4.96	0.0184	-5.6%	3	2.42	26
DD28 South	4.58E+09	5.04	0.0216	10.8%	2	1.81	58
GG29 East	6.82E+09	5.22	0.0194	-0.5%	6	1.82	12
FF30 North	7.30E+09	5.32	0.0185	-5.1%	6	1.18	4
EE29 West	7.42E+09	5.19	0.0192	-1.5%	3	1.21	10
CC29 West	8.13E+09	5.69	0.0196	0.5%	4	2.03	8
DD30 North	8.25E+09	4.77	0.0182	-6.7%	9	0.84	0
EE29 East	8.90E+09	4.88	0.0192	-1.5%	5	1.43	34
P7 North	1.45E+10	4.64	0.0183	-6.2%	5	1.58	12
DD28 North	1.55E+10	5.79	0.0173	-11.3%	2	2.19	2
T13 South	1.55E+10	4.63	0.0190	-2.6%	4	1.09	16
T13 North	1.60E+10	4.64	0.0197	1.0%	2	1.49	10
AA12 South	1.77E+10	4.63	0.0196	0.5%	3	1.94	8
CC27 South	2.24E+10	5.93	0.0182	-6.7%	3	1.38	4
EE27 East	2.89E+10	5.81	0.0202	3.6%	6	3.41	24
HH24 North	2.97E+10	5.79	0.0198	1.5%	3	1.43	2
DD26 South	2.97E+10	5.76	0.0188	-3.6%	10	1.06	8
HH24 South	2.98E+10	5.77	0.0178	-8.7%	6	1.14	12
HH24 East	2.99E+10	5.75	0.0190	-2.6%	6	9.60	20
HH22 North	3.02E+10	5.77	0.0213	9.2%	2	1.70	10
HH22 South	3.02E+10	5.81	0.0173	-11.3%	1	1.43	0
HH22 East	3.06E+10	5.82	0.0184	-5.6%	6	8.66	14
AA27 North	3.08E+10	5.93	0.0206	5.6%	2	1.50	6
CC27 West	3.33E+10	5.91	0.0183	-6.2%	4	2.64	20
AA27 West	3.53E+10	5.93	0.0220	12.8%	3	3.10	10
AA27 East	3.54E+10	5.93	0.0189	-3.1%	5	2.02	26
CC27 North	3.72E+10	5.94	0.0184	-5.6%	5	1.78	8
CC27 East	3.83E+10	5.93	0.0166	-14.9%	7	3.84	28

Table 4-1  
GGNS Areal Density and Panel Boron Carbide Loss

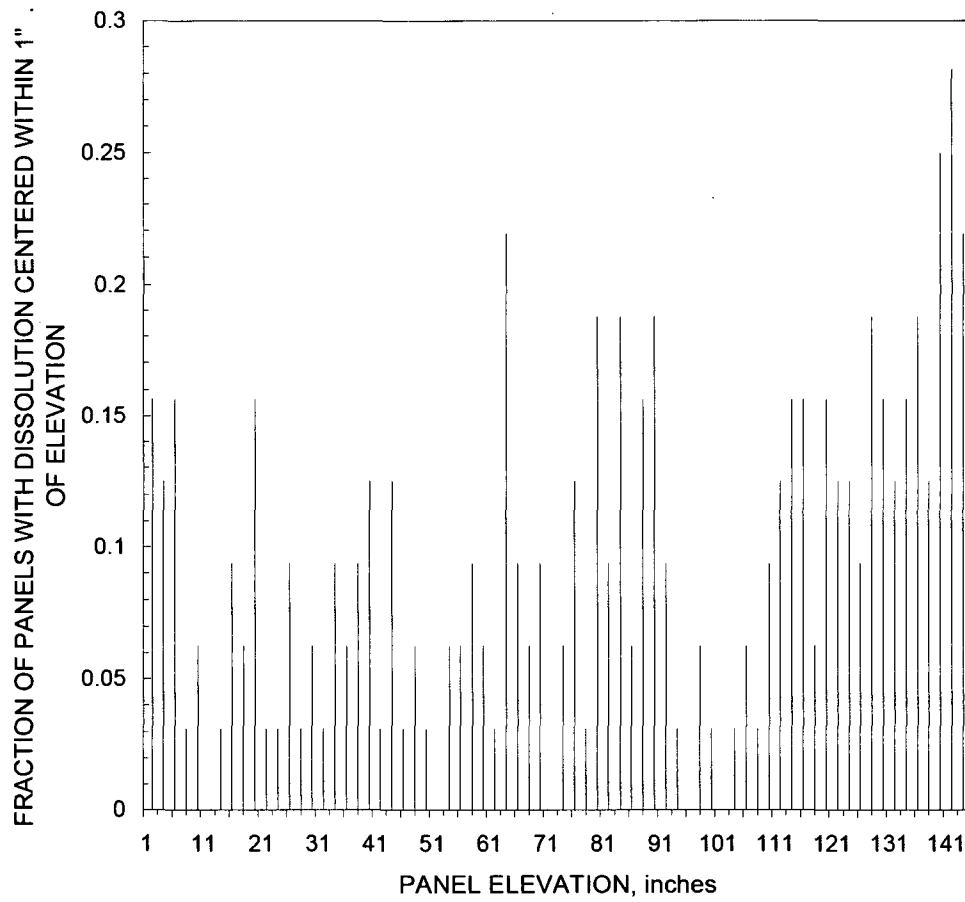


Figure 4-6  
Axial Distribution of Dissolution in Panels Tested

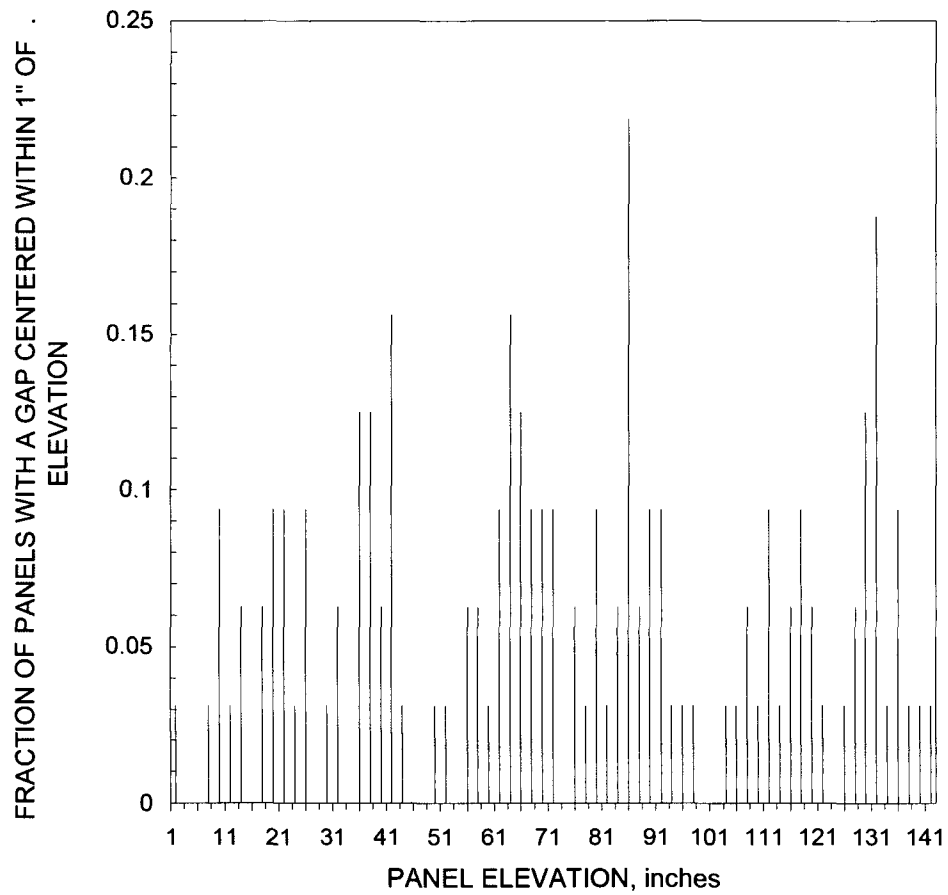


Figure 4-7  
Axial Distribution of Gaps in Panels Tested

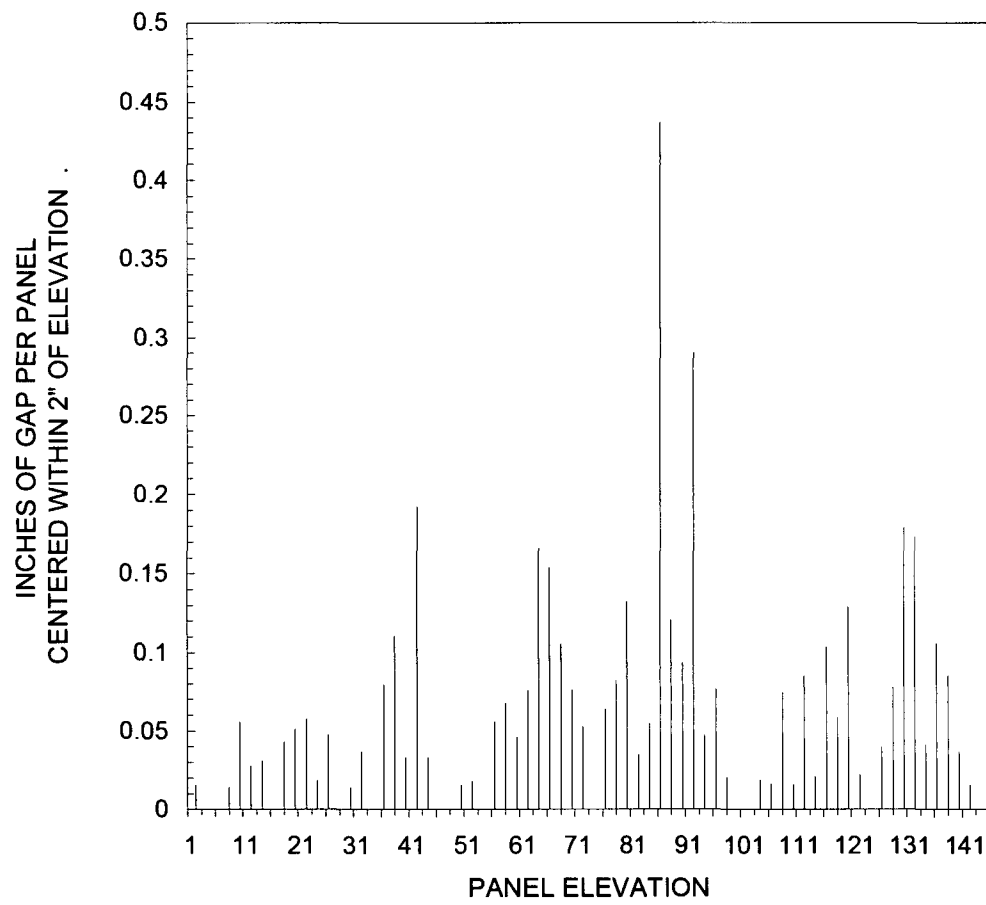


Figure 4-8  
Axial Distribution of Average Co-Planar Gapping in Panels Tested

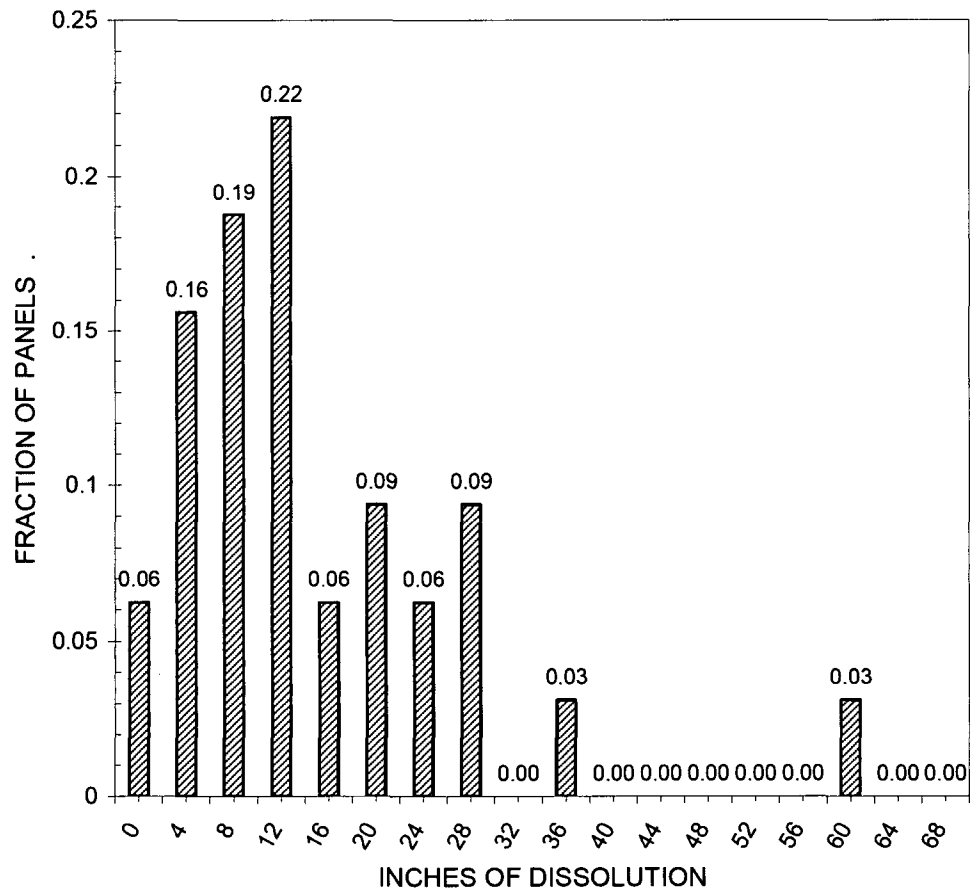


Figure 4-9  
Frequency Distribution of Total Dissolution Along the Panels Tested

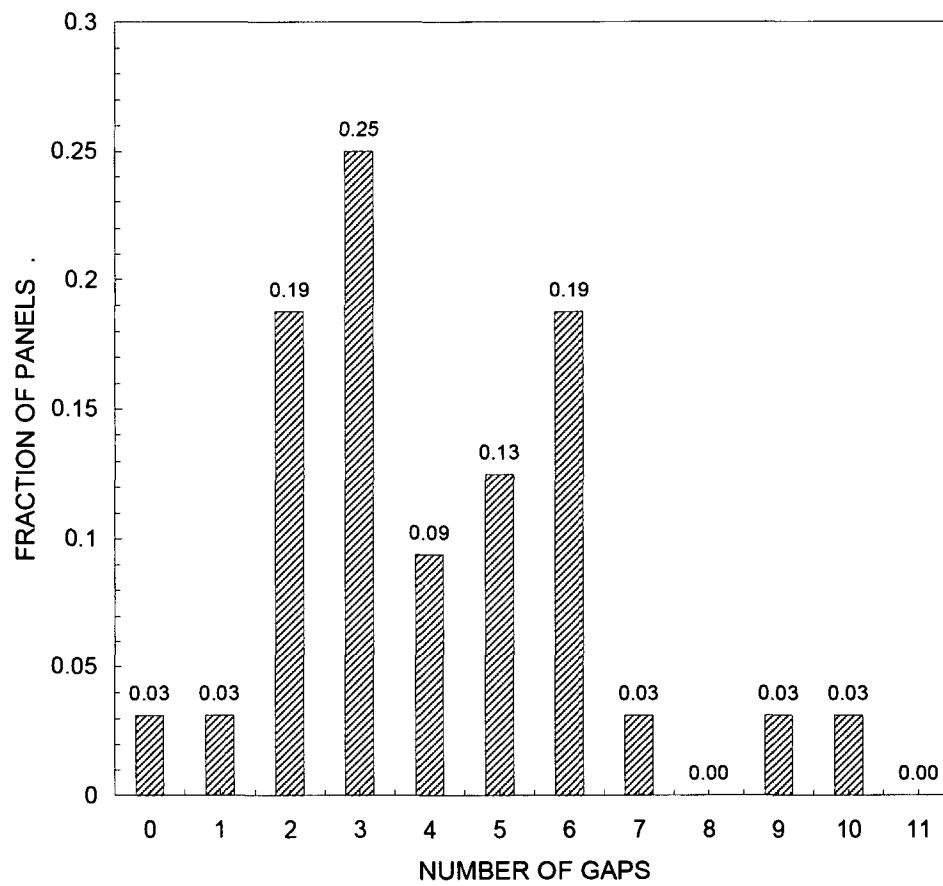


Figure 4-10  
Frequency Distribution of Number of Gaps in Panels Tested

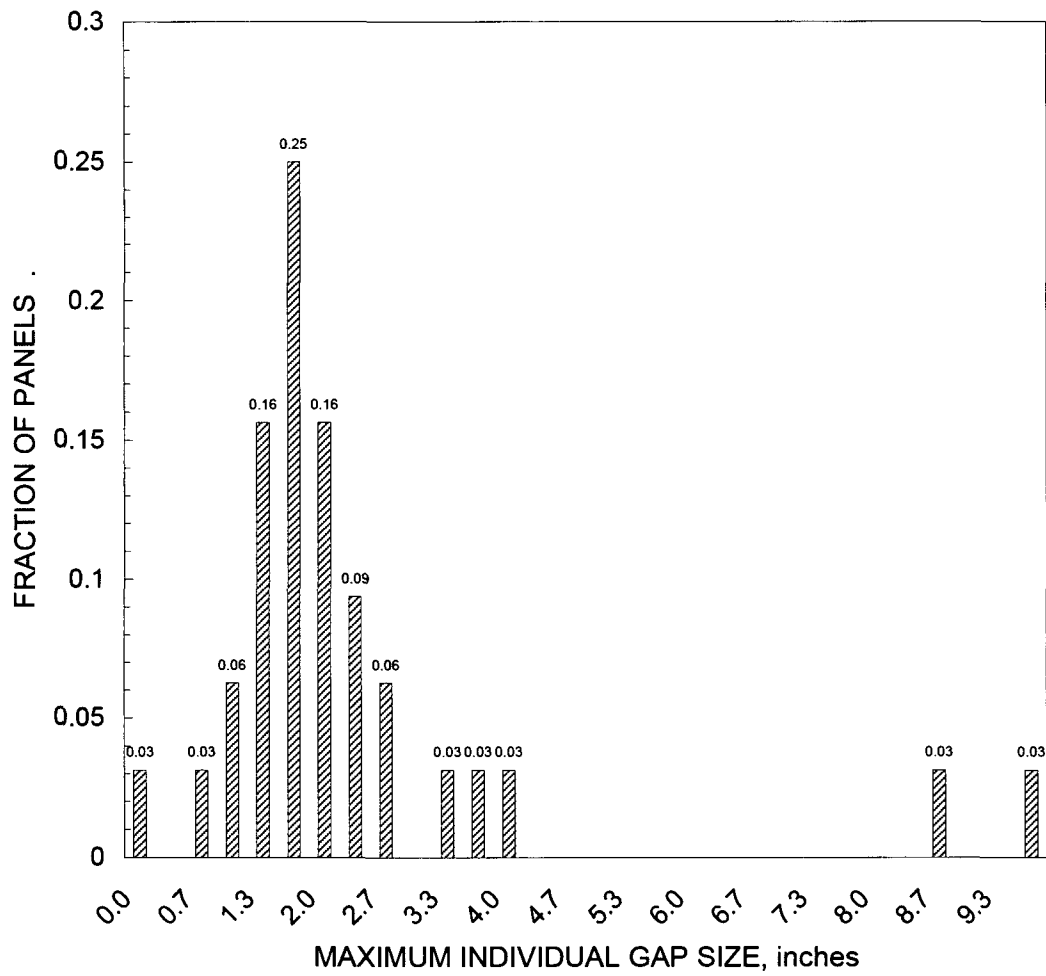


Figure 4-11  
Frequency Distribution of Maximum Gap Size in Panels Tested



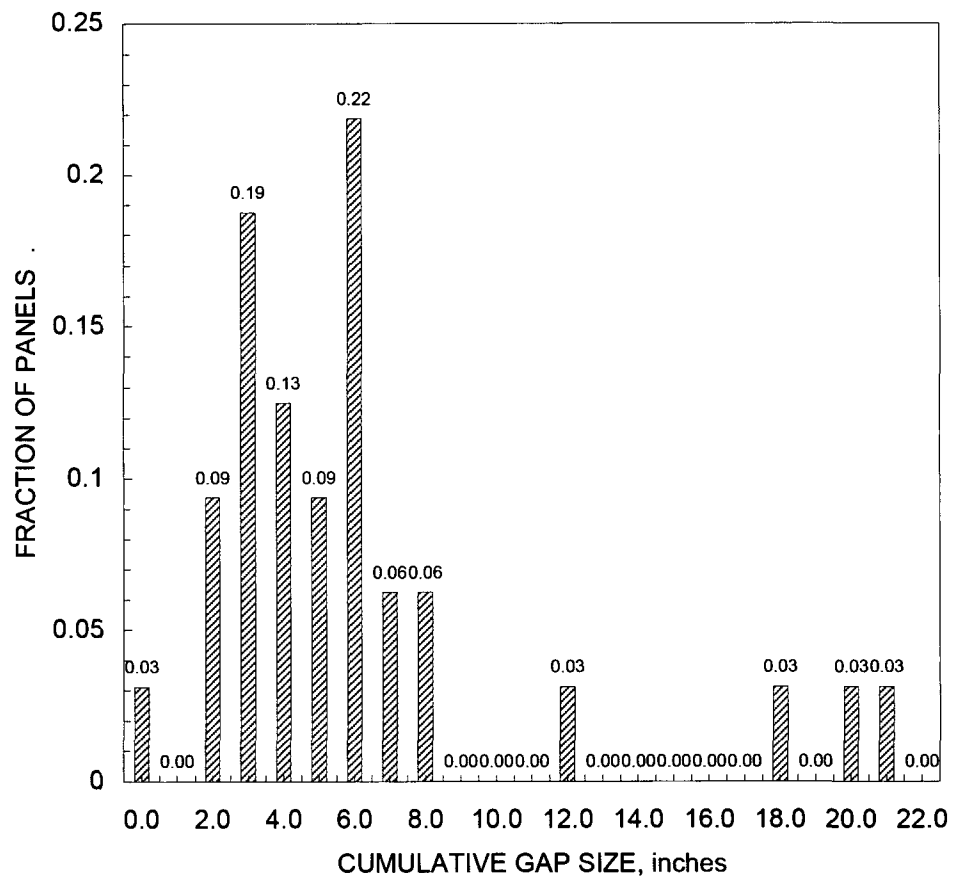


Figure 4-12  
Frequency Distribution of Cumulative Gap Size in Panels Tested

	Panel	Individual Gap Size		Elevation	
		Blackness	BADGER	Blackness	BADGER
CC-27	East	3.8	3.8	89	88
		3.7	3.5	139	138
		2.5	3	120	121
		2.0	3.1	97	96
		0.8	2	131	131
		0.7	1.6	79	79
		-----	1.5	-----	62
	North	0.9	1.4	84	84
		0.9	1.8	132	132
		0.7	1.1	118	118
		0.6	1.2	46	42
		0.6	1	66	64
	West	2.8	2.6	82	80
		2.3	2.5	66	64
		1.6	1.8	41	38
		-----	0.7	-----	88
	South	1.5	1.1	66	64
		0.7	1.4	113	112
		0.6	0.8	43	38
EE-27	East	1.2	3.4	85	86
		1.0	1.4	60	56
		0.8	2	128	128
		-----	2	-----	136
		-----	1.1	-----	19
		-----	1.1	-----	10
HH-22	East	5.0	8.7	89	86
		2.3	2.5	73	70
		2.0	2	66	60
		1.0	1.3	44	38
		1.0	2.1	133	130
		-----	0.6	-----	14
	North	2.2	1.7	137	134
HH-24	North	1.1	1.1	18	12
		1.2	1.4	116	112
		1.5	1.4	61	58
	South	1.2	1.4	86	86
		0.8	1.3	136	136
		0.6	1	71	68
		0.5	0.7	91	90
		-----	1.1	-----	132
		-----	1.1	-----	116
		-----	0.8	-----	104
		-----	0.6	-----	18
	East	6.0	9.6	91	92
		2.4	3.1	114	116
		1.7	1.7	56	54
		-----	0.9	-----	68
		-----	1.9	-----	80
AA-27	West	-----	2.9	-----	132
		3.0	3.1	45	42
		-----	1.2	-----	66
	North	-----	0.8	-----	72
		1.6	1.5	141	140
		1.0	1.4	47	44
	East	0.6	-----	23	-----
		-----	2	-----	86
		-----	1.2	-----	108
		-----	0.8	-----	118
		-----	1.6	-----	126.0
		-----	0.8	-----	132

Table 4-2 Comparison of BADGER Measured Gaps with Previous Blackness Test Measurements

## 5.0 CONCLUSIONS AND RECOMMENDATIONS

A series of 32 Boraflex panels from the GGNS fuel racks have been subjected to non-destructive BADGER testing to determine the condition of the Boraflex neutron absorber material. The average areal density of all panels tested is  $0.0191 \pm 0.0012$  grams B-10/cm<sup>2</sup>, which compares with a nominal as-built value of 0.0204 grams B-10/cm<sup>2</sup>. If there was no loss of boron carbide due to in-service degradation, the nominal as-built areal density could be as much as 0.0223 grams B-10/cm<sup>2</sup> due to densification effects. The average areal density of all panels tested is 0.0191 grams B-10/cm<sup>2</sup>. This represents a boron carbide loss of 14.1% that can be compared with a RACKLIFE predicted loss of 5.1%. RACKLIFE appears to be, on average, accurately predicting the degradation of the Boraflex panels in the GGNS spent fuel storage racks. ENO may want to increase the escape coefficient in their RACKLIFE model to account for the small differences between the RACKLIFE predictions and the average of the BADGER measurements.

The BADGER test results indicate that some of the Boraflex panels have sustained some in-service degradation and a few higher dose panels showed moderate loss of boron carbide. The types of degradation observed include:

- areas of local dissolution;
- general panel thinning;
- the formation of shrinkage-induced gaps.

Panel CC-27 East had the lowest measured areal density (0.0166 grams B-10/cm<sup>2</sup>). This value represents almost a 26% loss from the as-manufactured, densified areal density of 0.0223 grams B-10/cm<sup>2</sup>. This panel shows some areas of local dissolution and a gap at around 112." The reduction in panel average areal density, however, is most likely due to the areas of dissolution and to general panel thinning.

The local dissolution observed in the panels tested appears more prominently in the upper panel areas. Whether or not panels will be subject to dissolution is likely to depend on two factors: first, the fit-up of the panel enclosure and whether or not there is significant in flow and out flow of the pool water; and second, the time at which the panel accumulated a relatively high dose. Panels that accumulated dose early are subject to greater dissolution than are panels that accumulated high doses more recently.

Gamma radiation induced crosslinking of the polymer matrix and the associated densification of the matrix have actually caused the areal density to increase somewhat in some panels. This increase in areal density can be observed in some panels that show areal densities in the upper range of the expected areal density.

The largest cumulative length of gap observed in one panel was approximately 20 inches and the largest single gap measured was 9.6 inches. Gaps of this magnitude are considerably greater than the 4.1% asymptotic limit (or ~ 6.0 inches) of maximum gap size for gamma induced shrinkage of Boraflex<sup>[11]</sup>. This suggests rather substantial dissolution has and will continue to occur at the edges of some gaps.

With respect to the condition of the Boraflex panels in the GGNS spent fuel racks, the BADGER test results have revealed that the degradation of the Boraflex panels is primarily due to large shrinkage induced gaps followed by subsequent edge dissolution. This degradation is limited to specific regions(modules) within the spent fuel pool. The implementation of appropriate measures to mitigate degraded Boraflex may be effective in extending the useful service life the Boraflex rack modules and in some cases may recover currently restricted storage locations.

NETCO has developed a more sophisticated method of assessing the reactivity effects of local panel degradation, utilizing Monte-Carlo sampling techniques. This method samples the reactivity effects associated with local Boraflex degradation as measured by BADGER to create a more accurate rendering of the reactivity holddown capability of the Boraflex panels. This method has been employed at other spent fuel pools where BADGER measurements have been performed and has resulted in substantially increased reactivity margins and consequently longer projected useful service life of the spent fuel racks.

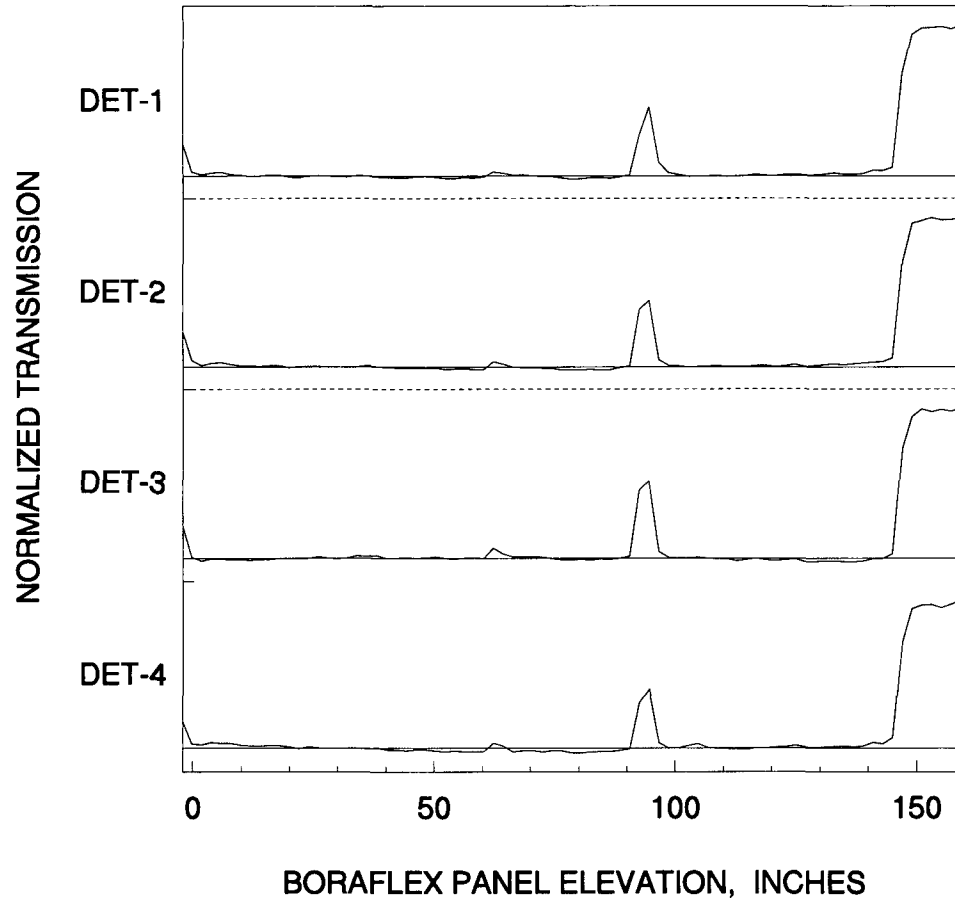
The most severe degradation was observed to occur in Module 6. In conjunction with the more sophisticated reactivity assessment methodology described above, it is possible that a two-region storage system could be identified for Module 6 to offset the reactivity effects due to gaps and dissolution. Using a selective loading in this module may allow the GGNS to recover storage locations that are currently administratively restricted.

## 6.0 REFERENCES

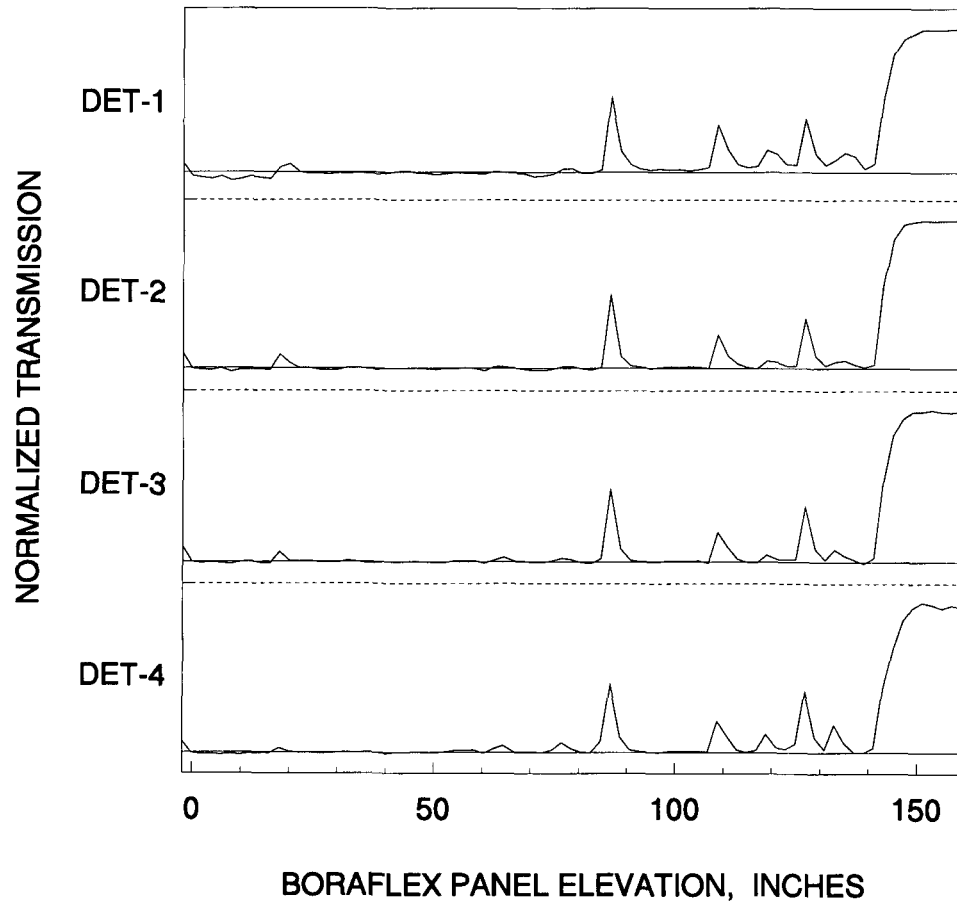
1. White Paper: "Boraflex Performance in Spent-Nuclear-Fuel Storage Racks", Electric Power Research Institute: Palo Alto, California; August 1996.
2. "Radiation Induced Changes in the Physical Properties of Boraflex™, a Neutron Absorber Material for Nuclear Applications", K. Lindquist, D. Kline, and R. Lambert, Journal of Nuclear Materials: Vol. 217, pp. 223-228; 1994.
3. "Boraflex Test Results and Evaluation", TR-101986, Electric Power Research Institute: Palo Alto, California; February 1993.
4. "BADGER, a Probe for Nondestructive Testing of Residual Boron-10 Absorber Density in Spent-Fuel Storage Racks: Development and Demonstration", TR-107335, Electric Power Research Institute: Palo Alto, California; October 1997.
5. "MCNP Validation of BADGER", GC-110539 Electric Power Research Institute: Palo Alto, California; May 1998.
6. SEP-287-01, Rev 0, "Procedure for Measuring the Boron-10 Areal Density of Boraflex in the Grand Gulf Nuclear Station Spent-Nuclear Fuel Storage Racks ", Northeast Technology Corp., Kingston, NY, August 10, 2007.
7. SEP-287-02, Rev 0, " Procedure for Assembly of the BWR Boron-10 Areal Density Meter at the Grand Gulf Nuclear Station", Northeast Technology Corp., Kingston, NY, August 10, 2007.
8. "The RACKLIFE Boraflex Rack Life Extension Computer Code: Theory and Numerics", TR-107333, Electric Power Research Institute: Palo Alto, California; July 1997.
9. Email from S. Stanchfield (ENO) to M. Harris(NETCO) dated 1/8/08 with attachments: EXMP-88/0079, "Design Input for GGNS-1 Spent Fuel Rack Criticality Analysis."
10. Amendment No. 17 to Facility Operating License NPF-29 Technical Specification 5.6 "Fuel Storage and Spent Fuel Storage Pool Temperature", August 18, 1986.
11. "A Synopsis of the Technology Developed to Address the Boraflex Degradation Issue", TR-108761, Electric Power Research Institute: Palo Alto, California; November 1997.

## **Appendix A**

# AA12SS1

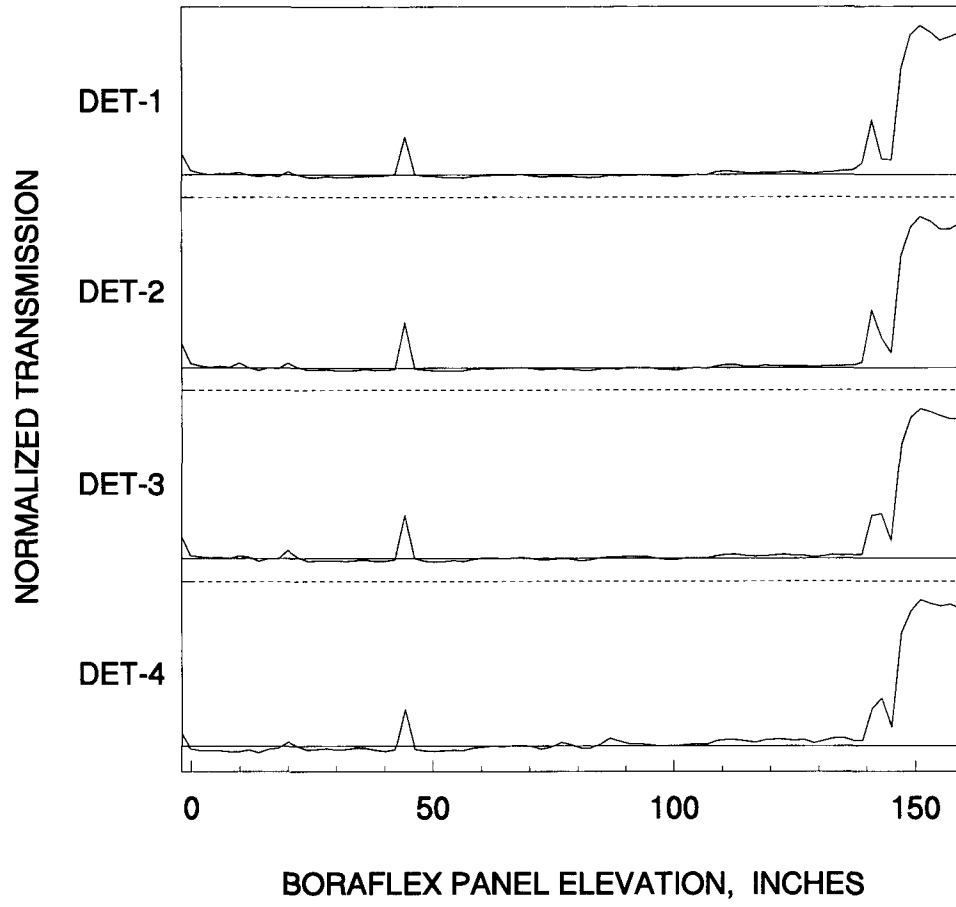


# AA27ES1

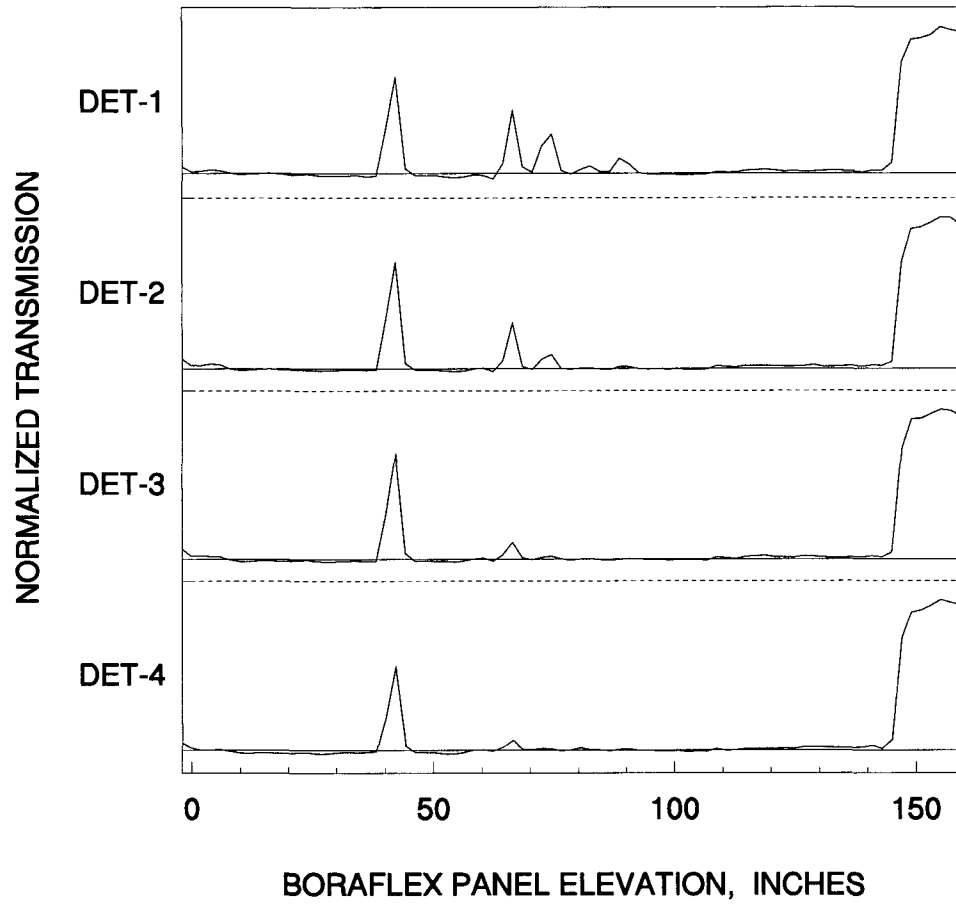




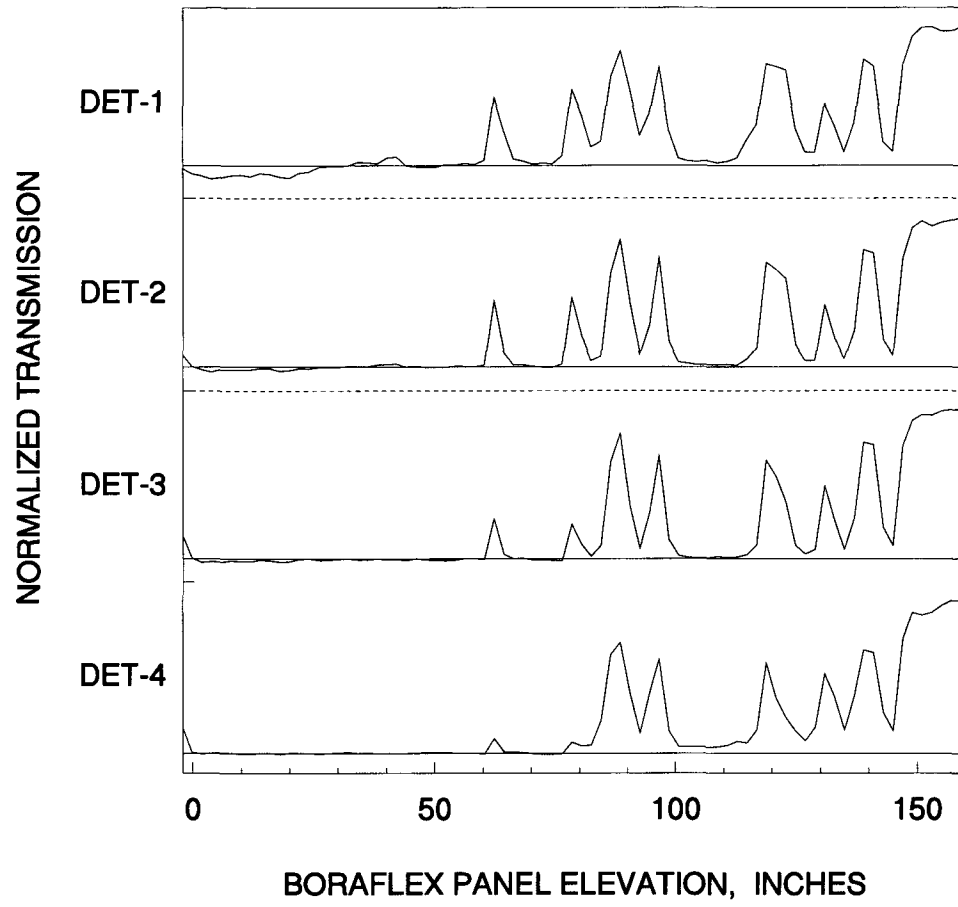
# AA27NS1



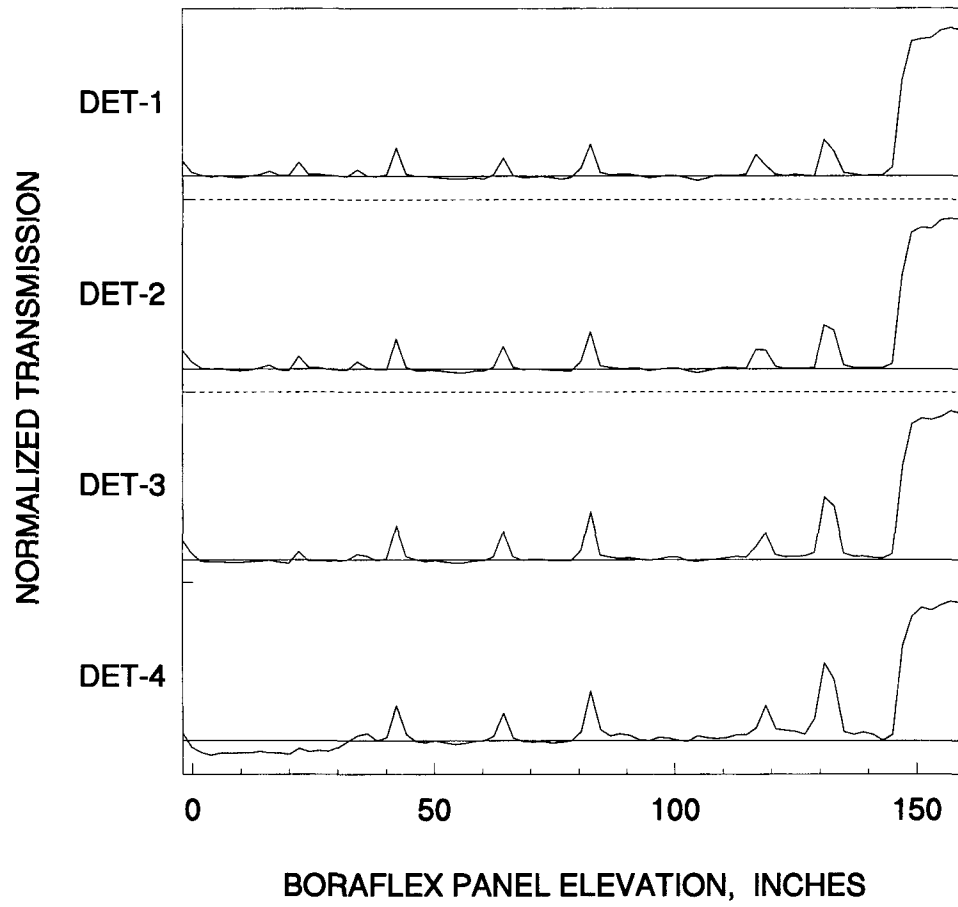
# AA27WS1



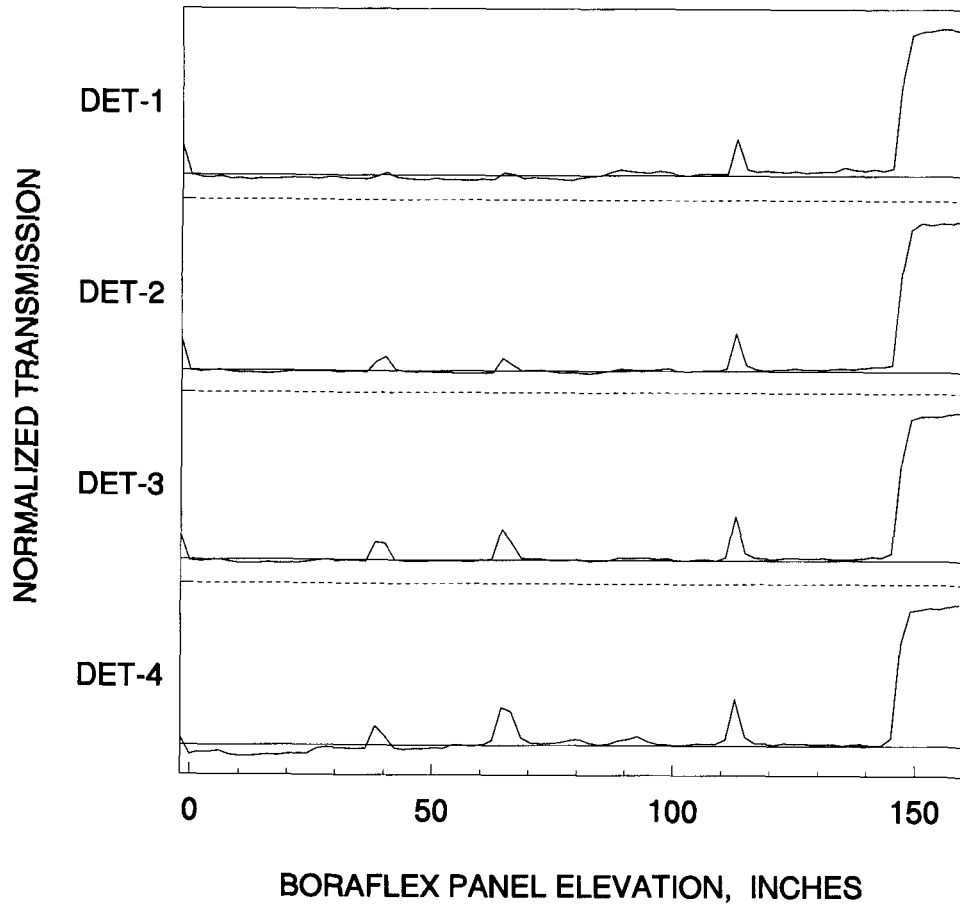
# CC27ES1



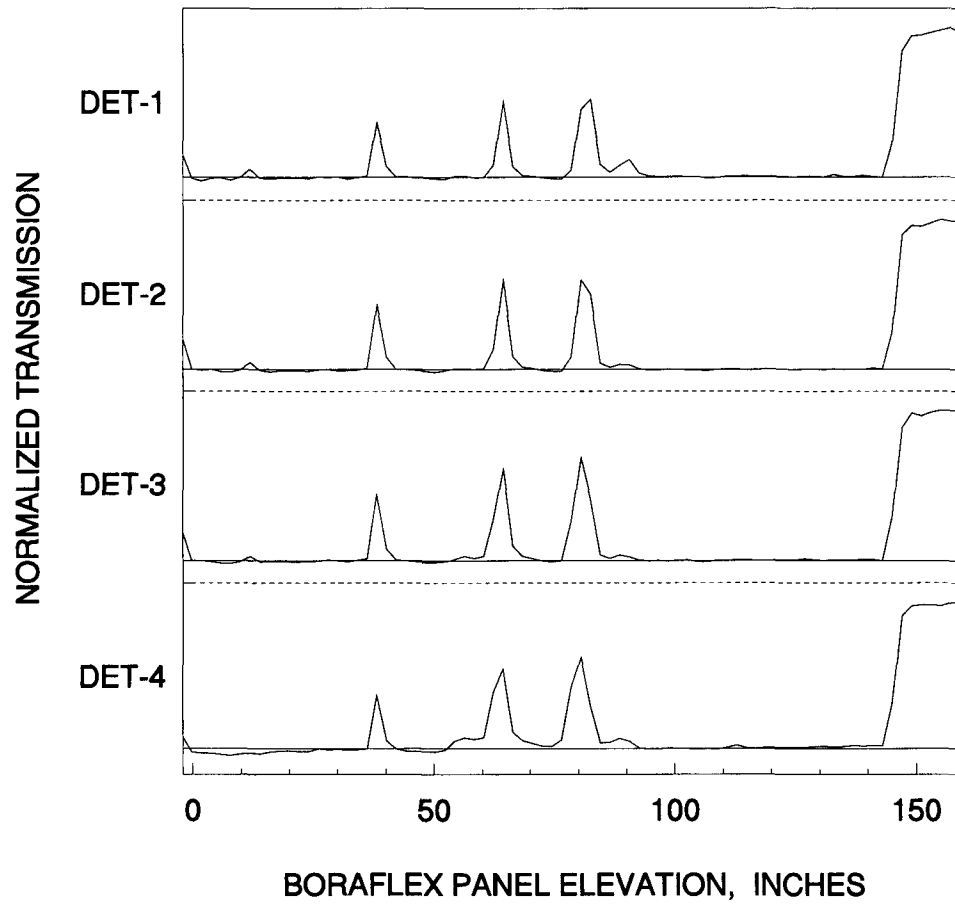
# CC27NS1



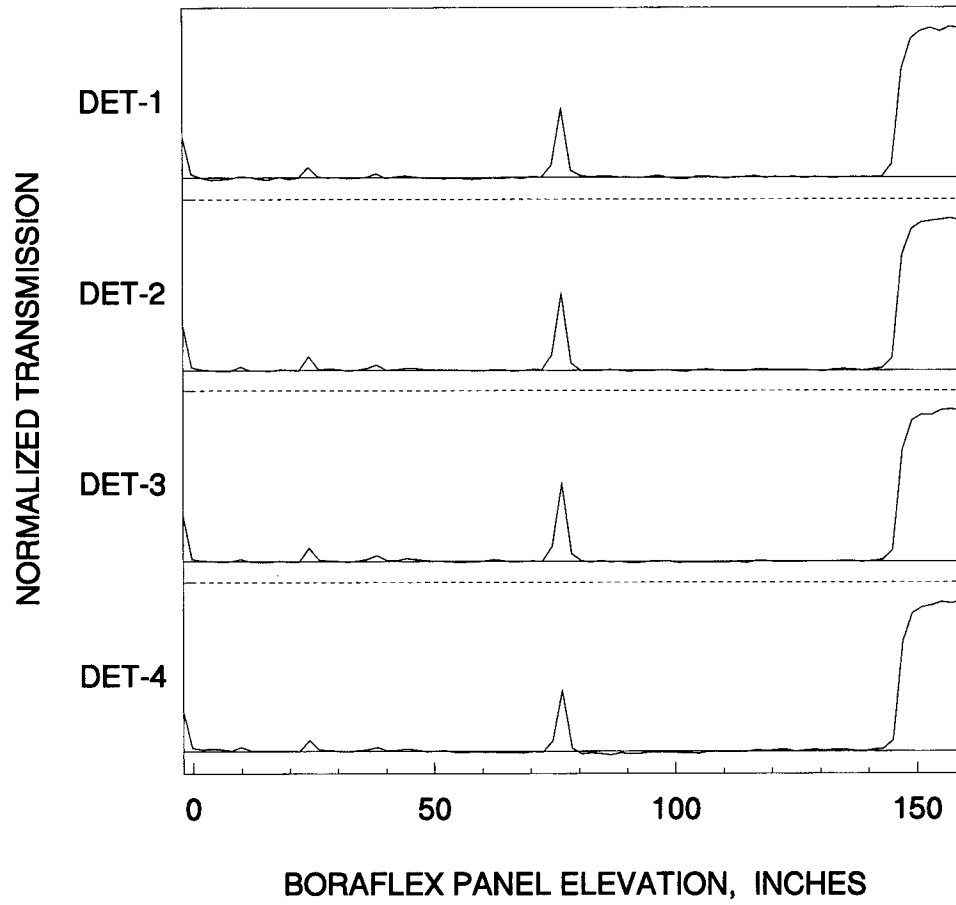
# CC27SS1



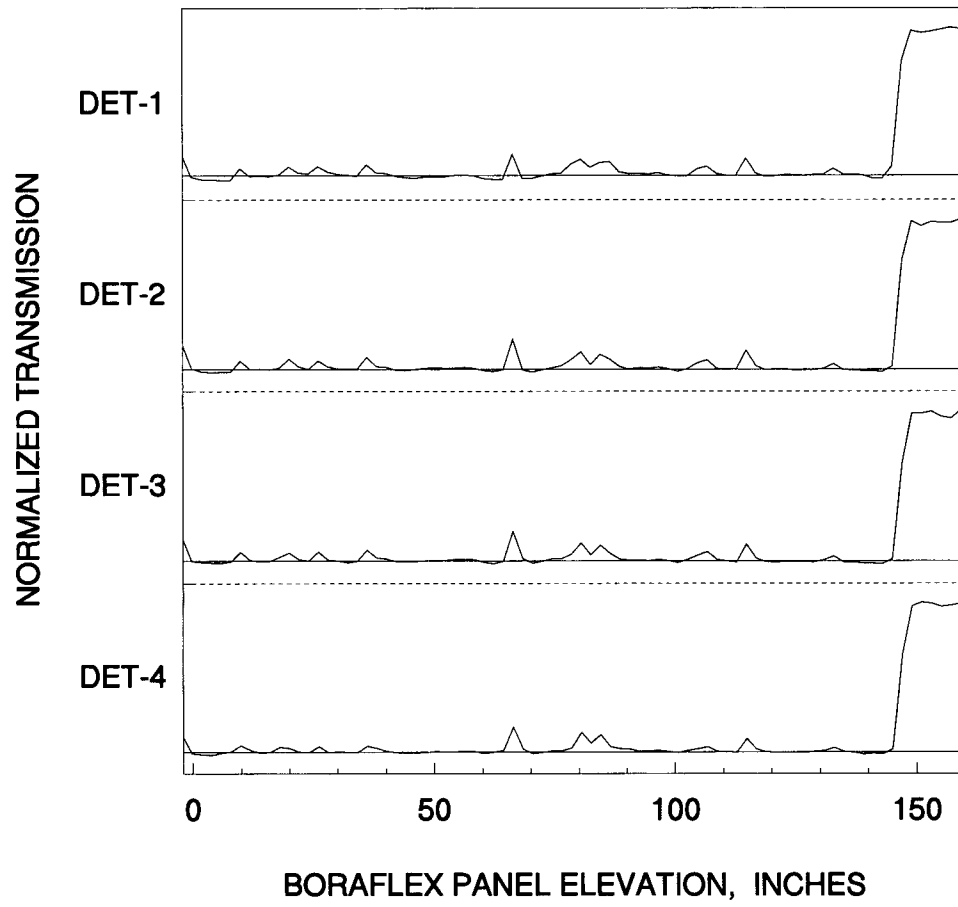
# CC27WS1



# CC29WS1

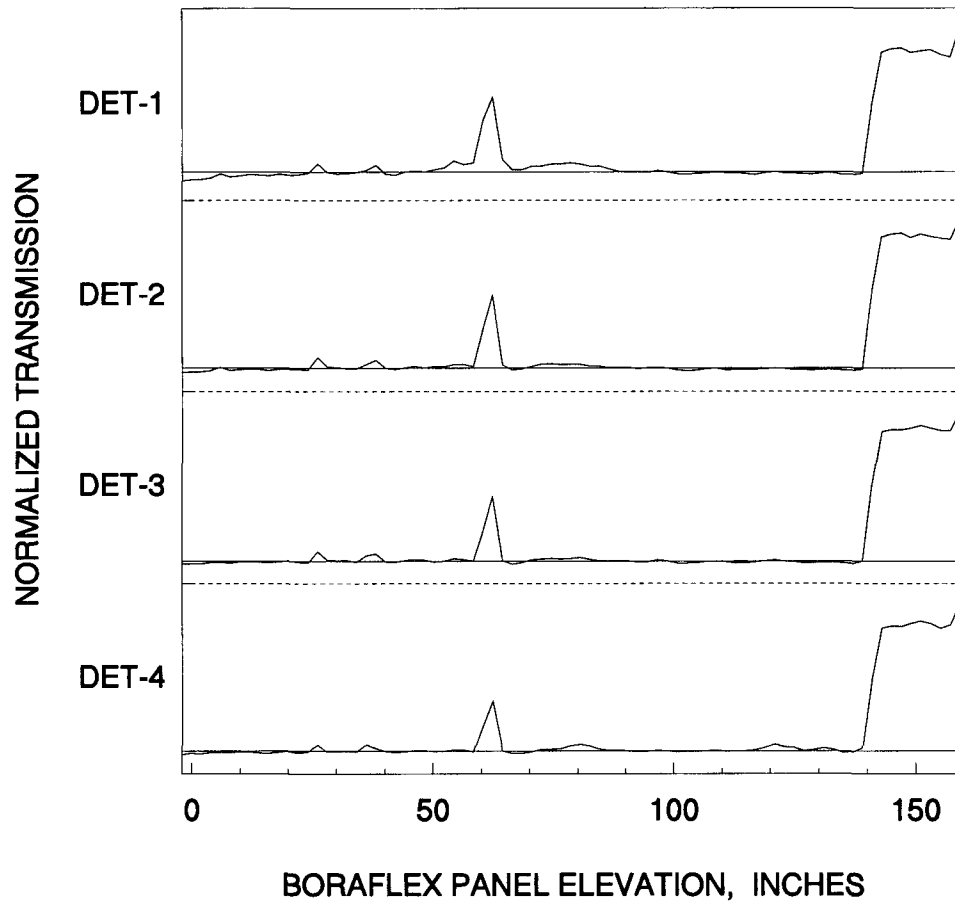


# DD26SS1

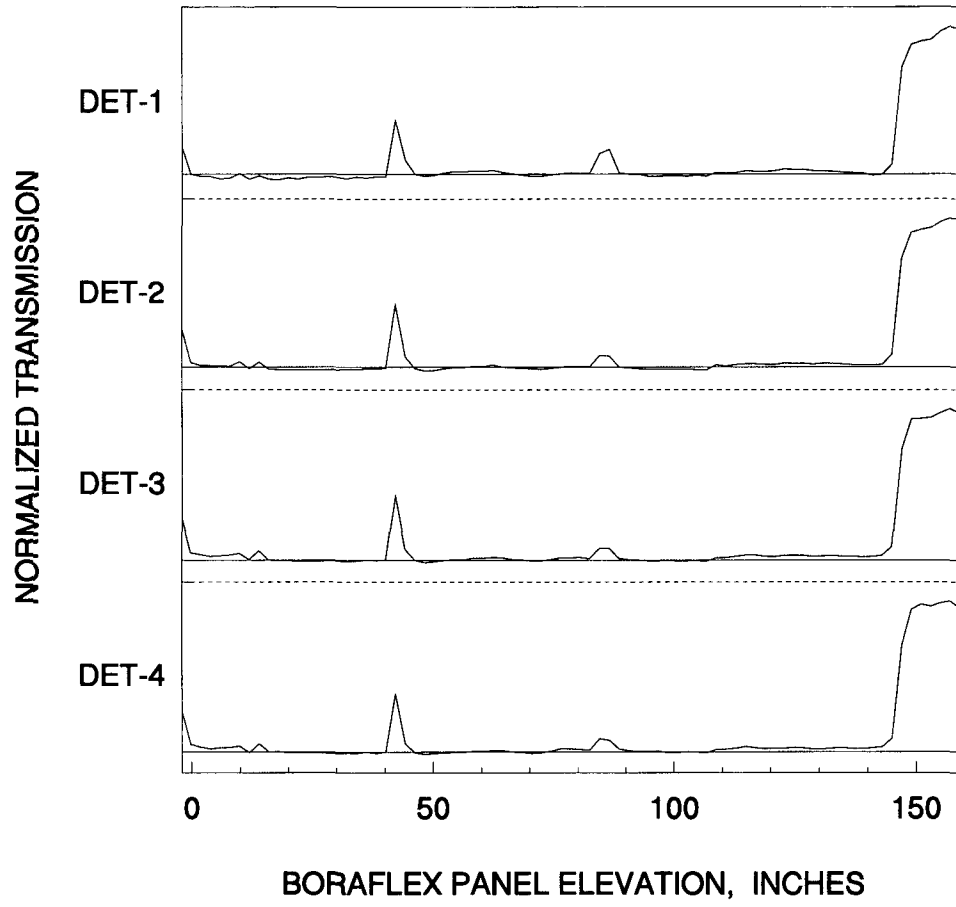




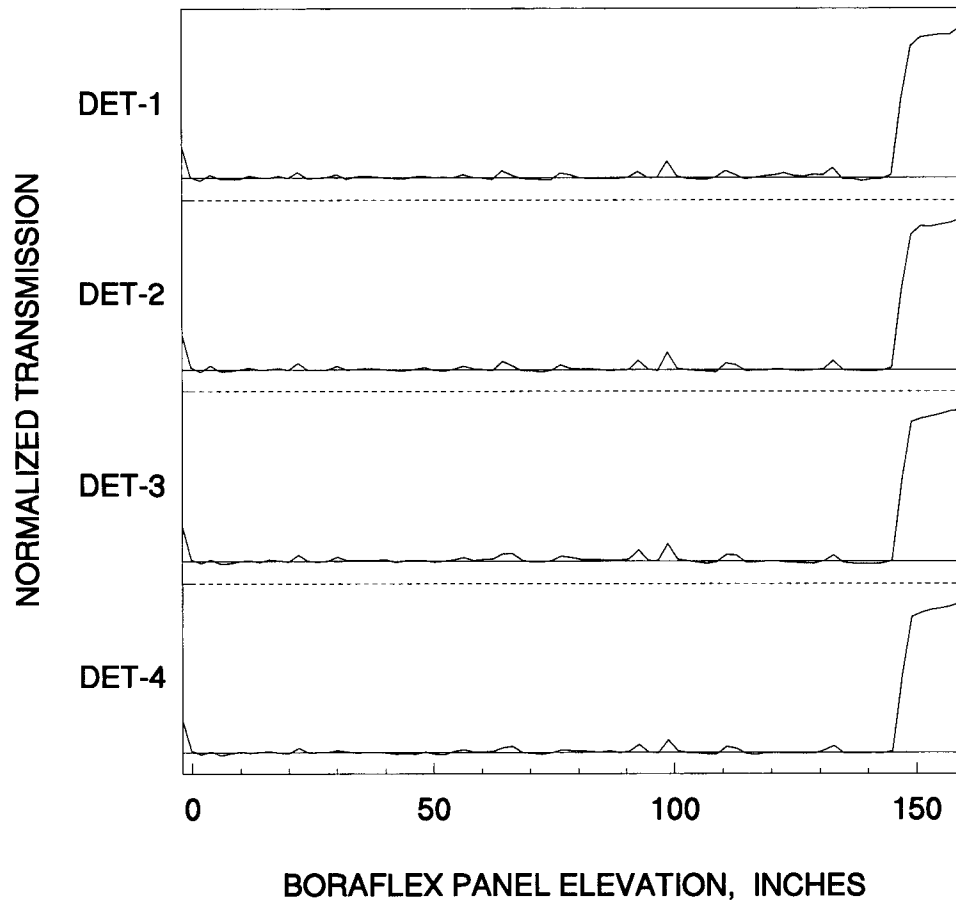
# DD28NS1



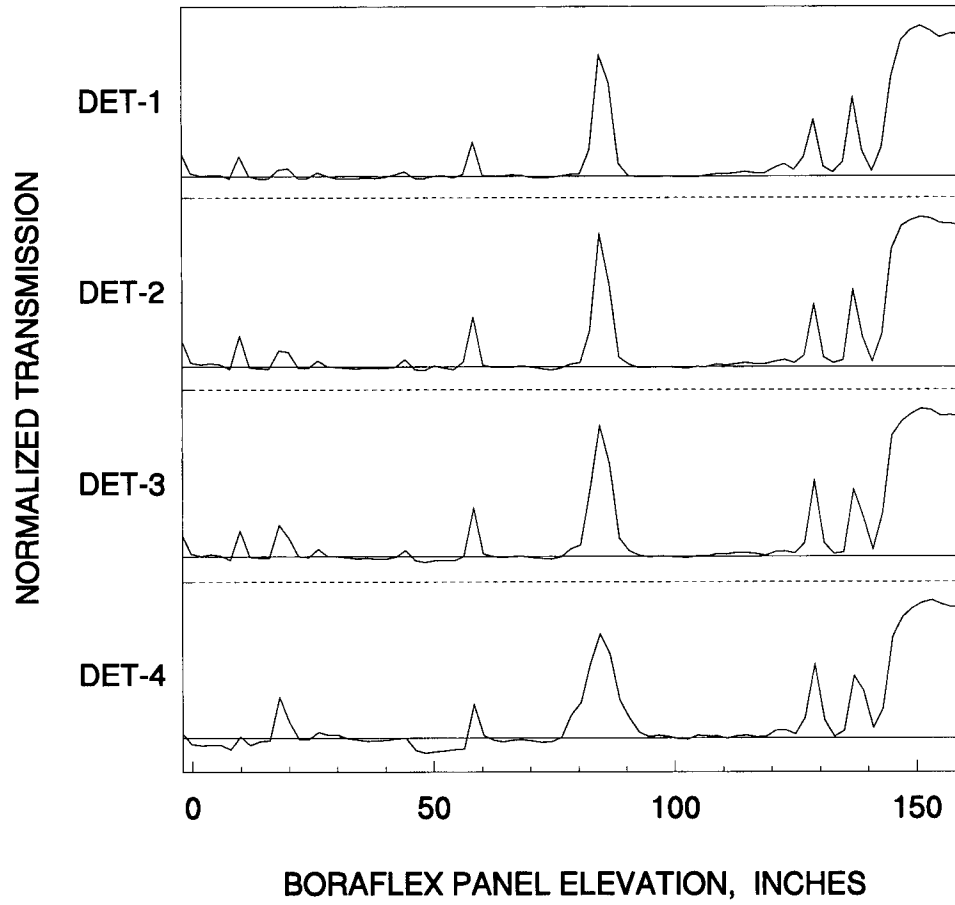
# DD28SS1



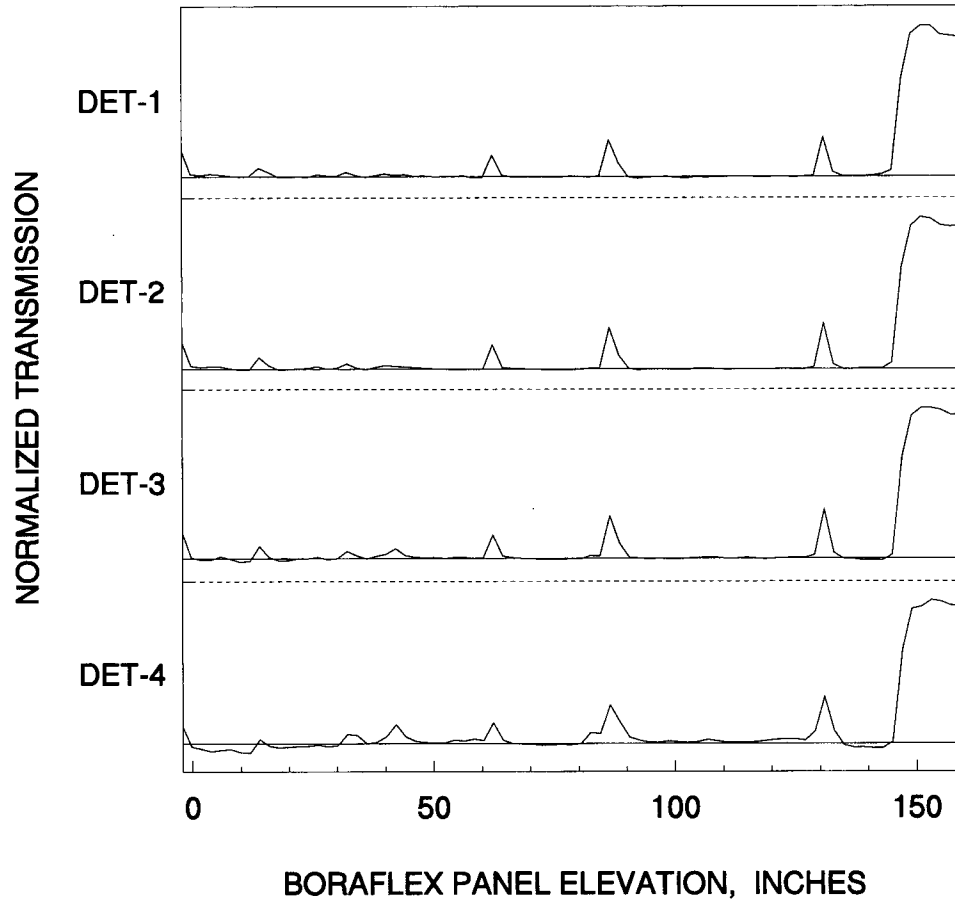
# DD30NS1



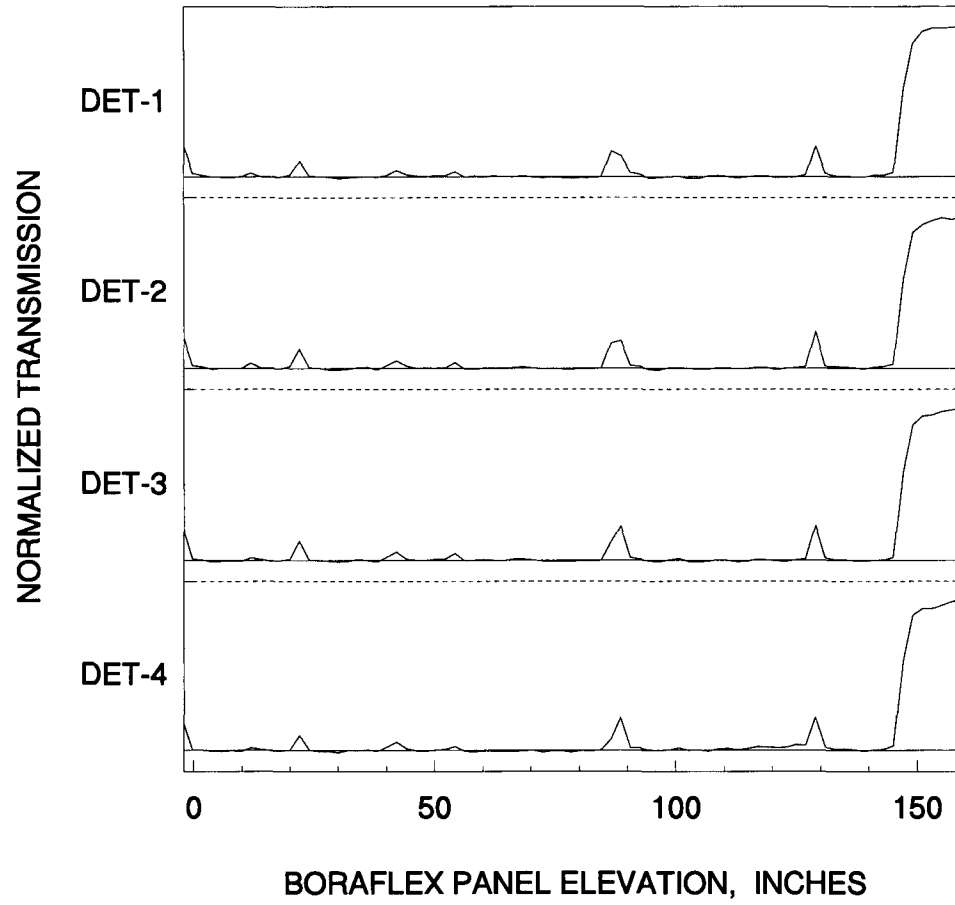
# EE27ES1



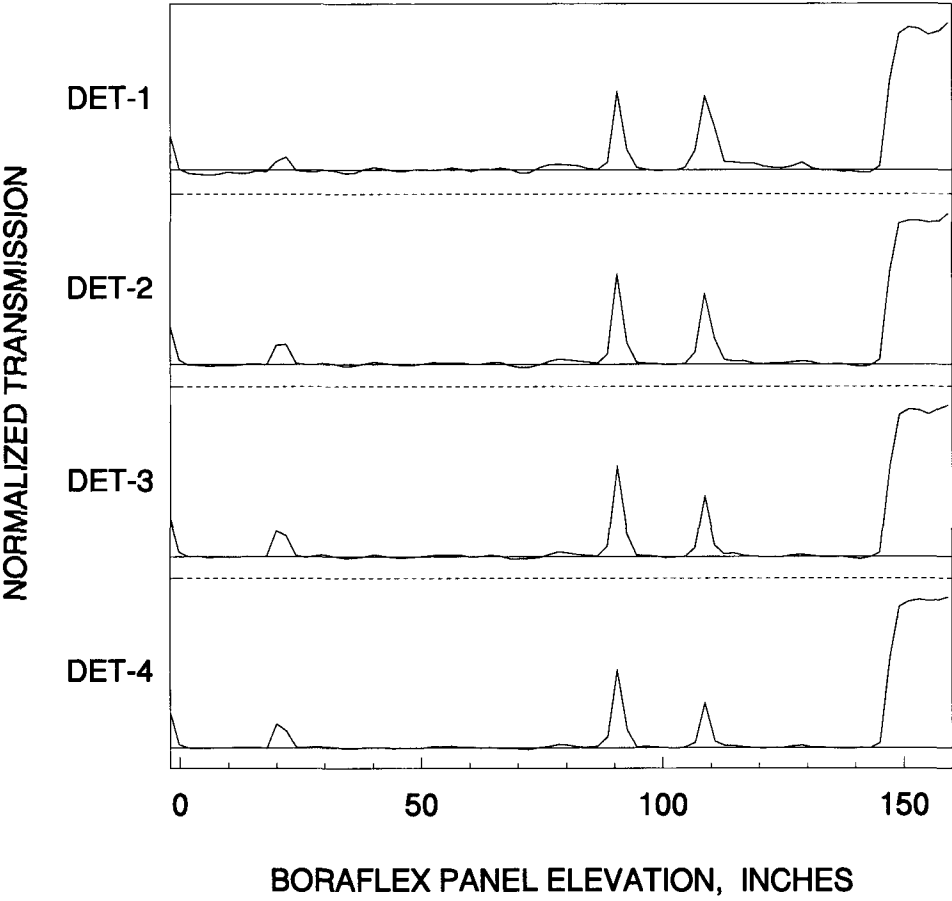
# EE29ES1



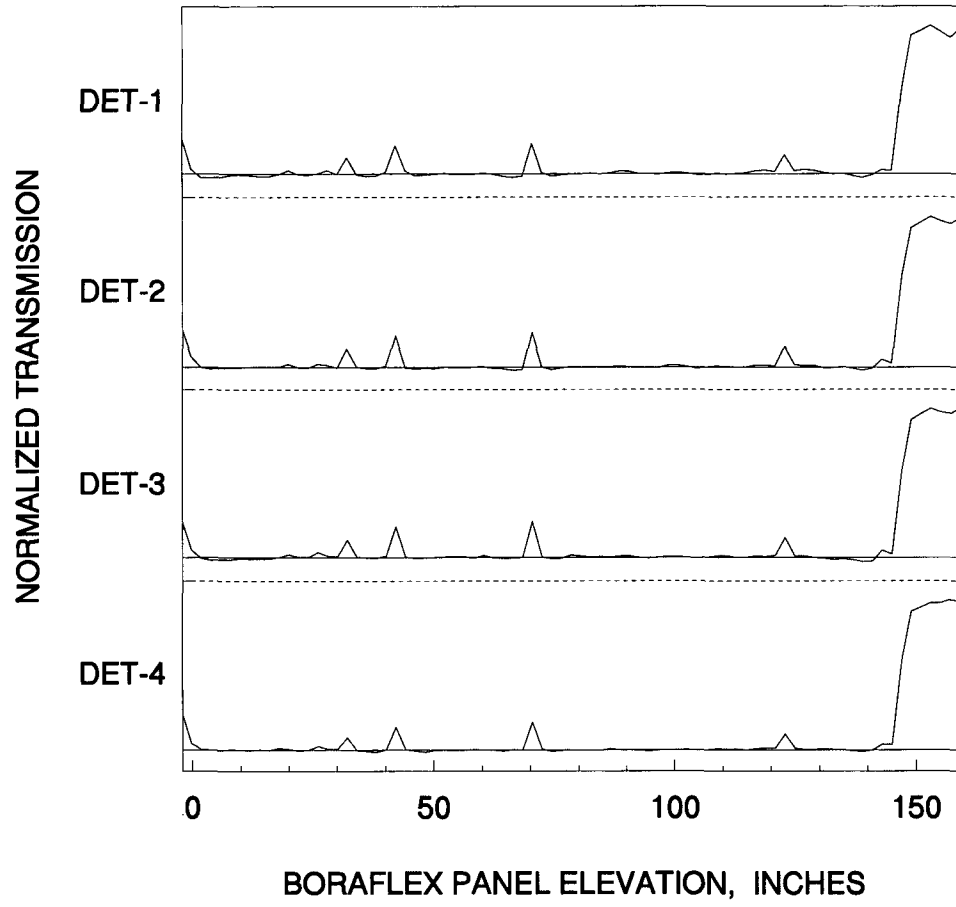
# EE29WS1



FF28SS1

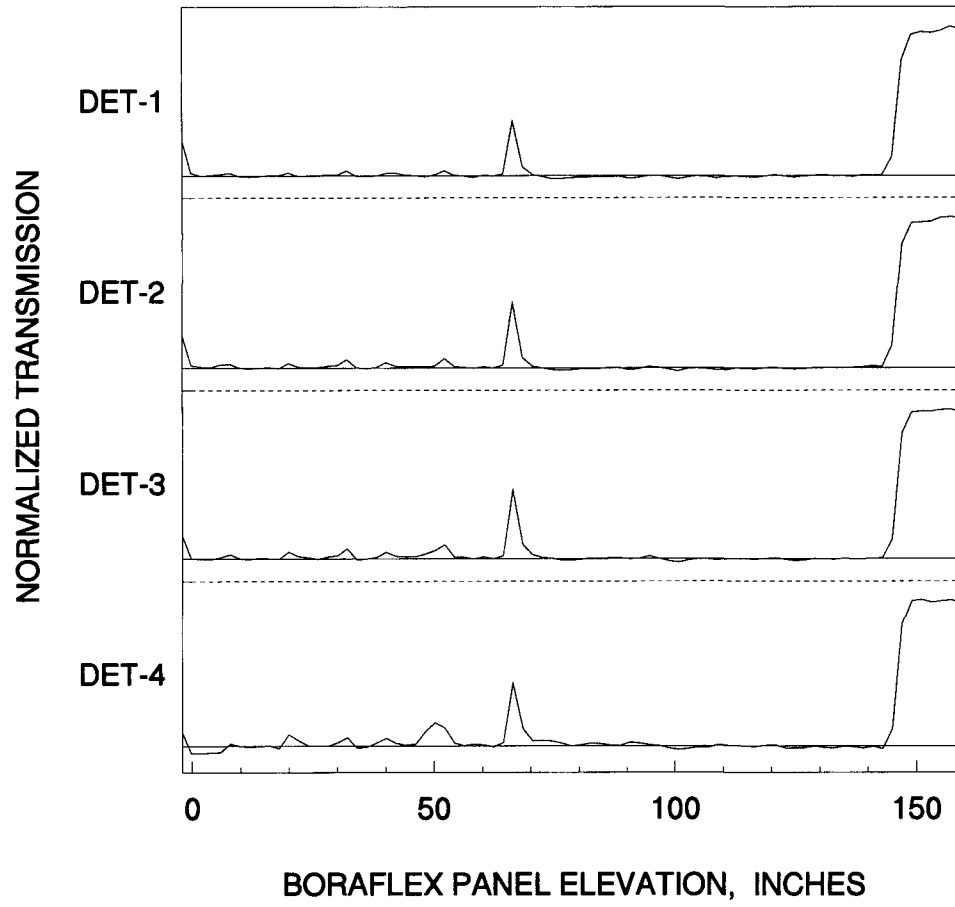


# FF30NS1

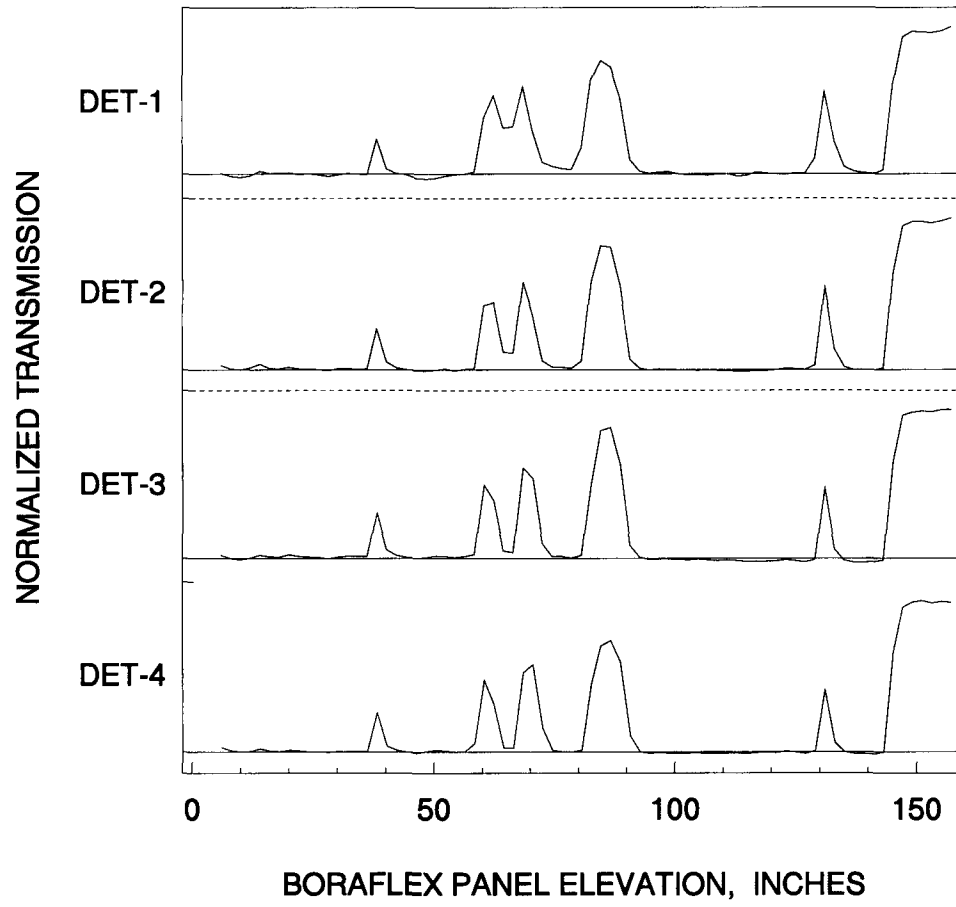




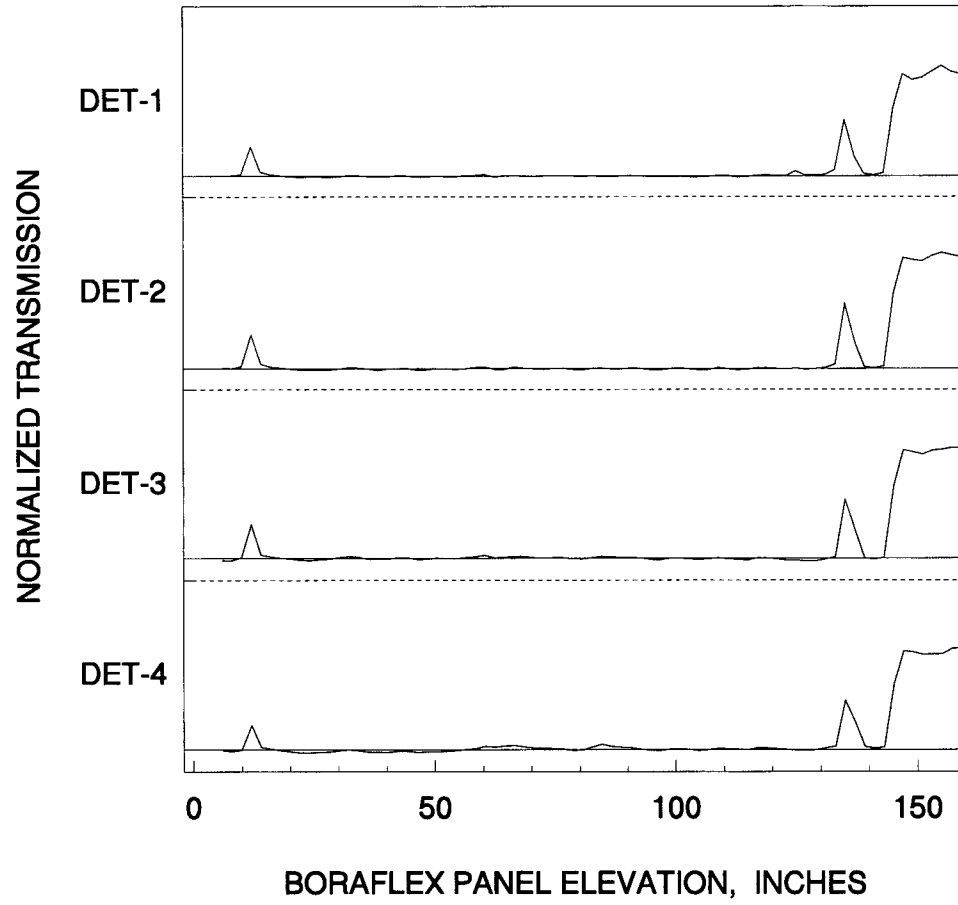
# GG29ES1



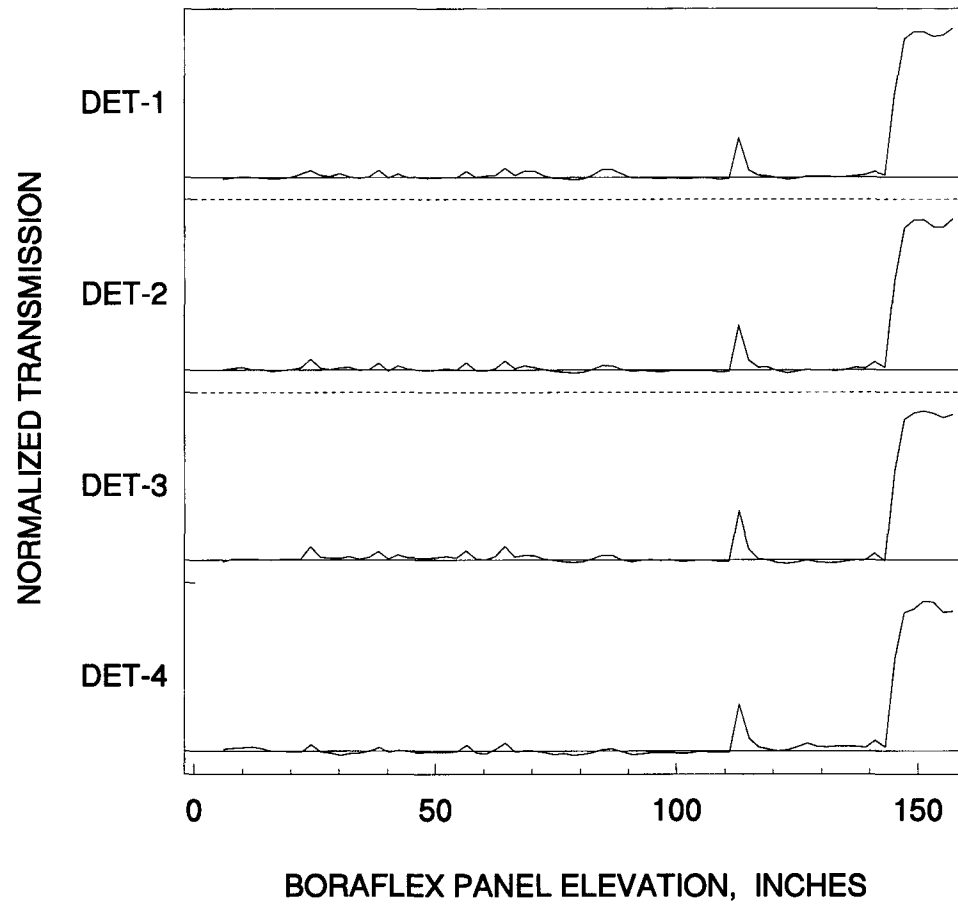
# HH22ES1



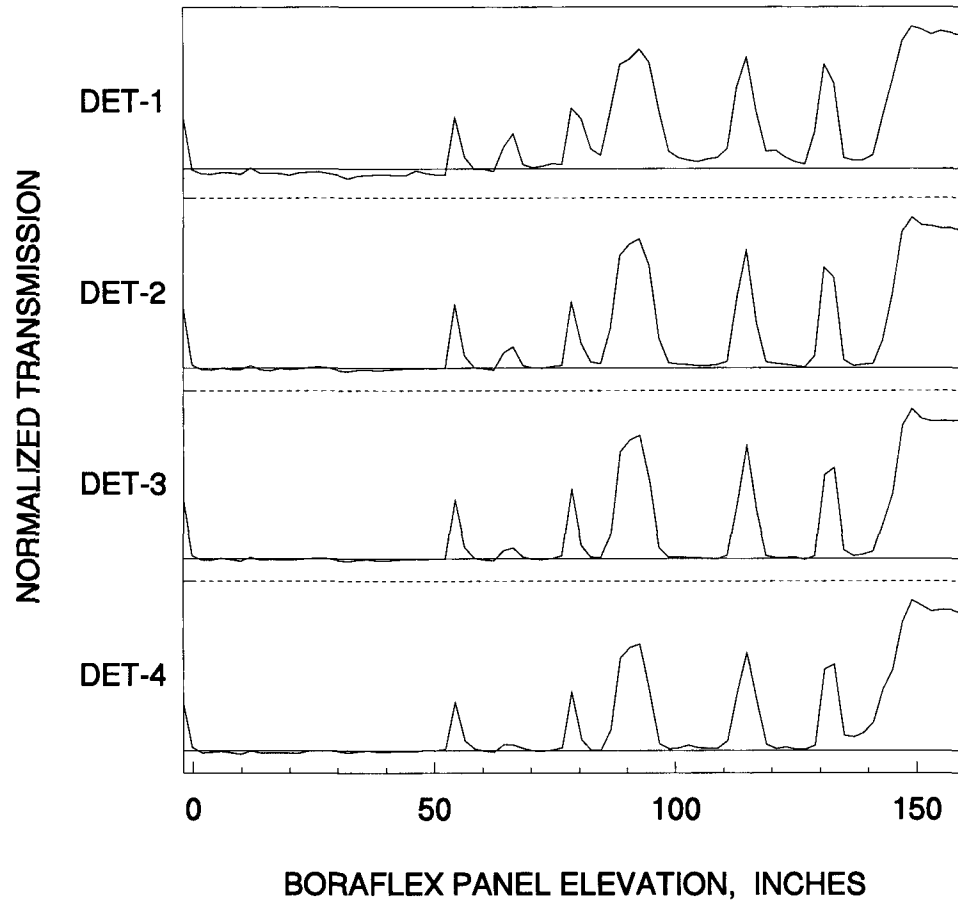
# HH22NS1



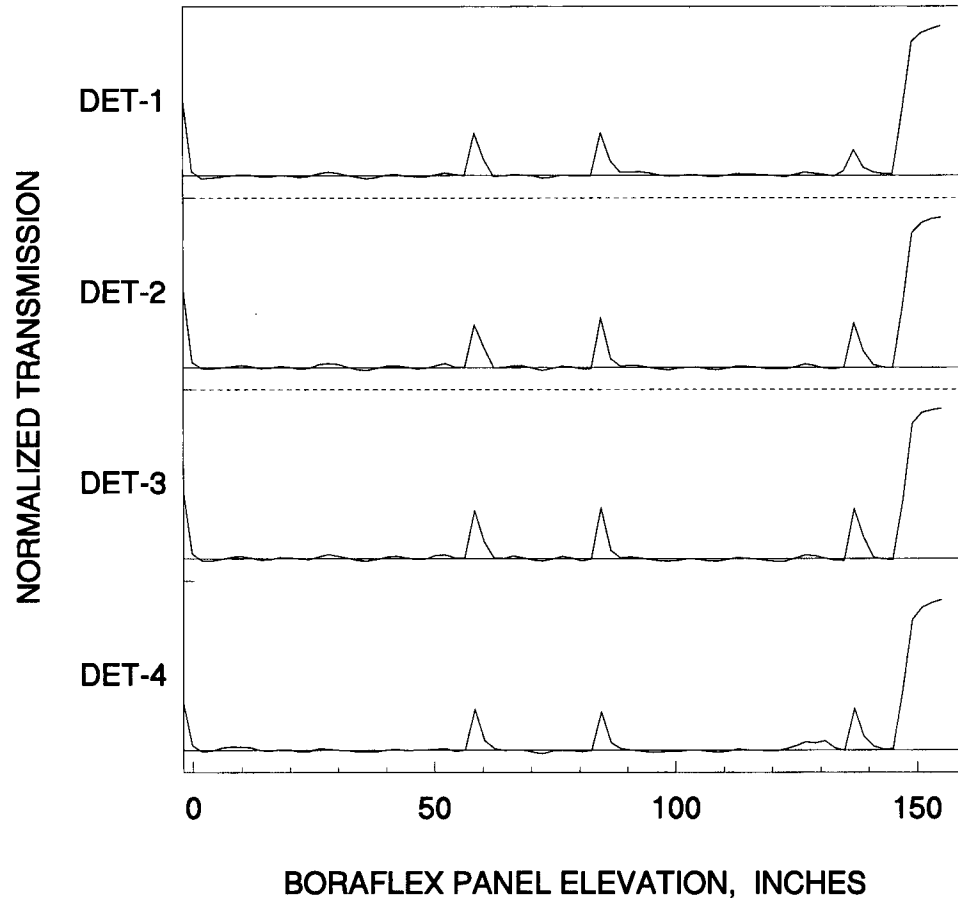
# HH22SS1



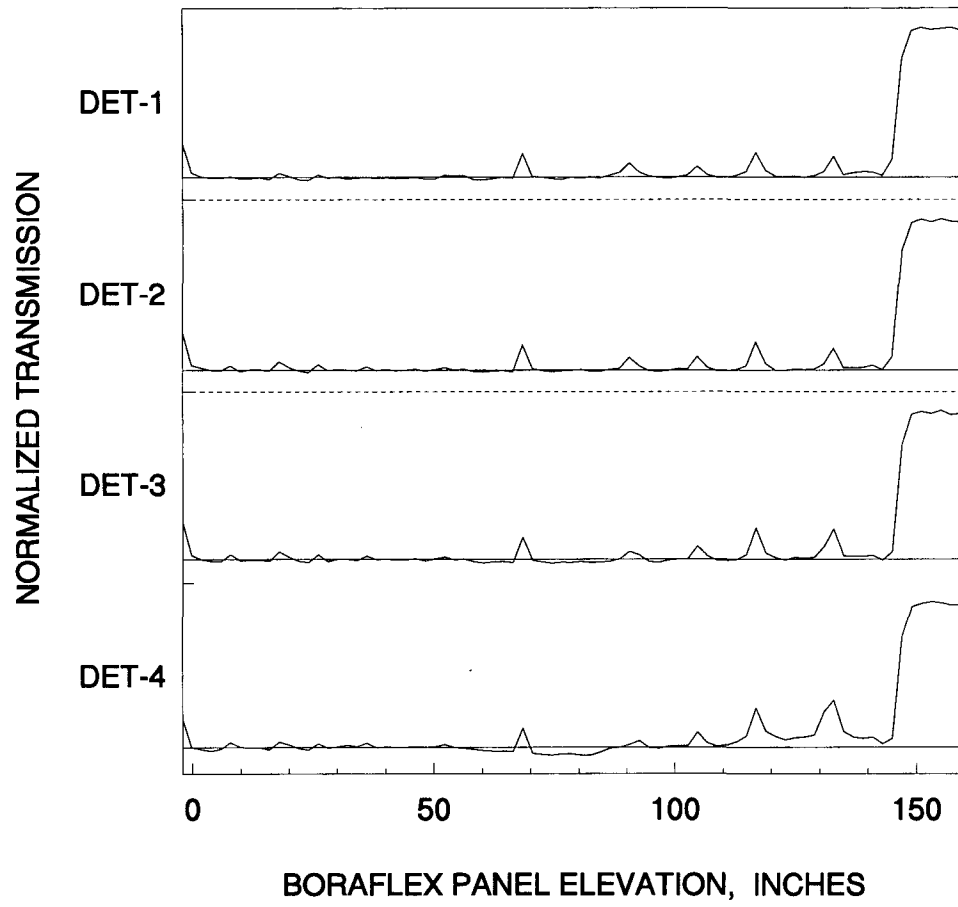
# HH24ES1



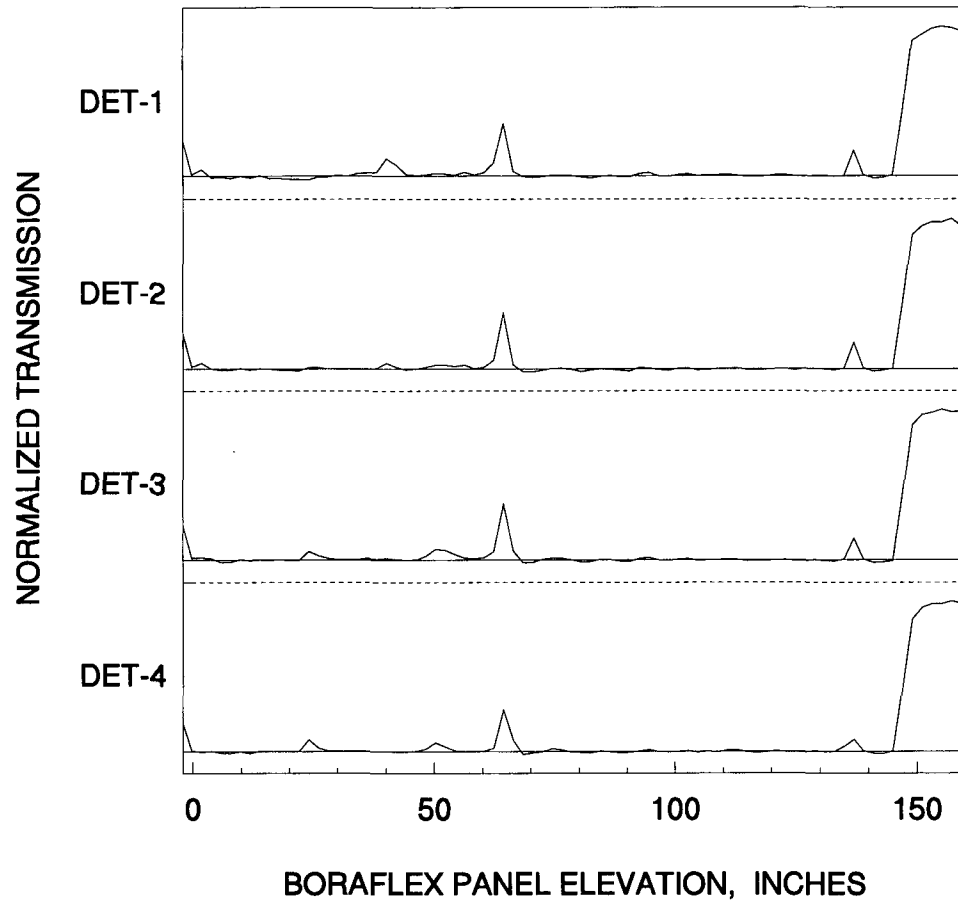
# HH24NS2



# HH24SS1

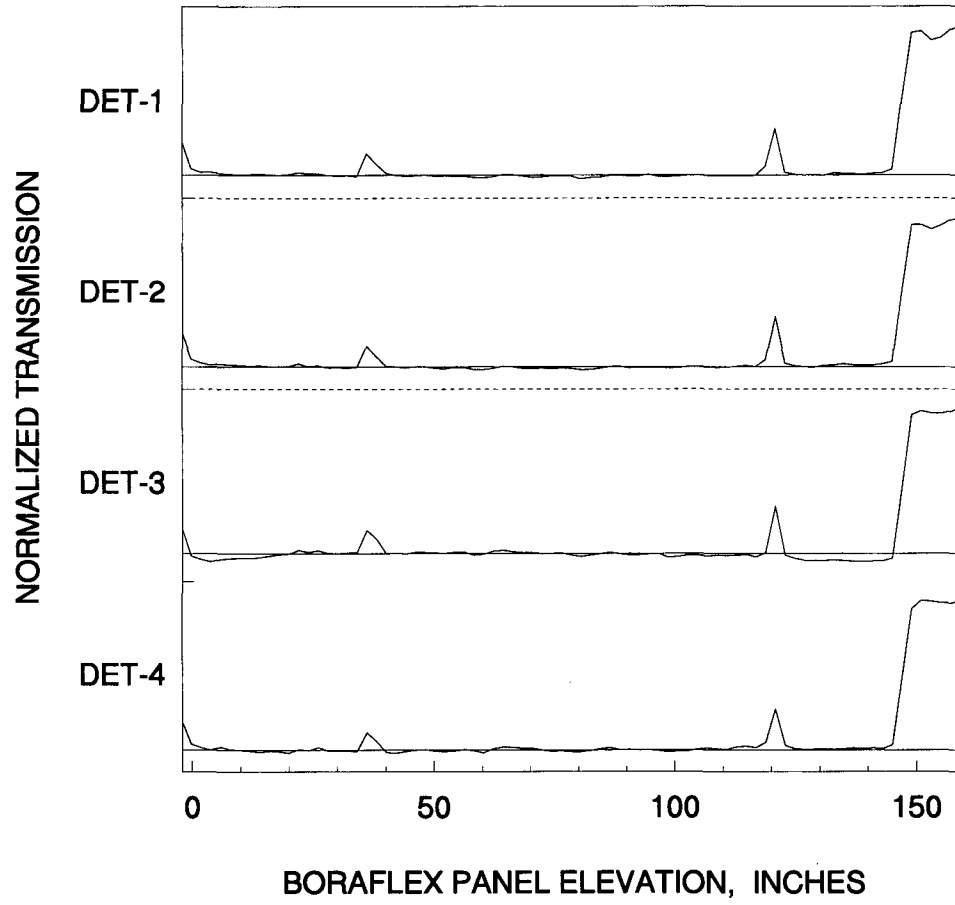


# P7NS1

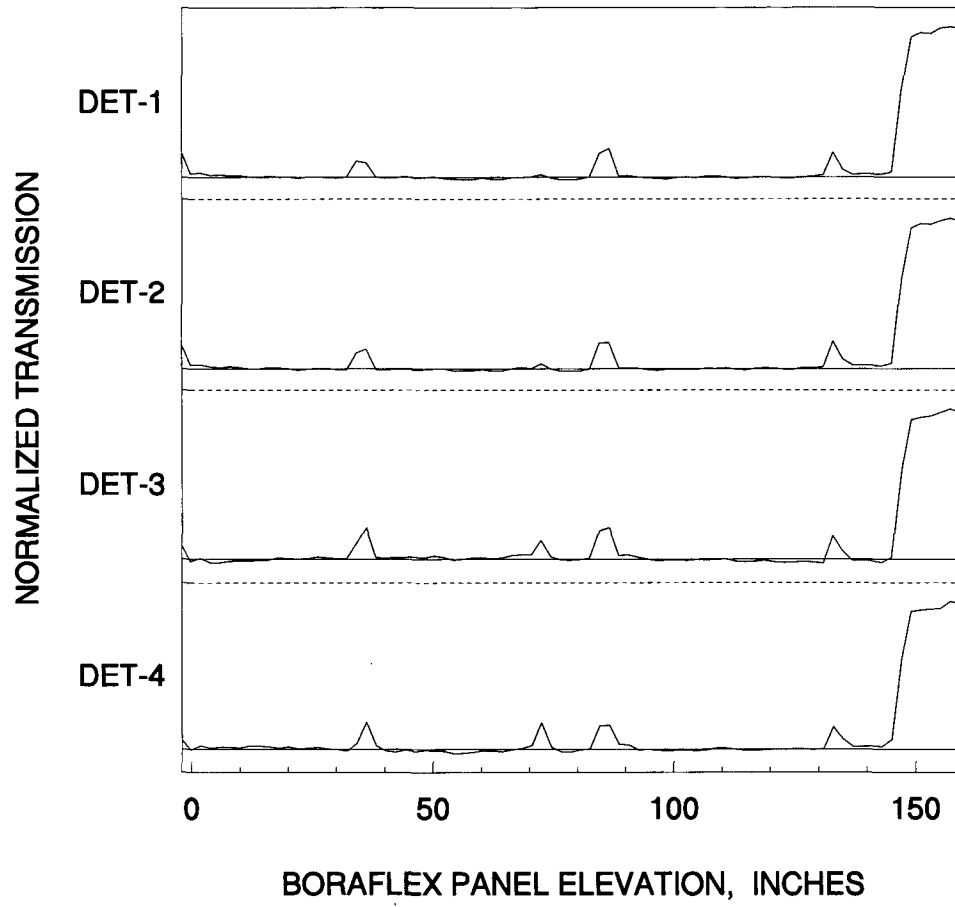




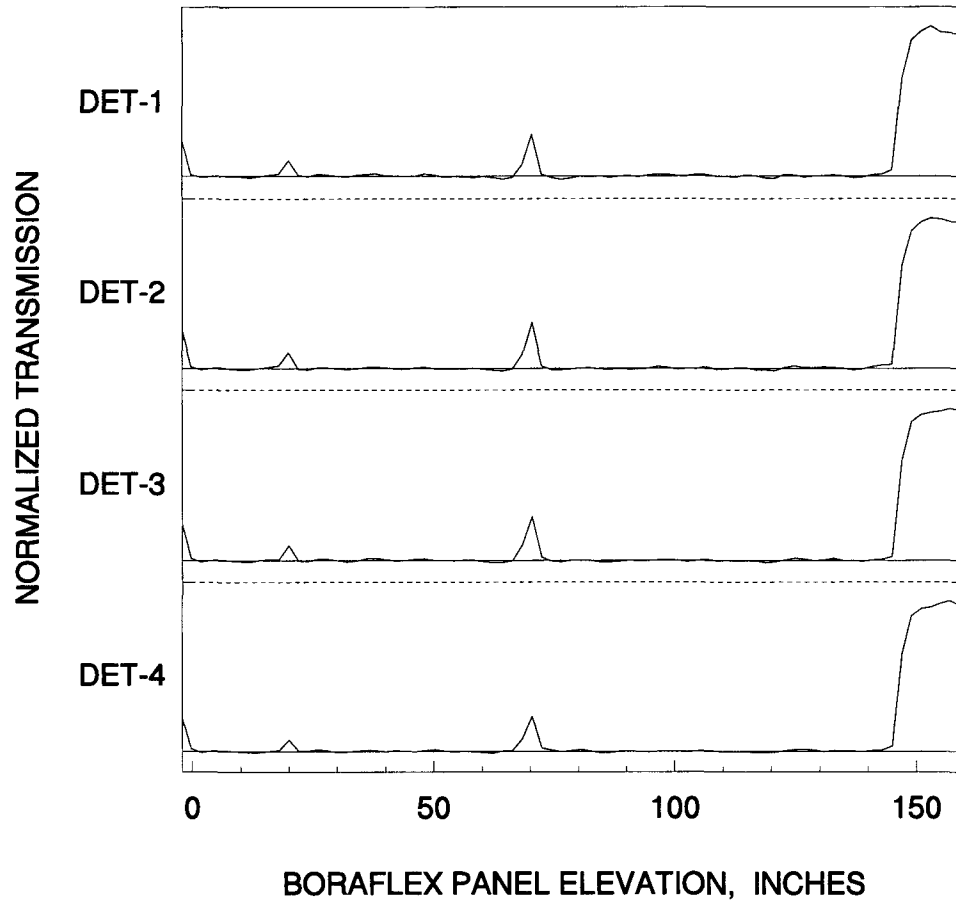
# T13NS1



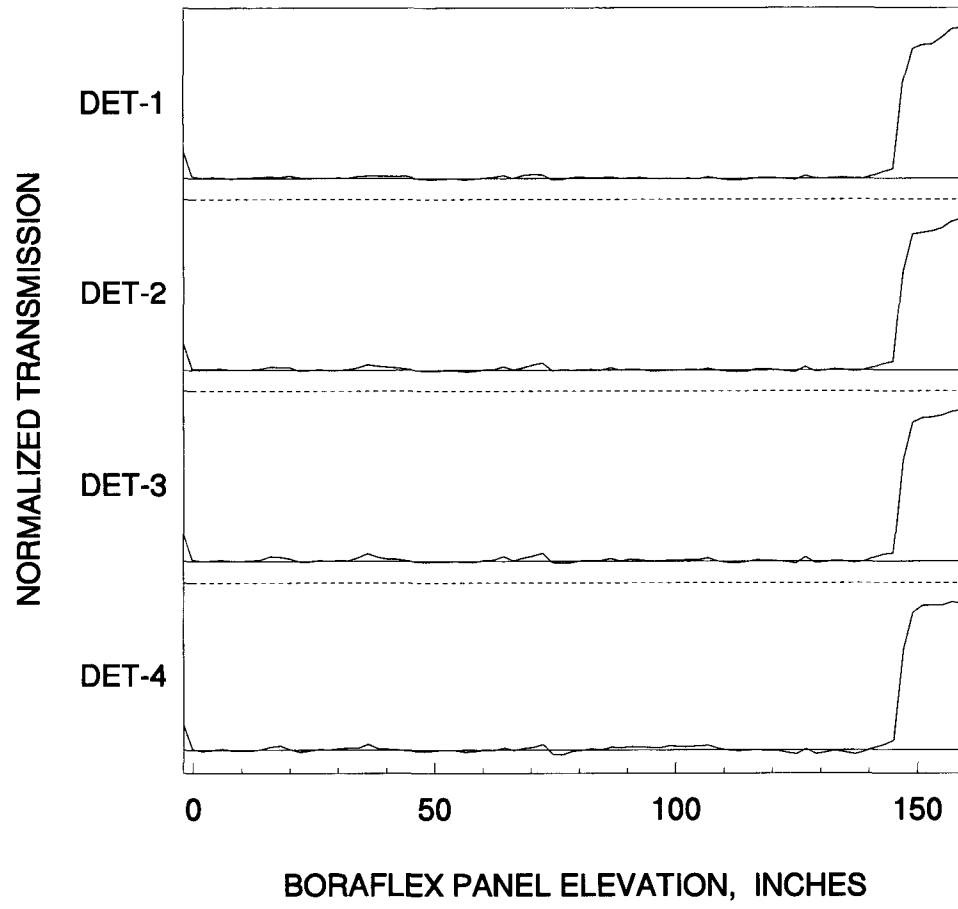
# T13SS1



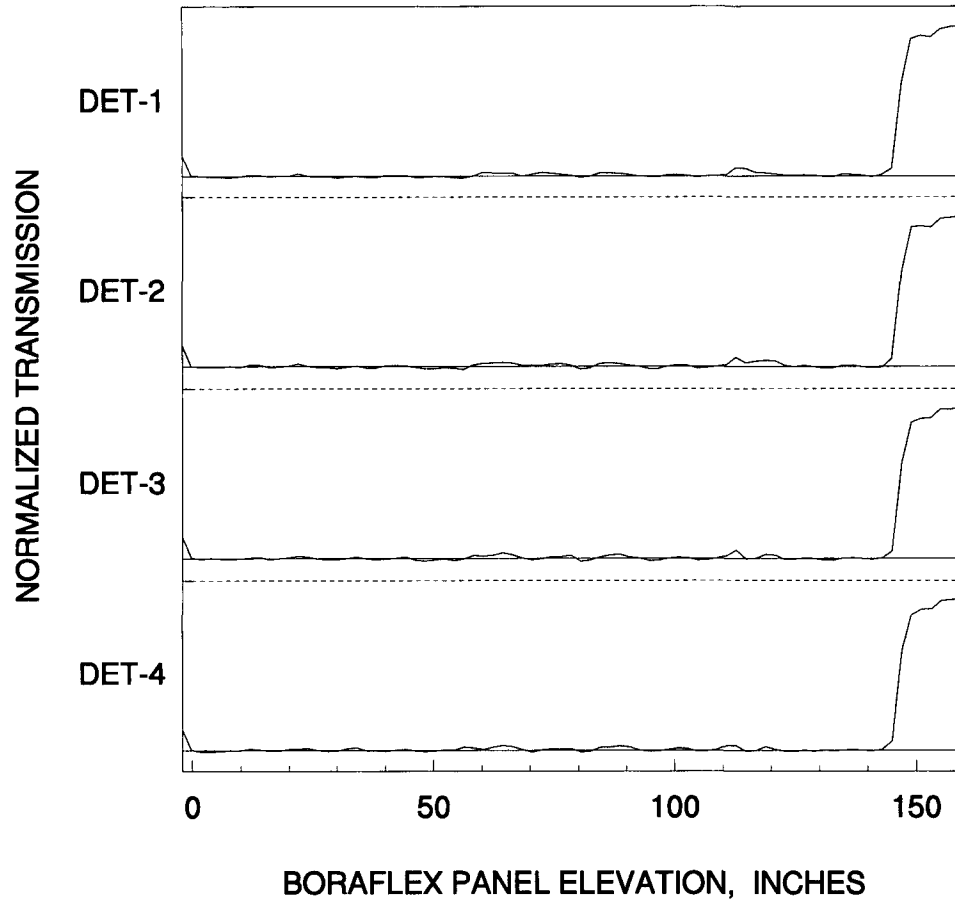
# ZP15WS1



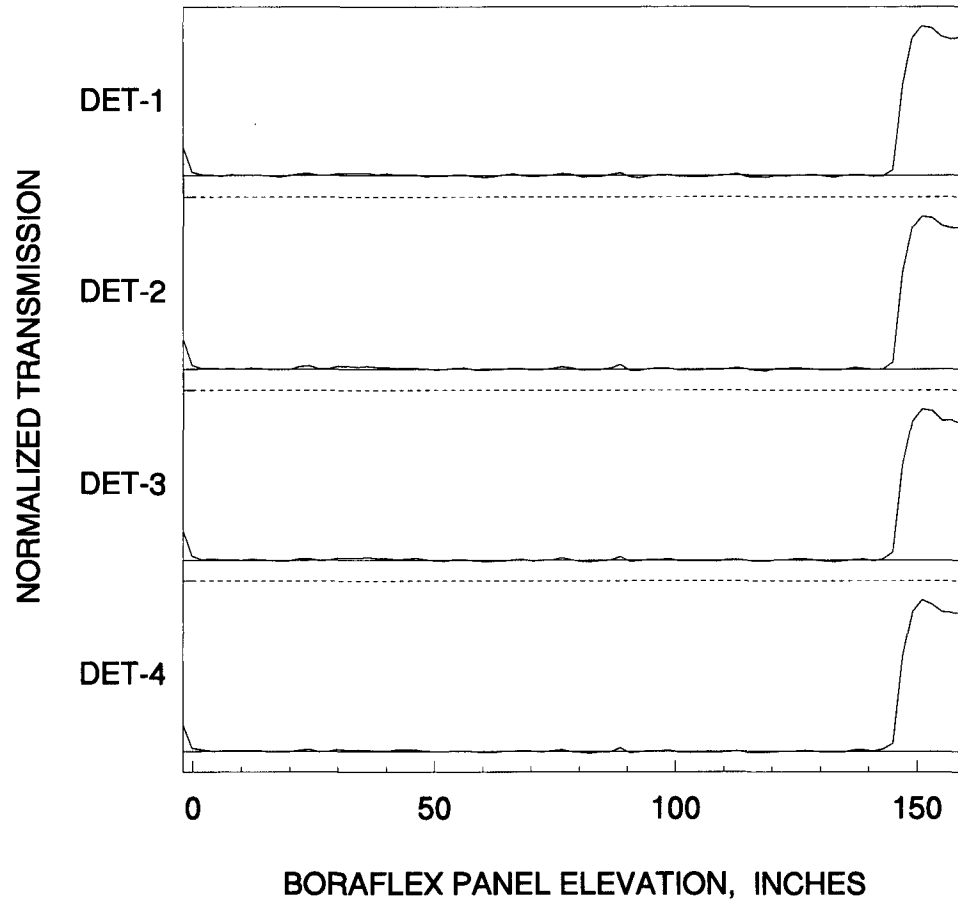
# ZQ14SS1



# ZQ16NS1



# ZR15ES1



## **Appendix B**

[illegible]





	ZQ14SS1.xls	ZQ16NS1.xls	ZR15ES1.xls	ZP15WS1.xls	FF28SS1.xls	DD28SS1.xls	GG29ES1.xls	FF30NS1.xls	EE29WS1.xls	CC29WS1.xls	DD30NS1.xls	EE29ES1.xls
106 inches	Local Dissolution(0)	0(0)	0(0)	0(0)	Local Dissolution(0)	Deposit(0)	0(0)	0(0)	0(0)	0(0)	0(0)	0(0)
107 inches												
108 inches	0(0)	0(0)	0(0)	0(0)	Gap(1.822361)	Local Dissolution(0)	0(0)	0(0)	0(0)	0(0)	0(0)	0(0)
109 inches												
110 inches	0(0)	Local Dissolution(0)	0(0)	0(0)	Local Dissolution(0)	Local Dissolution(0)	0(0)	0(0)	0(0)	0(0)	Gap(0.6399681)	0(0)
111 inches												
112 inches	0(0)	Gap(0.6665019)	0(0)	0(0)	Local Dissolution(0)	Local Dissolution(0)	0(0)	0(0)	0(0)	0(0)	0(0)	0(0)
113 inches												
114 inches	0(0)	Local Dissolution(0)	0(0)	0(0)	Local Dissolution(0)	Local Dissolution(0)	0(0)	0(0)	0(0)	0(0)	0(0)	0(0)
115 inches												
116 inches	0(0)	Local Dissolution(0)	0(0)	0(0)	Local Dissolution(0)	Local Dissolution(0)	0(0)	0(0)	0(0)	0(0)	0(0)	0(0)
117 inches												
118 inches	0(0)	Gap(0.6021392)	0(0)	0(0)	0(0)	Local Dissolution(0)	0(0)	0(0)	0(0)	0(0)	0(0)	0(0)
119 inches												
120 inches	0(0)	Local Dissolution(0)	0(0)	0(0)	0(0)	Local Dissolution(0)	0(0)	0(0)	0(0)	0(0)	0(0)	0(0)
121 inches												
122 inches	0(0)	0(0)	0(0)	0(0)	0(0)	Local Dissolution(0)	0(0)	Gap(0.8970988)	0(0)	0(0)	0(0)	0(0)
123 inches												
124 inches	Deposit(0)	0(0)	0(0)	Local Dissolution(0)	0(0)	Local Dissolution(0)	0(0)		0(0)	0(0)	0(0)	0(0)
125 inches												
126 inches	Local Dissolution(0)	0(0)	0(0)	0(0)	0(0)	Local Dissolution(0)	0(0)	0(0)	0(0)	0(0)	0(0)	0(0)
127 inches												
128 inches	0(0)	0(0)	0(0)	0(0)	Local Dissolution(0)	Local Dissolution(0)	0(0)	0(0)	Gap(1.212839)	0(0)	0(0)	Local Dissolution(0)
129 inches												
130 inches	0(0)	0(0)	0(0)	0(0)	0(0)	Local Dissolution(0)	0(0)	0(0)	Local Dissolution(0)	0(0)	0(0)	Gap(1.427787)
131 inches												
132 inches	0(0)	0(0)	0(0)	0(0)	0(0)	Local Dissolution(0)	0(0)	0(0)	0(0)	0(0)	Gap(0.6680537)	Local Dissolution(0)
133 inches												
134 inches	0(0)	0(0)	0(0)	0(0)	0(0)	Local Dissolution(0)	0(0)	0(0)	0(0)	0(0)	0(0)	0(0)
135 inches												
136 inches	0(0)	0(0)	0(0)	0(0)	0(0)	Local Dissolution(0)	0(0)	0(0)	0(0)	0(0)	0(0)	0(0)
137 inches												
138 inches	0(0)	0(0)	0(0)	0(0)	0(0)	Local Dissolution(0)	0(0)	Deposit(0)	0(0)	0(0)	0(0)	0(0)
139 inches												
140 inches	End Shrinkage(0)	0(0)	0(0)	0(0)	0(0)	Local Dissolution(0)	0(0)	0(0)	0(0)	0(0)	0(0)	0(0)
141 inches												
142 inches	End Transition(0)	0(0)	0(0)	0(0)	0(0)	Local Dissolution(0)	0(0)	Gap(0.6291444)	0(0)	Local Dissolution(0)	0(0)	
143 inches												
144 inches	End Transition(0)	End Transition(0)	End Transition(0)	End Transition(0)	Local Dissolution(0)	End Transition(0)	End Transition(0)	Local Dissolution(0)	End Transition(0)	End Transition(0)	0(0)	Local Dissolution(0)
145 inches												
146 inches	Beyond Panel(0)	Beyond Panel(0)	Beyond Panel(0)	Beyond Panel(0)	Beyond Panel(0)	Beyond Panel(0)	Beyond Panel(0)	Beyond Panel(0)	Beyond Panel(0)	Beyond Panel(0)	0(0)	Beyond Panel(0)
147 inches												
148 inches	Beyond Panel(0)	Beyond Panel(0)	Beyond Panel(0)	Beyond Panel(0)	Beyond Panel(0)	Beyond Panel(0)	Beyond Panel(0)	Beyond Panel(0)	Beyond Panel(0)	Beyond Panel(0)	0(0)	Beyond Panel(0)
149 inches												
150 inches	Beyond Panel(0)	Beyond Panel(0)	Beyond Panel(0)	Beyond Panel(0)	Beyond Panel(0)	Beyond Panel(0)	Beyond Panel(0)	Beyond Panel(0)	Beyond Panel(0)	Beyond Panel(0)	0(0)	Beyond Panel(0)
151 inches												
152 inches	Beyond Panel(0)	Beyond Panel(0)	Beyond Panel(0)	Beyond Panel(0)	Beyond Panel(0)	Beyond Panel(0)	Beyond Panel(0)	Beyond Panel(0)	Beyond Panel(0)	Beyond Panel(0)	0(0)	Beyond Panel(0)
153 inches												
154 inches	Beyond Panel(0)	Beyond Panel(0)	Beyond Panel(0)	Beyond Panel(0)	Beyond Panel(0)	Beyond Panel(0)	Beyond Panel(0)	Beyond Panel(0)	Beyond Panel(0)	Beyond Panel(0)		Beyond Panel(0)
155 inches												
156 inches	Beyond Panel(0)	Beyond Panel(0)	Beyond Panel(0)	Beyond Panel(0)	Beyond Panel(0)	Beyond Panel(0)	Beyond Panel(0)	Beyond Panel(0)	Beyond Panel(0)	Beyond Panel(0)		Beyond Panel(0)
157 inches												
158 inches	Beyond Panel(0)	Beyond Panel(0)	Beyond Panel(0)	Beyond Panel(0)	Beyond Panel(0)	Beyond Panel(0)	Beyond Panel(0)	Beyond Panel(0)	Beyond Panel(0)	Beyond Panel(0)		Beyond Panel(0)
159 inches												
#N/A	#N/A	#N/A	#N/A	#N/A	#N/A	#N/A	#N/A	#N/A	#N/A	#N/A	#N/A	#N/A

File	P7N81.xls	DD28N81.xls	T13881.xls	T13N81.xls	AA128S1.xls	CC278S1.xls	EE27ES1.xls	HH24NS2.xls	DD268S1.xls	HH248S1.xls	HH24ES1.xls	HH22NS1.xls
1 inches	Gap(0.6275532)	0(0)	Local Dissolution(0)	Local Dissolution(0)	0(0)	0(0)	0(0)	0(0)	0(0)	0(0)	End Transition(0)	
2 inches												
3 inches	0(0)	0(0)			Local Dissolution(0)	0(0)	0(0)	0(0)	Deposit(0)	0(0)	0(0)	
4 inches												
5 inches	Deposit(0)	0(0)			Local Dissolution(0)	0(0)	0(0)	0(0)	0(0)	0(0)	0(0)	0(0)
6 inches												
7 inches	Deposit(0)	0(0)	0(0)	0(0)	0(0)	0(0)	0(0)	0(0)	0(0)		0(0)	0(0)
8 inches												
9 inches	0(0)	0(0)	0(0)	0(0)	0(0)	0(0)	Gap(1.047555)	0(0)	Gap(0.6599327)	0(0)	0(0)	Local Dissolution(0)
10 inches												
11 inches	0(0)	0(0)	0(0)	0(0)	0(0)	0(0)	0(0)	0(0)	0(0)	0(0)	0(0)	Gap(1.137466)
12 inches												
13 inches	0(0)	0(0)	0(0)	0(0)	0(0)	0(0)	0(0)	0(0)	0(0)	0(0)	0(0)	0(0)
14 inches												
15 inches	0(0)	0(0)	0(0)	0(0)	0(0)	0(0)	0(0)	0(0)	0(0)	0(0)	0(0)	Local Dissolution(0)
16 inches												
17 inches	0(0)	0(0)	0(0)	0(0)	0(0)	0(0)	Gap(1.136057)	0(0)	Local Dissolution(0)	Gap(0.6357717)	0(0)	0(0)
18 inches												
19 inches	0(0)	0(0)	0(0)	0(0)	0(0)	0(0)	0(0)	0(0)	Gap(0.663238)	0(0)	0(0)	0(0)
20 inches												
21 inches	0(0)	0(0)	0(0)	Local Dissolution(0)	0(0)	0(0)	0(0)	0(0)	0(0)	0(0)	0(0)	0(0)
22 inches												
23 inches	Local Dissolution(0)	0(0)	0(0)	0(0)	0(0)	0(0)	0(0)	0(0)	0(0)	0(0)	0(0)	0(0)
24 inches												
25 inches	Local Dissolution(0)	Gap(0.7062877)	0(0)	0(0)	0(0)	0(0)	Local Dissolution(0)	0(0)	Gap(0.6688465)	0(0)	0(0)	0(0)
26 inches												
27 inches	0(0)	0(0)	0(0)	0(0)	0(0)	0(0)	0(0)	Local Dissolution(0)	0(0)	0(0)	0(0)	0(0)
28 inches												
29 inches	0(0)	0(0)	0(0)	0(0)	0(0)	0(0)	0(0)	0(0)	0(0)	0(0)	0(0)	0(0)
30 inches												
31 inches	0(0)	0(0)	0(0)	0(0)	0(0)	0(0)	0(0)	0(0)	0(0)	0(0)	0(0)	0(0)
32 inches												
33 inches	0(0)	0(0)	0(0)	0(0)	0(0)	0(0)	0(0)	0(0)	0(0)	0(0)	0(0)	0(0)
34 inches												
35 inches	0(0)	0(0)	0(0)	0(0)	0(0)	0(0)	0(0)	0(0)	0(0)	0(0)	0(0)	0(0)
36 inches												
37 inches	0(0)	0(0)	Gap(0.9987267)	Gap(0.9458284)	0(0)	0(0)	0(0)	0(0)	Gap(0.7100115)		0(0)	0(0)
38 inches												
39 inches	0(0)	0(0)	0(0)	0(0)	0(0)	Gap(0.8320309)	0(0)	0(0)	Local Dissolution(0)	0(0)	0(0)	0(0)
40 inches												
41 inches	Gap(0.7389989)	0(0)	0(0)	0(0)	0(0)	0(0)	0(0)	0(0)	0(0)	0(0)	0(0)	0(0)
42 inches												
43 inches	0(0)	0(0)	0(0)	0(0)	0(0)	0(0)	0(0)	0(0)	0(0)	0(0)	0(0)	0(0)
44 inches												
45 inches	0(0)	0(0)	0(0)	0(0)	0(0)	0(0)	Local Dissolution(0)	0(0)	0(0)	0(0)	0(0)	0(0)
46 inches												
47 inches	0(0)	0(0)	0(0)	0(0)	0(0)	0(0)	0(0)	0(0)	0(0)	0(0)	0(0)	0(0)
48 inches												
49 inches	Local Dissolution(0)	0(0)	0(0)	0(0)	0(0)	0(0)	Deposit(0)	0(0)	0(0)	0(0)	0(0)	0(0)

[illegible]

	P7NS1.xls	DD28NS1.xls	T13SS1.xls	T13NS1.xls	AA12SS1.xls	CC27SS1.xls	EE27ES1.xls	HH24NS2.xls	DD26SS1.xls	HH24SS1.xls	HH24ES1.xls	HH22NS1.xls
108 inches	0(0)	0(0)	0(0)	0(0)	0(0)	0(0)	0(0)	0(0)	Gap(0.6725909)		0(0)	0(0)
107 inches												
108 inches	0(0)	0(0)	0(0)	0(0)	0(0)	0(0)	0(0)	0(0)	0(0)	0(0)	0(0)	0(0)
109 inches												
110 inches	0(0)	0(0)	0(0)	0(0)	0(0)	0(0)	0(0)	0(0)	0(0)	0(0)	0(0)	0(0)
111 inches												
112 inches	0(0)	0(0)	0(0)	0(0)	0(0)	Gap(1.378061)	0(0)	0(0)	0(0)	0(0)	Local Dissolution(0)	0(0)
113 inches												
114 inches	0(0)	0(0)	0(0)	0(0)	0(0)	0(0)	0(0)	0(0)	Gap(0.8481258)	Local Dissolution(0)	0(0)	0(0)
115 inches												
116 inches	0(0)	0(0)	0(0)	0(0)	0(0)	0(0)	0(0)	0(0)		Gap(1.137095)	Gap(3.1)	0(0)
117 inches												
118 inches	0(0)	0(0)	0(0)	Local Dissolution(0)	0(0)	0(0)	0(0)	0(0)	0(0)	Gap Transition(0)	0(0)	0(0)
119 inches												
120 inches	0(0)	0(0)	0(0)	Gap(1.492237)	0(0)	0(0)	Local Dissolution(0)	0(0)	0(0)	0(0)	Local Dissolution(0)	0(0)
121 inches												
122 inches	0(0)	0(0)	0(0)	Local Dissolution(0)	0(0)	0(0)	Local Dissolution(0)	0(0)	0(0)	0(0)	0(0)	0(0)
123 inches												
124 inches	0(0)	0(0)	0(0)	0(0)	0(0)	0(0)	0(0)	0(0)	0(0)	0(0)	0(0)	0(0)
125 inches												
126 inches	0(0)	0(0)	0(0)	0(0)	0(0)	0(0)	Local Dissolution(0)	Crack(0)	0(0)	0(0)	0(0)	0(0)
127 inches												
128 inches	0(0)	0(0)	0(0)	0(0)	0(0)	0(0)	Gap(1.977307)	0(0)	0(0)	0(0)	0(0)	0(0)
129 inches												
130 inches	0(0)	0(0)		0(0)	0(0)	0(0)	Local Dissolution(0)	0(0)	0(0)	Gap Transition(0)	Local Dissolution(0)	0(0)
131 inches												
132 inches	0(0)	0(0)	Gap(1.022896)		0(0)	0(0)	0(0)	0(0)	Gap(0.610092)	Gap(1.11659)	Gap(2.872049)	Local Dissolution(0)
133 inches												
134 inches	0(0)	0(0)	Gap Transition(0)		0(0)	0(0)	Local Dissolution(0)	0(0)	0(0)		0(0)	Gap(1.703739)
135 inches												
136 inches	Gap(0.9470838)	0(0)	Local Dissolution(0)	0(0)	0(0)	0(0)	Gap(2.04534)	Gap(1.332045)	0(0)	Local Dissolution(0)	Local Dissolution(0)	0(0)
137 inches												
138 inches	0(0)	0(0)	Local Dissolution(0)	0(0)	0(0)	0(0)	0(0)	0(0)	0(0)	Local Dissolution(0)	0(0)	Local Dissolution(0)
139 inches												
140 inches	Deposit(0)	Beyond Panel(0)	Local Dissolution(0)	0(0)	Local Dissolution(0)	Local Dissolution(0)	Local Dissolution(0)	0(0)	0(0)	Local Dissolution(0)	Local Dissolution(0)	0(0)
141 inches												
142 inches	Deposit(0)	Beyond Panel(0)	Local Dissolution(0)	Local Dissolution(0)	Local Dissolution(0)	0(0)	End Shrinkage(0)	0(0)	0(0)	0(0)	Local Dissolution(0)	Local Dissolution(0)
143 inches												
144 inches	0(0)	Beyond Panel(0)	Beyond Panel(0)	End Transition(0)	End Transition(0)	Local Dissolution(0)	Beyond Panel(0)	0(0)	Beyond Panel(0)	Local Dissolution(0)	End Transition(0)	Beyond Panel(0)
145 inches												
146 inches	Beyond Panel(0)	Beyond Panel(0)	Beyond Panel(0)	Beyond Panel(0)	Beyond Panel(0)	Beyond Panel(0)	Beyond Panel(0)	Beyond Panel(0)	Beyond Panel(0)	Beyond Panel(0)	Beyond Panel(0)	Beyond Panel(0)
147 inches												
148 inches	Beyond Panel(0)	Beyond Panel(0)	Beyond Panel(0)	Beyond Panel(0)	Beyond Panel(0)	Beyond Panel(0)	Beyond Panel(0)	Beyond Panel(0)	Beyond Panel(0)	Beyond Panel(0)	Beyond Panel(0)	Beyond Panel(0)
149 inches												
150 inches	Beyond Panel(0)	Beyond Panel(0)	Beyond Panel(0)	Beyond Panel(0)	Beyond Panel(0)	Beyond Panel(0)	Beyond Panel(0)	Beyond Panel(0)	Beyond Panel(0)	Beyond Panel(0)	Beyond Panel(0)	Beyond Panel(0)
151 inches												
152 inches	Beyond Panel(0)	Beyond Panel(0)	Beyond Panel(0)	Beyond Panel(0)	Beyond Panel(0)	Beyond Panel(0)	Beyond Panel(0)	Beyond Panel(0)	Beyond Panel(0)	Beyond Panel(0)	Beyond Panel(0)	Beyond Panel(0)
153 inches												
154 inches	Beyond Panel(0)	Beyond Panel(0)	Beyond Panel(0)	Beyond Panel(0)	Beyond Panel(0)	Beyond Panel(0)	Beyond Panel(0)	Beyond Panel(0)	Beyond Panel(0)	Beyond Panel(0)	Beyond Panel(0)	Beyond Panel(0)
155 inches												
156 inches	Beyond Panel(0)	Beyond Panel(0)	Beyond Panel(0)	Beyond Panel(0)	Beyond Panel(0)	Beyond Panel(0)	Beyond Panel(0)	Beyond Panel(0)	Beyond Panel(0)	Beyond Panel(0)	Beyond Panel(0)	Beyond Panel(0)
157 inches												
158 inches	Beyond Panel(0)	Beyond Panel(0)	Beyond Panel(0)	Beyond Panel(0)	Beyond Panel(0)	Beyond Panel(0)	Beyond Panel(0)		Beyond Panel(0)	Beyond Panel(0)	Beyond Panel(0)	Beyond Panel(0)
159 inches												
#N/A	#N/A	#N/A	#N/A	#N/A	#N/A	#N/A	#N/A	#N/A	#N/A	#N/A	#N/A	#N/A

File	HH22SS1.xls	HH22ES1.xls	AA27NS1.xls	CC27WS1.xls	AA27WS1.xls	AA27ES1.xls	CC27NS1.xls	CC27ES1.xls
1 inches			0(0)	0(0)	Local Dissolution(0)	0(0)	0(0)	0(0)
2 inches								
3 inches			0(0)	0(0)	Local Dissolution(0)	0(0)	0(0)	0(0)
4 inches								
5 inches			0(0)	0(0)	Local Dissolution(0)	0(0)	0(0)	0(0)
6 inches	0(0)		0(0)	Deposit(0)	Local Dissolution(0)	0(0)	0(0)	0(0)
7 inches								
8 inches	0(0)	0(0)	0(0)	Deposit(0)	0(0)	Deposit(0)	0(0)	0(0)
9 inches								
10 inches	0(0)	0(0)	0(0)	0(0)	0(0)	0(0)	0(0)	0(0)
11 inches								
12 inches	0(0)	0(0)	0(0)	Crack(0)	0(0)	0(0)	0(0)	0(0)
13 inches								
14 inches	0(0)	Gap(0.5784192)	0(0)	0(0)	0(0)	0(0)	0(0)	0(0)
15 inches								
16 inches	0(0)	0(0)	0(0)	0(0)	0(0)	0(0)	0(0)	0(0)
17 inches								
18 inches	0(0)	0(0)	0(0)	0(0)	0(0)	Crack(0)	0(0)	0(0)
19 inches								
20 inches	0(0)	0(0)	Local Dissolution(0)	0(0)	0(0)	Local Dissolution(0)	0(0)	0(0)
21 inches								
22 inches	0(0)	0(0)	0(0)	0(0)	0(0)	0(0)	Crack(0)	0(0)
23 inches								
24 inches	Crack(0)	0(0)	0(0)	0(0)	0(0)	0(0)	0(0)	0(0)
25 inches								
26 inches	0(0)	0(0)	0(0)	0(0)	0(0)	0(0)	0(0)	0(0)
27 inches								
28 inches	0(0)	0(0)	0(0)	0(0)	0(0)	0(0)	0(0)	0(0)
29 inches								
30 inches	0(0)	0(0)	0(0)	0(0)	0(0)	0(0)	0(0)	0(0)
31 inches								
32 inches	0(0)	0(0)	0(0)	0(0)	0(0)	0(0)	0(0)	0(0)
33 inches								
34 inches	0(0)	0(0)	0(0)	0(0)	0(0)	0(0)	Crack(0)	0(0)
35 inches								
36 inches	0(0)	0(0)	0(0)	0(0)	0(0)	0(0)	0(0)	0(0)
37 inches								
38 inches	Crack(0)	Gap(1.331661)	0(0)	Gap(1.769279)	0(0)	0(0)	0(0)	0(0)
39 inches								
40 inches	0(0)	0(0)	0(0)	Local Dissolution(0)	0(0)	0(0)	0(0)	0(0)
41 inches								
42 inches	Crack(0)	0(0)	0(0)	0(0)	Gap(3.1)	0(0)	Gap(1.207938)	0(0)
43 inches								
44 inches	0(0)	0(0)	Gap(1.348176)	0(0)	Gap Transition(0)	0(0)	0(0)	0(0)
45 inches								
46 inches	0(0)	0(0)	0(0)	0(0)	0(0)	0(0)	0(0)	0(0)
47 inches								
48 inches	0(0)	0(0)	0(0)	0(0)	0(0)	0(0)	0(0)	0(0)
49 inches								

File	HH22S1.xls	HH22ES1.xls	AA27NS1.xls	CC27WS1.xls	AA27WS1.xls	AA27ES1.xls	CC27NS1.xls	CC27ES1.xls
50 inches	0(0)	0(0)	0(0)	0(0)	0(0)	0(0)	0(0)	0(0)
51 inches								
52 inches	0(0)	0(0)	0(0)	0(0)	0(0)	0(0)	0(0)	0(0)
53 inches								
54 inches	0(0)	0(0)	0(0)	0(0)	0(0)	0(0)	0(0)	0(0)
55 inches								
56 inches	Crack(0)	0(0)	0(0)	Local Dissolution(0)	0(0)	0(0)	0(0)	0(0)
57 inches								
58 inches	0(0)	0(0)	0(0)	Local Dissolution(0)	0(0)	0(0)	0(0)	0(0)
59 inches								
60 inches	0(0)	Gap(1.883188)	0(0)	Local Dissolution(0)	0(0)	0(0)	0(0)	0(0)
61 inches								
62 inches	0(0)	0(0)	0(0)	Gap Transition(0)	0(0)	0(0)	0(0)	Gap(1.516175)
63 inches								
64 inches	Crack(0)	Local Dissolution(0)	0(0)	Gap(2.470895)	Local Dissolution(0)	Local Dissolution(0)	Gap(1.039085)	Local Dissolution(0)
65 inches								
66 inches	0(0)	Local Dissolution(0)	0(0)	Local Dissolution(0)	Gap(1.240775)	0(0)	0(0)	0(0)
67 inches								
68 inches	Crack(0)	Gap(2.454301)	0(0)	Local Dissolution(0)	0(0)	0(0)	0(0)	0(0)
69 inches								
70 inches			0(0)	Local Dissolution(0)	0(0)	0(0)	0(0)	0(0)
71 inches								
72 inches	0(0)	Gap Transition(0)	0(0)	0(0)	Gap(0.75)	0(0)	0(0)	0(0)
73 inches								
74 inches	0(0)	Local Dissolution(0)	0(0)	0(0)	Local Dissolution(0)	0(0)	0(0)	0(0)
75 inches								
76 inches	0(0)	Local Dissolution(0)	0(0)	0(0)	0(0)	Local Dissolution(0)	0(0)	0(0)
77 inches								
78 inches	0(0)	0(0)	0(0)	Local Dissolution(0)	0(0)	0(0)	0(0)	Gap(1.560965)
79 inches								
80 inches	0(0)	Local Dissolution(0)	0(0)	Gap(2.640054)	0(0)	0(0)	0(0)	Local Dissolution(0)
81 inches								
82 inches	0(0)	0(0)	0(0)	0(0)	0(0)	0(0)	Gap(1.428534)	0(0)
83 inches								
84 inches	Crack(0)	0(0)	0(0)	Local Dissolution(0)	0(0)	Local Dissolution(0)	Local Dissolution(0)	Local Dissolution(0)
85 inches								
86 inches	Crack(0)	Gap(8.66)	0(0)	Local Dissolution(0)	0(0)	Gap(2.019037)	0(0)	0(0)
87 inches								
88 inches	0(0)	0(0)	0(0)	0(0)	0(0)	Gap Transition(0)	0(0)	Gap(3.840339)
89 inches								
90 inches	0(0)	0(0)	0(0)	Gap(0.6752482)	0(0)	Local Dissolution(0)	0(0)	Local Dissolution(0)
91 inches								
92 inches	0(0)	0(0)	0(0)	0(0)	0(0)	0(0)	0(0)	Local Dissolution(0)
93 inches								
94 inches	0(0)	0(0)	0(0)	0(0)	0(0)	0(0)	0(0)	0(0)
95 inches								
96 inches	0(0)	0(0)	0(0)	0(0)	0(0)	0(0)	0(0)	Gap(3.148992)
97 inches								
98 inches	0(0)	0(0)	0(0)	0(0)	0(0)	0(0)	0(0)	Local Dissolution(0)
99 inches								
100 inches	0(0)	0(0)	0(0)	0(0)	0(0)	0(0)	0(0)	0(0)
101 inches								
102 inches	0(0)	0(0)	0(0)	0(0)	0(0)	0(0)	0(0)	0(0)
103 inches								
104 inches	0(0)	0(0)	0(0)	0(0)	0(0)	0(0)	0(0)	0(0)
105 inches								

[illegible]



**Enclosure 2 to**

**Attachment 1**

**GNRO-2011/00025**

**Grand Gulf Nuclear Station Extended Power Uprate**

**Response to Request for Additional Information**

**Reactor Systems Branch**

**Excerpts from the Blackness Testing of Boraflex in Selected  
Spent Fuel Storage Rack Cells  
(Seventh Measurement Campaign)**

**BLACKNESS TESTING OF BORAFLEX  
IN SELECTED SPENT FUEL STORAGE RACK CELLS  
OF THE GRAND GULF NUCLEAR STATION  
SEVENTH MEASUREMENT CAMPAIGN**

**HOLTEC REPORT HI-992255  
HOLTEC PROJECT 81055  
DISTRIBUTION: C, F**

**Prepared for  
ENERGY OPERATIONS, INC.**

REVISION BLOCK				
REVISION NUMBER	AUTHOR & DATE	REVIEWER & DATE	QA & DATE	APPROVED & DATE
ORIGINAL	W. MITCHELL <i>W. Mitchell</i> 6/23/99	S. TURNER <i>S. Turner</i> 6/23/99	V. GUPTA <i>V. Gupta</i> 7-1-99	M. MURPHY <i>M. Murphy</i> 7-1-99 <i>For STN</i>
REVISION 1				
REVISION 2				

## TABLE OF CONTENTS

		<u>PAGE</u>
1.0	INTRODUCTION . . . . .	1
2.0	RESULTS AND CONCLUSIONS . . . . .	4
3.0	EQUIPMENT DESCRIPTION . . . . .	8
4.0	OPERATING PROCEDURES AND QUALITY ASSURANCE . . . . .	9

## LIST OF TABLES

Table 1	SEVENTH-CAMPAIGN DATA AND COMPARISON WITH PREVIOUS CAMPAIGN RESULTS
Table 2	COMPARISON OF GAP SIZES FOR SEVEN CAMPAIGNS
Table 3	COMPARISON OF GAP LOCATIONS FOR SEVEN CAMPAIGNS

## LIST OF FIGURES

Fig. 1	A portion of the chart traces for cell HH24
Fig. 2	Correlation curve for gap size
Fig. 3	Number of gaps found in each of the six campaigns
Fig. 4	Number of gaps found as a function of time
Fig. 5	Average gap size for each of the six campaigns
Fig. 6	Maximum gap size for each of the six campaigns
Fig. 7	Distribution of gaps within specific size ranges
Fig. 8	Axial distribution of gap locations in Campaign 7

## 1.0 INTRODUCTION

The seventh campaign of blackness (neutron absorption) testing was performed in selected cells of the Grand Gulf spent fuel storage rack on March 24-27, 1999. The testing was carried out for the purpose of revealing any changes in the number and sizes of gaps observed in the following, earlier campaigns:

- The first campaign (August 1988);
- the second campaign (April 1990);
- the third campaign (September 1991);
- the fourth campaign (May 1993);
- the fifth campaign (December 1994); and
- the sixth campaign (May 1996).

As in the previous campaigns, the seventh campaign used a specially-designed logging tool containing a Californium-252 neutron source and four boron trifluoride (BF<sub>3</sub>) thermal neutron detectors.

The Grand Gulf storage pool contains storage racks with Boraflex panels of 0.0208 g B-10/cm<sup>2</sup> areal density between each storage cell. The cells have an inside diameter of 6.06 inches and a lattice spacing of 6.259 inches, and the Boraflex panels are sandwiched between the stainless steel walls of adjacent cells. Consequently, the Boraflex is mechanically restrained and some random gaps would be expected to form as the Boraflex shrinks under irradiation.

Blackness testing is an adaptation of well-established neutron logging techniques used extensively in the oil industry over the past few decades. For blackness testing, a logging tool containing the neutron source and the four thermal neutron detectors is lowered into the storage pool and vertically traverses a designated storage cell. Fast neutrons from the Californium source pass through the walls of the cell, become thermalized (moderated) in the water of adjacent cells and diffuse (scatter) back toward the logging tool. These back-scattered thermal neutrons are absorbed in areas of the rack walls where the Boraflex absorber material is present and intact. However, in areas where the Boraflex is missing or significantly degraded, the thermal neutrons will pass

through and register as an increase in counting rate by the detectors inside the logging tool. Increases in thermal neutron counting rates are interpreted as indicators of missing Boraflex in the storage cell being tested, while low counting rates confirm that the Boraflex is intact.

In making the tests, a logging speed of approximately 1 ft/min is used: the outputs from the four counting channels, one associated with each wall of the cell, are recorded using a multi-channel strip chart recorder. Each strip chart recording is examined to determine gap sizes and axial locations, and a correlation curve is used to relate trace deflections (peaks) to gap size. Measurement accuracy for the width of a gap in the Boraflex absorber is estimated to be  $\pm 20\%$ . Gaps of 1/2 inch are considered to represent the lower limit of reliable detection, although indications of smaller gaps are recognizable in the recorder charts. Because of the small amplitude of the signals, these deflections are not reliable indicators of gaps; however, they have the characteristic shape corresponding to a gap and are considered evidence that a small gap probably exists.

The axial location of a gap is determined from the position of the peak counting rate on the strip chart record and the known logging speed of the test tool. Comparisons of gap positions measured in the seven campaigns, and in replicate runs, generally show an expected uncertainty in axial position of a few inches. Differences in location of several inches occur in a very limited number of instances. The frequency of this occurrence is too low to permit definitive statements or conclusions regarding location accuracy.

In the seventh campaign, the "standard" 52 cells (208 Boraflex panels) were tested, with second, confirming runs made in five of the 52. The confirming runs were made with tool orientations different from those used in the initial runs. The 52 cells had previously held spent fuel and therefore had been subjected to radiation. (An early check run was made in a cell that had not contained fuel. As expected, the cell had no gaps in any side; it will not be included in the data and discussion that follow.) All but one of the "standard" 52 cells tested had gaps in at least three sides, with more than half of the cells showing gaps in all four sides.

In addition to the tests of the "standard" 52 cells, runs were made in a specially-fabricated test cell containing a broad range of gaps of known sizes. The purpose of these runs was to develop a Grand-Gulf-specific correlation between percent deflection and gap size. The generic correlation used earlier did not extend to the

high deflections encountered in recent Grand Gulf tests, so it had been necessary to extrapolate the correlation. This was done very conservatively to insure that the sizes of the larger gaps were over-estimated. Data taken in the test cell were used to check the accuracy of the generic correlation for smaller deflections/gaps and to develop relationships applicable to the very large deflections encountered in the recent Grand Gulf tests. The correlation developed in Campaign 7 with the test cell was compared to the generic correlation used earlier. The comparison showed there is acceptable agreement between the old correlation and the new up to gap sizes of 3.0 inches. Above that size, the old, generic correlation over-predicted the size of the gap; this was conservative, as intended. With the newly-developed, plant-specific correlation, that conservatism/over-estimation is not necessary. Consequently, all gaps larger than 3.0 inches shown previously for Campaigns 4, 5, and 6 were re-evaluated using the new correlation. This resulted in reductions in the sizes of the gaps. The reduced sizes are given here.

In this report, the text is followed by the numbered tables, which in turn are followed by the illustrations.

## 2.0 RESULTS AND CONCLUSIONS

The seventh campaign of testing in the Grand Gulf spent fuel racks included a total of 52 cells, all of which had been used to store spent fuel. Five cells were re-tested to verify results. In the 208 full length Boraflex panels tested, there were 362 gaps 0.5-inch in size or larger. In addition, there were numerous chart peaks that are thought to indicate gaps smaller than the 0.5-inch lower limit of reliable detection.<sup>1</sup>

A portion of the chart for cell HH24 is reproduced here as Fig. 1. In the illustration, the large peak represents the largest gap found in Campaign 7; this gap is in the Boraflex of the east side of the cell and is estimated to be 6.0 inches in size. The smaller peaks in the traces are for a 1.2-inch gap in the north Boraflex, an 0.5-inch gap in the south, and an 0.7-inch gap in the west. There is also an indication of another gap (smaller than 0.5-inch) in the trace for the north side. There are 15 gaps greater than 0.5-inch in cell HH24. As is the case in the other strip chart recordings, the shapes of the peaks are well defined; this indicates clean breaks with no significant edge erosion.

The correlation curve used to determine gap sizes in this campaign and to correct gaps shown as 3.1 inches and larger in Campaigns 4, 5, and 6 is given as Fig. 2. As stated in the *last* report, for Campaign 6, "...the large gaps are very likely smaller than reported here." The over-estimation has been removed from the values reported here.

Nearly 90% of the panels tested contained gaps, a figure that continues the steady increase in percentage of affected panels found since the first campaign. It follows that the number of gaps also increases, and the totals found in the seven campaigns are shown in the illustration given as Fig. 3. That chart shows a dramatic increase in the number of new gaps discovered in Campaign 7, reversing the earlier trend of decreases in the rate of increase in number of total gaps from campaign to campaign. Since the time periods between campaigns have not been the same length, the total-gaps data were plotted as a function of time after the first campaign to

---

<sup>1</sup> In early, past reports, some gaps smaller than 0.5 inch, and "suspect" gaps, were included in tabulations and in the count of total gaps. Due to the large number of small-gap indications in this and recent campaigns, the increasing size and number of gaps in the size range of reliable detection, and the desire to focus on these more significant gaps, this report deals only with gaps whose size is 0.5 inch or larger. Listings here of gaps found in past campaigns are consistent with this convention.

confirm, as indicated in Fig. 3, the apparent increase in the rate of gap generation between the sixth and seventh campaigns. Figure 4 shows the total number of gaps found in each campaign versus the time line extending from Campaign 1 to Campaign 7. This illustration confirms that Campaign 7 reveals a significant, recent increase in the rate of gap generation. The reason or reasons for this increase are not known.

The average gap size resumes its tendency to increase with time, as shown in Fig. 5, which gives the average gap size for each of the campaigns. As the illustration shows, the average gap size had remained constant at 1.3 inches for Campaigns 4, 5, and 6, but now shows an increase to 1.4 inches for Campaign 7.

The *maximum* gap size continues to increase with time, as Fig. 6 shows. In addition to the increase in the size of the largest gap, there has been a substantial increase in the total width of all gaps found in a given Boraflex panel. The Campaign 6 report contained a table that listed Boraflex panels having gaps whose total width was greater than 5.5 inches (based on the old, generic correlation curve). That table, as modified by the use of the new correlation and the addition of the Campaign 7 results, is given below.

<u>CELL</u>	<u>SIDE</u>	<u>TOTAL WIDTH OF GAPS, IN.</u>		<u>TOTAL NO. OF GAPS</u>	
		<u>CAMP. 6</u>	<u>CAMP. 7</u>	<u>CAMP. 6</u>	<u>CAMP. 7</u>
Y21	E	6.5	9.2	3	4
W21	N	5.6	7.8	5	5
V24	S	5.6	9.8	3	4
HH24	E	6.1	10.1	2	3
CC27	E	8.0	13.5	4	6

In addition to the panels listed in the Campaign 6 report as containing gaps totaling more than 5.5 inches, Campaign 7 revealed additional panels that exceed that arbitrary total width. These panels are shown in the table given on the following page.



<u>CELL</u>	<u>SIDE</u>	<u>TOTAL WIDTH OF GAPS, IN.</u>	<u>TOTAL NO. OF GAPS</u>
EE21	E	5.6	3
AA25	E	5.8	5
Y27	E	6.0	3
W21	E	6.7	5
CC27	W	6.7	3
DD20	S	6.8	5
DD22	E	6.8	3
V26	S	7.2	3
HH22	E	11.3	5

A panel does not have to contain one of the largest gaps to have a very large total gap width. For example, the largest gap found in Campaign 7 (6.0 inches) combines with two others in the east side cell HH24 to give a total panel gap width of 10.1 inches, yet the east side of cell CC27 has a total gap width of 13.5 inches and has no gap as large as four inches.

A panel that has numerous gaps does not necessarily have a large total gap width. The west side of cell HH24 contains seven gaps whose total width is less than 5.0 inches, while the north side of W23 has five gaps with a total width of only 3.6 inches.

Figure 7 shows the distribution of gap sizes for each of the four campaigns. The distributions are similar, with later campaigns reflecting higher radiation doses to the Boraflex panels -- as evidenced by the increased number of small and large gaps.

The third campaign report showed the axial distribution of gaps for the first three campaigns and concluded there did not seem to be a trend in axial locations of gaps<sup>2</sup> beyond an obvious increase in the number of axial intervals containing gaps. The fourth campaign results appeared to contradict this observation, with some concentration of gaps in the axial zones between 60 and 90 inches up the Boraflex. This concentration of gaps

---

<sup>2</sup> The axial location specified for a gap is the distance, in inches, above the design position of the bottom of the Boraflex panel.

in the 60- to 90-inch range continued in the fifth campaign, with an un-mentioned small concentration of gaps in the 130- to 140-inch range, high up the cells. In the sixth campaign, the concentration in the 60-90 range continued, while the 130-140 interval showed a pronounced peak in the number of contained gaps. This trend continues in the seventh campaign, as can be seen in Fig. 7.

Results of the seventh measurement campaign are summarized and compared with results from the earlier campaigns in Table 1. As has been the case in corresponding tables of earlier reports, Table 1 lists only those gaps determined to be 0.5 inch or larger, the lower limit of reliable detection. While blanks in the table define locations where no gaps 0.5 inches or larger were found, the chart traces for many of those locations give indications of small, developing gaps.

A comparison of gap sizes for the seven campaigns is given in Table 2, which lists data used to prepare Figs. 3, 6, and 7. Table 3 gives a comparison of gap locations for the seven campaigns.

The report on Campaign 6 contained a discussion of *reductions* in gap sizes that appeared to exceed the estimated uncertainty associated with the calculations. That discussion will not be repeated here, for there are few instances of gap-size reduction revealed by Campaign 7; instead, the results of the campaign are notable for the substantial *increases* in gap sizes, as emphasized by the data given in the comparison table shown earlier in this section.

### 3.0 EQUIPMENT DESCRIPTION

The measuring (logging) equipment consists of four nearly identical channels, each including a boron trifluoride (BF<sub>3</sub>) counter tube (1-1/2 inch diameter by 5 inch length) located in a water-tight stainless steel box that constitutes the underwater logging tool. A small positive air pressure is maintained in the tool to prevent water intrusion in the event of a leak.

The logging tool also contains a Californium-252 source and is sized to fit closely into the storage cells. Insulated cabling connects the logging tool to surface instrumentation, which includes a high-voltage power supply, linear amplifier, single channel analyzer (integral bias), and count-rate meters for each channel, in addition to a multi-channel strip chart recorder and timer/counter circuits.

The position of the logging tool is controlled by an operator standing on the pool bridge. A second individual controls and monitors the recording equipment, which is located adjacent to the pool.

#### 4.0 OPERATING PROCEDURES AND QUALITY ASSURANCE

Grand Gulf Nuclear Station Performance and System Engineering Instruction No. 17-S-02-30, Blackness Testing, prepared by Entergy Operations, Inc., was closely followed in making the tests. The tests were witnessed by a Grand Gulf representative, and the data sheets in the data package (Revision 7) were appropriately signed-off by the Grand Gulf Test Supervisor and the Grand Gulf Reactor Engineering Superintendent.

During the traverse of each storage cell, the thermal neutron counting rate in each of the four channels was continuously recorded. An increase in counting rate in any channel is indicative of a possible gap in the Boraflex of the associated wall, with the magnitude of the increase being proportional to the width of the gap. Sensitivity to gap size depends upon the relative neutron counting rates in the Boraflex region and in the unpoisoned region of the cell and is not dependent upon the absolute counting rates. The principal sources of error in the measurements are:

- (1) Normal statistical variation in counting rates;
- (2) unavoidable changes in counting rate as the logging tool moves from side-to-side within the cell (because of the changing neutron moderation in the water around the tool);
- (3) interference from background gamma radiation, if any;
- (4) drift in amplifier gain and counting efficiency;
- (5) changes in logging speed (from which the axial position of a potential gap is determined); and
- (6) differences in channel response due to internal detector alignment and to the presence of electrical noise requiring differing bias settings.

In the seventh campaign the sources of error were minimal, resulting in runs that demonstrated very good consistency. The data sheets incorporated into the procedures call for a verification count at the beginning and end of each working day, intended to reveal any major changes in performance of the counting instrumentation.

In addition, periodic check counts were made in the water above each cell. These data confirm that the instrumentation remained stable and was performing consistently.

TABLE 1. SEVENTH CAMPAIGN DATA AND COMPARISON WITH PREVIOUS CAMPAIGN RESULTS (PAGE 1 OF 11)

CELL AND SIDE		CAMPAIGN 1 SIZE LOC.		CAMPAIGN 2 SIZE LOC.		CAMPAIGN 3 SIZE LOC.		CAMPAIGN 4 SIZE LOC.		CAMPAIGN 5 SIZE LOC.		CAMPAIGN 6 SIZE LOC.		CAMPAIGN 7 SIZE LOC.	
V-20	N			0.6	34	0.7	37	0.7	37	0.9	39	1.1	39	1.3	39
	E			0.6	89	1.0	92	0.9	90	1.0	93	1.5	91	1.4	91
	S							0.6	74	0.5	77	0.7	76	0.8	75
	W			1.4	136	2.5	139	2.7	136	2.9	140	3.0	137	2.9	137
X-20	N			0.5	48	0.8	49	1.0	44	1.4	51	1.8	50	1.6	52
	E	0.5	78	0.5	84	1.0	84	0.9	80	1.2	87	2.0	85	1.6	88
	S			0.6	78	1.0	77	1.3	73	1.2	80	1.7	78	1.4	81
										0.6	116	0.7	113	0.6	117
						0.6	40	0.8	35	0.7	42	0.7	41	1.0	42
												0.5	66	0.8	68
										0.5	91	0.7	89	0.6	93
	W					0.7	121	0.7	117	0.6	124	0.7	120	1.0	125
Z-20	N					0.6	74	0.5	74	0.8	76	0.9	75	1.1	76
	E	0.6	82	0.9	80	1.2	82	1.3	82	1.6	84	1.6	83	1.9	84
	S	0.8	69	1.0	66	1.4	68	1.9	70	1.8	71	1.8	69	2.2	70
	W			0.6	65	0.7	67	0.8	67	1.0	69	0.9	67	1.3	69
BB-20	N					0.8	86	0.8	86	1.0	87	1.0	85	1.3	87
	E					0.6	107	0.5	108	0.6	109	0.6	106	0.8	108
	S	0.7	80	1.2	78	1.8	80	2.9	78	3.0	82	2.0	80	2.4	81
	W											0.5	130	1.4	133
DD-20	N													0.6	40
	E					0.6	84	0.5	51	0.5	53	0.5	53	0.8	53
	S	0.5	84	0.9	82	1.1	85	0.6	83	0.6	86	0.7	84	0.9	85
								0.7	129	0.8	132	0.8	129	0.9	131
								1.4	84	1.5	86	1.2	84	1.5	86
				0.6	63	1.0	64	1.2	64	1.0	65	1.1	65	1.5	66
				0.7	93	1.2	95	1.5	94	1.4	98	1.2	94	1.6	96
	W											1.0	134	1.6	137

TABLE 1. SEVENTH CAMPAIGN DATA AND COMPARISON WITH PREVIOUS CAMPAIGN RESULTS (PAGE 2 OF 11)

CELL AND SIDE		CAMPAIGN 1 SIZE LOC.		CAMPAIGN 2 SIZE LOC.		CAMPAIGN 3 SIZE LOC.		CAMPAIGN 4 SIZE LOC.		CAMPAIGN 5 SIZE LOC.		CAMPAIGN 6 SIZE LOC.		CAMPAIGN 7 SIZE LOC.	
FF-20	N													0.6	18
														0.6	41
	E					0.7	85	0.8	86	0.8	86	0.7	84	0.5	134
	S			1.2	86	2.3	89	2.9	88	3.1	90	2.9	88	1.0	85
	W													3.4	89
HH-20														0.9	114
	N					1.1	86	1.6	87	1.9	88	2.0	87	2.4	87
						0.8	127	0.9	129	1.2	131	1.3	129	1.7	130
	E							0.5	27	0.5	28	0.6	29	0.6	28
				1.0	87	2.1	89	2.9	90	3.0	91	2.5	91	2.7	91
	S					0.6	46	0.8	46	0.8	47	1.3	48	1.0	47
						0.7	91	0.8	90	1.0	92	0.8	91	1.1	92
	W									0.5	135	0.6	134	0.6	135
W-21								0.5	25	0.6	26	0.6	26	1.1	26
														0.8	49
	N	0.5	63	0.6	61	0.8	63	0.5	44	0.5	46	0.6	45	0.8	45
								0.9	62	1.1	64	1.2	63	1.8	64
								1.1	70	1.3	72	1.6	70	2.1	71
										1.1	89	1.5	86	2.2	88
								0.6	117	0.6	120	0.7	117	0.9	119
	E													0.8	41
										1.6	71	1.6	70	1.8	71
												0.9	78	1.3	80
								0.7	102	0.6	106	0.9	102	1.5	104
	S									0.5	140	0.7	136	1.3	139
Y-21						0.6	38	0.6	114	0.5	116	0.5	113	0.7	39
	W													0.6	115
														0.6	69
														0.6	79
	N	1.2	65	1.3	64	2.0	67	0.5	45	2.6	68	2.5	67	2.8	68
								2.4	64			0.6	24	1.2	25
	E							0.9	72	3.0	78	2.9	77	3.3	78
								0.5	84	3.0	87	3.0	86	3.4	87
														1.3	129
	S	0.7	73	0.9	73	1.3	74	1.5	71	1.5	76	1.5	75	1.9	76
	W	1.0	91	1.3	90	1.8	92	1.9	90	1.9	94	2.0	93	2.4	94

TABLE 1. SEVENTH CAMPAIGN DATA AND COMPARISON WITH PREVIOUS CAMPAIGN RESULTS (PAGE 3 OF 11)

CELL AND SIDE		CAMPAIGN 1 SIZE LOC.		CAMPAIGN 2 SIZE LOC.		CAMPAIGN 3 SIZE LOC.		CAMPAIGN 4 SIZE LOC.		CAMPAIGN 5 SIZE LOC.		CAMPAIGN 6 SIZE LOC.		CAMPAIGN 7 SIZE LOC.	
AA-21	N													0.8	64
	E	1.1	135	1.5	135	2.7	136	3.4	138	3.7	139	3.5	138	3.5	139
	S	0.7	69	0.9	67	0.6	77	0.9	79	0.9	80	0.8	79	1.2	80
	W					1.2	68	1.5	68	1.3	70	1.5	70	1.9	70
CC-21	N									0.8	142	0.9	139	1.1	141
	E					0.7	78	0.7	79	0.7	80	0.7	79	1.0	80
	S	1.3	83	1.4	82	2.1	83	2.5	82	2.7	85	2.5	87	2.7	85
	W	0.5	95	0.8	94	1.1	95	1.5	95	1.5	97	1.4	99	0.8	5
EE-21	N	0.7	88	0.9	88	1.6	89	1.8	88	1.9	91	1.7	92	1.7	98
	E													0.6	125
	S													2.3	91
	W														
GG-21	N					0.5	87	0.5	87	0.5	89	0.6	90	0.7	88
	E											0.5	53	1.0	51
	S					0.8	85	1.0	86	1.2	88	2.3	90	4.0	89
	W													0.6	133
V-22	N													0.6	75
	E					0.7	104	0.8	104	0.6	106	0.7	108	0.9	104
	S													0.6	21
	W					0.6	64	0.9	64	0.7	66	0.9	68	1.1	65
V-22	N													0.5	92
	E							0.5	102					0.6	104
	S					0.6	62	0.7	63	0.6	65	0.7	65	1.1	64
	W					0.8	87	0.9	87	0.8	90	0.7	89	0.9	89
V-22	N							0.6	39	0.5	40			0.7	38
	E					1.0	127	1.2	126	1.2	130	1.2	128	1.5	129
	S					0.6	62	0.8	62	0.9	65	0.9	64	1.1	64
	W					0.6	86	0.7	85	0.8	89	1.1	87	1.9	88
V-22	N					0.5	70	0.6	71	0.5	73	0.6	74	0.8	72
	E					0.5	105	0.6	104	0.6	105	0.6	105	0.8	105
	S							0.7	64	0.6	66	0.6	66	0.8	65
	W							0.8	138	0.7	140	0.8	138	1.2	138
V-22	N													0.6	10
	E	0.8	128	1.5	127	2.5	129	3.2	130	2.7	131	2.7	130	2.7	130
	S					0.9	65	0.9	65	0.9	67	1.0	68	1.2	66
	W					0.6	115	0.7	113	0.7	117	0.7	116	0.8	116

TABLE 1. SEVENTH CAMPAIGN DATA AND COMPARISON WITH PREVIOUS CAMPAIGN RESULTS (PAGE 4 OF 11)

CELL AND SIDE		CAMPAIGN 1 SIZE LOC.	CAMPAIGN 2 SIZE LOC.	CAMPAIGN 3 SIZE LOC.	CAMPAIGN 4 SIZE LOC.	CAMPAIGN 5 SIZE LOC.	CAMPAIGN 6 SIZE LOC.	CAMPAIGN 7 SIZE LOC.
X-22	N				0.5 78		0.5 77	0.7 76
	E	0.6 136	0.6 136	0.8 138	0.9 139	1.1 140	1.0 138	1.2 140
	S			0.6 41	0.7 42	0.5 44	0.5 45	0.8 43
	W	0.8 71	1.1 137 1.2 71	2.2 137 1.8 73	2.6 138 1.8 73	2.4 140 2.1 75	2.3 137 2.1 75	2.5 139 2.4 75
Z-22	N				0.5 107			0.5 109
	E	0.6 104	0.9 103	1.3 105	1.7 105	1.5 107	1.3 106	1.6 107
	W	0.7 66	1.0 66	1.6 69	0.7 71 1.9 69	0.5 73 2.0 70	0.8 73 2.0 71	0.8 73 2.4 70
BB-22	N							
	E		0.6 84	0.7 85	1.0 88 0.7 122	0.9 88 0.6 124	0.9 86 0.6 121	1.0 87 0.9 123
	S			0.6 33	0.7 33	0.6 35	0.7 35	0.8 34
	W	1.0 82 0.6 108	1.3 81 0.8 106	2.1 82 1.3 108	2.8 83 1.3 108	2.0 85 1.4 111	2.5 83 1.5 109	2.4 84 1.7 109
DD-22	N		0.5 125	0.7 126	0.8 128	0.9 130	0.8 128	1.2 131
	E	0.5 85	0.9 84	1.1 85	1.7 87	3.0 89	4.5 89	4.8 91
								0.6 123
								1.4 139
	S						0.5 24	0.6 25
				0.6 63	0.8 63	0.7 65	0.8 65	0.7 49 1.2 66
								0.6 89
	W			0.7 109 0.9 72	1.0 110 1.3 72	0.8 112 1.2 74	0.8 111 1.3 74	1.1 113 1.7 75
FF-22	N							0.5 89
	E		0.7 67	1.5 69	2.2 69	2.1 71	2.1 70	2.3 71
								1.0 132
	SW		1.1 43 0.8 64	2.0 44 1.8 66	2.7 45 2.3 67	2.6 47 2.5 68	2.7 46 2.6 68	2.8 46 2.7 68



TABLE 1. SEVENTH CAMPAIGN DATA AND COMPARISON WITH PREVIOUS CAMPAIGN RESULTS (PAGE 5 OF 11)

CELL AND SIDE		CAMPAIGN 1 SIZE LOC.		CAMPAIGN 2 SIZE LOC.		CAMPAIGN 3 SIZE LOC.		CAMPAIGN 4 SIZE LOC.		CAMPAIGN 5 SIZE LOC.		CAMPAIGN 6 SIZE LOC.		CAMPAIGN 7 SIZE LOC.	
HH-22	N					0.7	17	0.7	17	0.9	18	0.9	18	1.1	18
						1.2	134	1.6	136	1.9	137	1.8	134	2.2	137
	E			0.5	39	0.8	41	1.0	42	0.8	43	0.8	43	1.0	44
														2.0	66
						0.8	70	1.6	71	1.3	73	1.3	72	2.3	73
												1.8	86	5.0	89
	S W			0.6	111	0.9	112	1.7	113	1.0	115	1.0	113	1.0	133
														1.2	116
														0.6	7
												0.6	111	0.8	114
W-23	N							0.6	27	0.6	29	0.6	29	0.7	29
										0.5	73			0.6	74
										0.5	81			0.6	81
										0.6	120	0.5	119	0.8	122
	E							0.5	128			0.8	139	0.9	144
														0.6	34
										0.6	125	1.2	123	2.4	127
														1.8	136
	S W														
						0.8	68	0.9	68	0.8	70	1.0	70	0.6	14
Y-23	N			0.8	136	1.4	138	1.6	136	1.9	140	1.7	138	2.1	136
	E	0.8	76	1.0	75	1.4	77	2.0	75	1.9	79	1.8	78	2.1	76
	S	1.0	81	1.3	79	2.0	82	2.0	79	2.2	83	2.2	82	2.7	80
	W			0.8	70	1.1	72	1.5	72	1.3	74	1.5	74	1.9	71
										1.0	141	1.2	140	1.5	137
AA-23	N							0.7	28	0.6	30	0.6	29	0.8	29
	E	0.5	38	0.5	40	0.6	41	0.9	42	0.8	44	0.7	43	0.8	43
						0.6	85	0.9	85	0.8	88	0.7	86	0.9	87
	S W											0.9	140	1.2	141
														0.9	88
				1.1	137	2.1	137	2.9	139	2.7	141	2.3	138	2.5	139
								0.5	16	0.5	19			0.6	18
		1.1	82	1.3	83	2.1	85	2.4	85	2.2	88	2.5	86	2.5	87

TABLE 1. SEVENTH CAMPAIGN DATA AND COMPARISON WITH PREVIOUS CAMPAIGN RESULTS (PAGE 6 OF 11)

CELL AND SIDE		CAMPAIGN 1 SIZE LOC.		CAMPAIGN 2 SIZE LOC.		CAMPAIGN 3 SIZE LOC.		CAMPAIGN 4 SIZE LOC.		CAMPAIGN 5 SIZE LOC.		CAMPAIGN 6 SIZE LOC.		CAMPAIGN 7 SIZE LOC.	
CC-23	N	0.5	67	0.5	65	0.9	67	0.9	67	1.0	69	0.9	68	1.1	69
	E													0.6	45
	S	0.6	111	0.9	110	1.3	112	1.6	113	1.4	115	1.3	112	1.9	114
	W	0.5	77	0.7	76	1.0	79	1.1	79	1.0	81	1.0	79	1.5	80
EE-23	N			0.5	98	1.1	100	1.3	101	1.6	103	1.6	100	1.9	103
	E					1.2	138	1.5	138	1.3	142	1.2	138	1.6	141
	S					0.8	85	1.1	86	1.0	89	0.9	86	1.3	88
	W			0.8	60	1.7	62	1.9	63	1.8	65	1.9	63	2.1	65
GG-23	N														
	E			0.6	74	1.2	77	1.8	78	1.8	81	1.5	78	2.1	79
	S							0.5	84	0.5	88			0.7	85
	W			0.8	68	1.5	71	0.7	121	0.6	120	0.6	118	0.8	119
V-24	N														
	E	0.5	136	0.8	134	1.0	137	1.2	137	1.2	139	0.8	142	1.1	140
	S							0.6	59			0.6	65	1.0	34
	W	0.5	128	0.7	126	1.2	128	1.6	131	1.6	130	1.6	134	2.2	130
X-24	N														
	E														
	S														
	W	1.3	130	1.9	127	3.5	129	3.5	129	3.8	131	3.5	135	3.5	132
X-24	N			0.6	78	0.7	81	1.0	81	1.0	82	0.9	81	1.1	81
	E			0.5	109	0.6	112	0.8	112	0.7	113	0.7	112	0.9	111
	S													0.8	55
	W	0.9	111	1.2	110	1.8	112			2.2	113	2.6	111	2.7	111



TABLE 1. SEVENTH CAMPAIGN DATA AND COMPARISON WITH PREVIOUS CAMPAIGN RESULTS (PAGE 8 OF 11)

CELL AND SIDE		CAMPAIGN 1 SIZE LOC.		CAMPAIGN 2 SIZE LOC.		CAMPAIGN 3 SIZE LOC.		CAMPAIGN 4 SIZE LOC.		CAMPAIGN 5 SIZE LOC.		CAMPAIGN 6 SIZE LOC.		CAMPAIGN 7 SIZE LOC.	
W-25	N					0.6	37	0.7	39	0.7	39	0.6	39	0.8	39
	E													0.8	88
	S	1.4	99	1.7	97	3.3	98	3.5	100	3.5	100	3.5	98	3.6	100
	W					0.6	13	0.6	13	0.6	15	0.6	16	0.8	15
Y-25	N	1.2	81	1.3	80	1.6	81	2.0	81	2.5	83	1.9	81	2.3	83
	E	0.5	76	0.8	76	1.0	77	1.1	77	1.1	79	1.0	77	1.2	79
	S	1.1	101	1.4	101	2.2	102	2.7	101	2.5	104	2.3	101	2.7	103
	W													0.5	24
AA-25	N													0.6	26
	E	1.4	103	1.4	104	2.3	106	2.7	106	2.9	108	3.0	106	2.9	108
												0.5	20	0.9	12
														1.4	21
								0.6	68	0.5	70	0.6	69	1.0	26
				0.7	136	1.3	138	1.6	137	1.4	140	1.3	137	0.8	70
	S													0.7	78
		1.3	111	1.8	110	2.8	113	3.3	112	3.2	115	3.0	113	3.0	115
	W													0.5	26
				0.6	56	0.8	59	1.0	58	0.9	60	1.0	58	1.1	59
CC-25	N					0.7	138	0.9	137	0.9	140	0.9	136	1.2	139
								0.6	44	0.5	45	0.6	44	0.7	44
	E							0.6	114	1.1	115			0.6	115
	S	0.8	47	0.8	45	1.4	46	1.5	47	1.5	48	1.2	48	1.9	47
						0.8	88	1.0	88	0.9	90	0.9	88	1.2	89
	W			0.7	66	1.0	67	1.3	67	1.0	69	1.1	68	1.3	68
EE-25	N			0.7	88	1.0	88	1.3	86	1.3	89	1.1	87	1.5	88
						0.6	138								
	E													0.7	27
				0.5	86	0.8	84	1.0	84	1.0	87	0.9	85	1.2	86
	S			0.6	91	0.9	90	1.1	87	1.1	92	1.1	90	1.2	91
										0.7	141	0.7	139	1.0	140
	W					0.8	67	0.9	66	0.8	68	0.9	67	1.1	67
GG-25								0.8	140			1.0	138	1.4	140
	N							0.6	103	0.6	109	0.5	106	0.7	103
	E														
	S			0.5	59	1.1	60	1.5	61	1.3	64	1.2	62	1.7	58
						0.6	127	0.9	128	0.8	133	0.8	128	1.1	126
	W			0.7	134	1.8	134	2.3	136	2.4	140	2.7	135	2.5	133

TABLE 1. SEVENTH CAMPAIGN DATA AND COMPARISON WITH PREVIOUS CAMPAIGN RESULTS (PAGE 9 OF 11)

CELL AND SIDE		CAMPAIGN 1 SIZE LOC.		CAMPAIGN 2 SIZE LOC.		CAMPAIGN 3 SIZE LOC.		CAMPAIGN 4 SIZE LOC.		CAMPAIGN 5 SIZE LOC.		CAMPAIGN 6 SIZE LOC.		CAMPAIGN 7 SIZE LOC.	
V-26	N													0.6	68
	E											1.0	139	1.4	142
	S	0.7	104	0.6	102	1.0	104	1.4	103	1.2	106	1.2	103	0.6	55
										0.8	27	1.8	26	1.6	104
	W	1.0	86	1.6	89	2.5	90	2.7	90	2.8	92	2.9	90	2.5	26
X-26						2.2	40	2.4	138	2.3	141	2.5	138	1.8	51
	N					0.7	70	0.9	68	0.8	72	0.8	70	2.9	91
	E	0.7	115	0.8	113	1.1	116	1.3	114	1.3	118	1.1	116	2.5	140
	S	1.2	88	1.7	87	2.9	88	3.5	88	3.4	91	3.0	88	1.0	72
	W	0.7	62	0.8	60	1.5	62	1.8	61	1.7	64	1.8	63	1.6	118
Z-26	N														
	E	0.5	35	0.6	38	0.8	39	0.9	41	0.8	41	0.6	41	0.9	41
	S	1.3	82	2.0	85	3.3	86	3.5	86	3.2	88	3.1	87	3.8	88
	W	1.2	78	1.3	75	2.3	75	2.7	77	2.5	78	2.5	77	2.5	78
BB-26	N	1.3	110	1.4	110	2.0	113	2.1	112	2.9	114	2.3	113	2.5	114
	E	1.0	135	1.3	134	2.0	137	2.8	137	2.9	138	2.9	137	2.8	138
	S	0.9	78	1.1	79	1.8	80	1.9	80	1.7	81	1.6	81	2.1	82
						0.6	124	0.8	124	0.6	126	0.7	125	0.9	126
	W					0.6	45	0.6	48	0.5	47	0.6	47	0.8	47
DD-26														1.2	133
	N	0.5	136	0.8	136	2.0	138	2.1	138	2.0	140	1.9	139	2.3	140
	E											0.8	138	0.6	85
	S	0.8	81	1.1	80	1.6	82	2.5	82	2.2	84	2.1	82	0.9	140
FF-26	W									0.6	69	0.5	68	2.4	82
	N			0.6	63	1.3	65	1.9	66	2.1	67	2.1	66	0.8	69
	E									0.5	46	0.5	45	0.7	46
	S			0.7	90	1.2	91	1.7	92	1.6	94	1.5	92	1.7	94
	W			1.2	42	2.7	44	3.3	44	3.4	46	3.0	45	3.5	45

TABLE 1. SEVENTH CAMPAIGN DATA AND COMPARISON WITH PREVIOUS CAMPAIGN RESULTS (PAGE 10 OF 11)

CELL AND SIDE		CAMPAIGN 1 SIZE LOC.		CAMPAIGN 2 SIZE LOC.		CAMPAIGN 3 SIZE LOC.		CAMPAIGN 4 SIZE LOC.		CAMPAIGN 5 SIZE LOC.		CAMPAIGN 6 SIZE LOC.		CAMPAIGN 7 SIZE LOC.	
HH-26	N					0.7	15	1.1	14	1.1	16	1.0	15	1.4	15
														0.5	87
	E S W			0.9	64	2.1	65	0.7	101	0.5	103			0.6	102
						3.3	65	3.0	66	3.0	66	3.0	65	3.6	67
						0.8	85	1.0	85	0.9	87	0.9	85	1.1	87
														0.6	23
						0.6	39	1.1	39	0.7	40	0.9	39	1.1	39
						0.5	77	0.8	76	0.6	78			0.8	77
												0.8	137	0.9	140
W-27	N							0.5	30					0.6	40
								0.7	38	0.6	40			1.3	137
	E S W			0.5	132	0.7	135	1.1	135	1.1	137	1.1	134	1.3	137
				0.7	105	1.0	106	1.2	106	1.1	108	1.0	106	1.3	108
						0.7	96	1.3	96	1.1	98	1.2	96	1.8	98
				1.1	42	0.6	43	2.2	43	1.8	45	1.6	44	2.3	45
Y-27	N E			1.0	89	1.3	91	2.2	91	1.7	92	1.8	89	2.1	93
														1.0	85
	S W											1.3	90	2.5	93
				1.2	136	2.2	137	3.0	138	3.0	138	2.7	134	2.5	139
				1.2	50	2.0	51	1.9	51	2.4	52	2.3	51	2.5	52
						0.7	130	0.9	130	0.8	131	0.9	127	1.4	86
AA-27	N			0.5	46	0.7	44	0.9	45	0.9	47	0.8	46	1.0	47
						1.1	137	1.0	139	1.4	142	1.3	138	1.6	141
	E S W									0.6	22			0.6	23
		0.7	59	0.7	58	1.2	57	1.3	58	1.3	60	1.3	59	1.7	60
		0.5	120	0.5	120	0.9	118	0.9	120	0.8	123	0.9	120	1.2	122
		1.1	43	1.4	43	2.3	42	2.8	43	2.6	45	3.0	43	3.0	45

TABLE 1. SEVENTH CAMPAIGN DATA AND COMPARISON WITH PREVIOUS CAMPAIGN RESULTS (PAGE 11 OF 11)

CELL AND SIDE		CAMPAIGN 1 SIZE LOC.		CAMPAIGN 2 SIZE LOC.		CAMPAIGN 3 SIZE LOC.		CAMPAIGN 4 SIZE LOC.		CAMPAIGN 5 SIZE LOC.		CAMPAIGN 6 SIZE LOC.		CAMPAIGN 7 SIZE LOC.	
CC-27	N							0.6	43	0.5	46	0.5	45	0.6	46
														0.6	66
								0.5	82	0.5	84	0.6	83	0.9	84
	E							0.6	129	0.6	133	0.6	130	0.7	118
								0.6	42					0.9	132
														0.7	79
	S									1.9	90	2.9	88	3.8	89
										0.5	98	1.1	96	2.0	97
		1.0	117	1.1	116	1.7	117	2.5	116	2.1	120	1.8	117	2.5	120
	W											2.2	137	0.8	131
				0.6	39	0.8	40	1.0	40	0.9	42	0.9	41	3.7	139
		0.5	65	0.7	64	1.0	65	1.2	65	1.1	67	1.1	66	0.6	43
EE-27	N									0.5	114	0.5	111	1.5	66
										1.3	42	1.3	41	0.7	113
		0.8	40	0.9	38	1.1	40	1.3	40	0.7	67	1.2	66	1.6	41
	E							0.8	64			0.6	81	2.3	66
														2.8	82
	S					0.7	30	1.0	30	1.0	32	0.9	31	0.9	32
				0.7	88	1.0	90	1.6	87	1.7	93	1.6	91	1.9	91
						0.6	83	1.1	85	1.0	86	1.4	84	1.0	60
	W													1.2	85
						0.7	63	0.9	63	0.9	66	0.9	65	0.8	128
								0.6	124	0.5	127			1.3	65
GG-27	N													0.6	125
						1.0	22	1.2	22	1.2	24	1.3	23	1.6	24
						1.1	134	1.4	133	1.4	136	1.6	133	1.9	136
	E							0.5	91						
						0.7	117	1.2	120	1.1	120	0.9	117	0.6	77
												0.8	128	1.2	119
	S					0.6	78	0.8	79	0.7	81	0.7	79	2.0	130
								0.7	106	0.7	109	0.7	106	0.9	80
								0.5	64	0.5	67	0.7	66	0.9	107
	W													2.2	65
				0.7	119	1.4	118	1.8	119	1.8	121	1.9	118	2.2	119



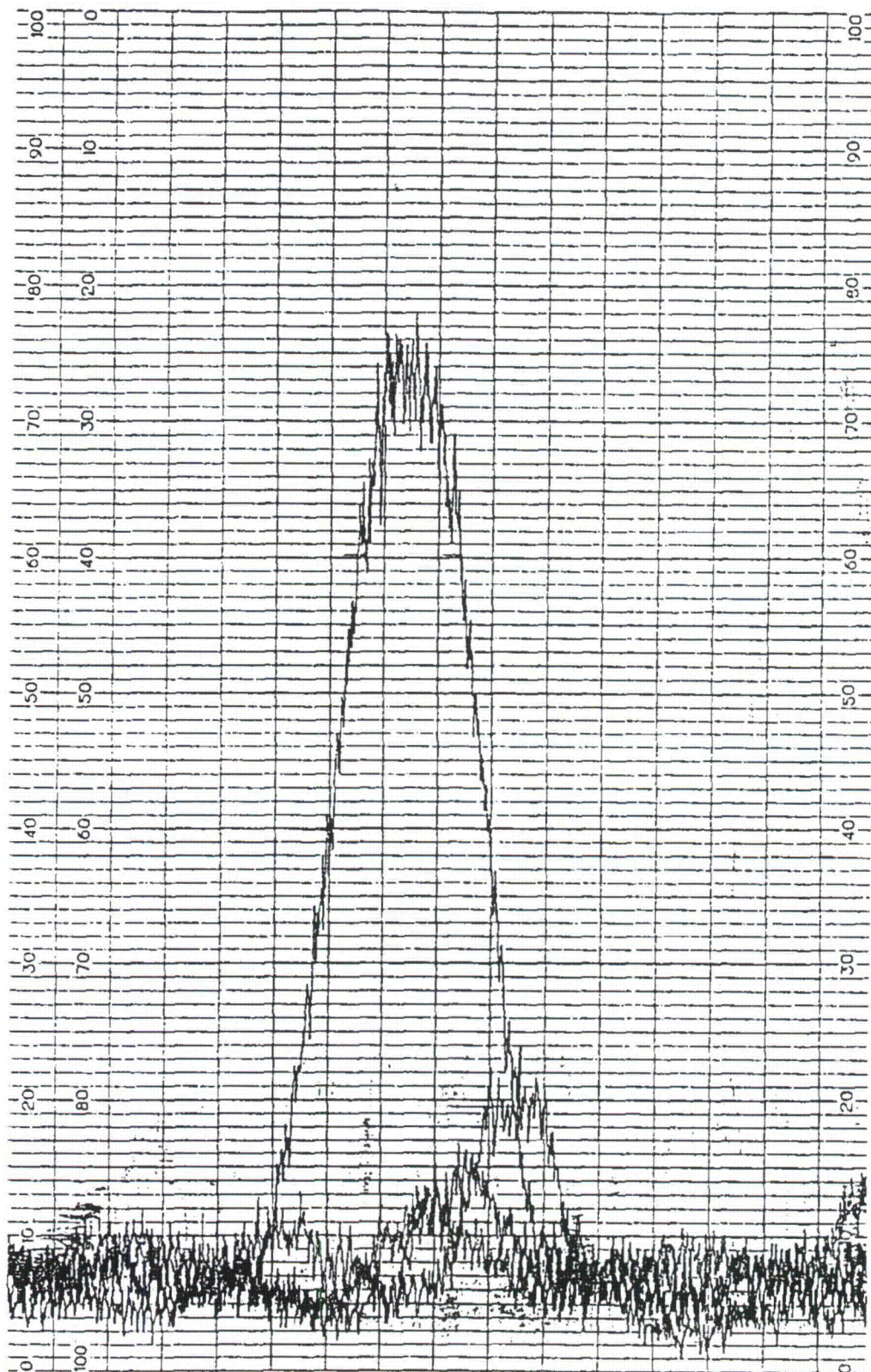


Fig. 1 A portion of the chart traces for cell HH24



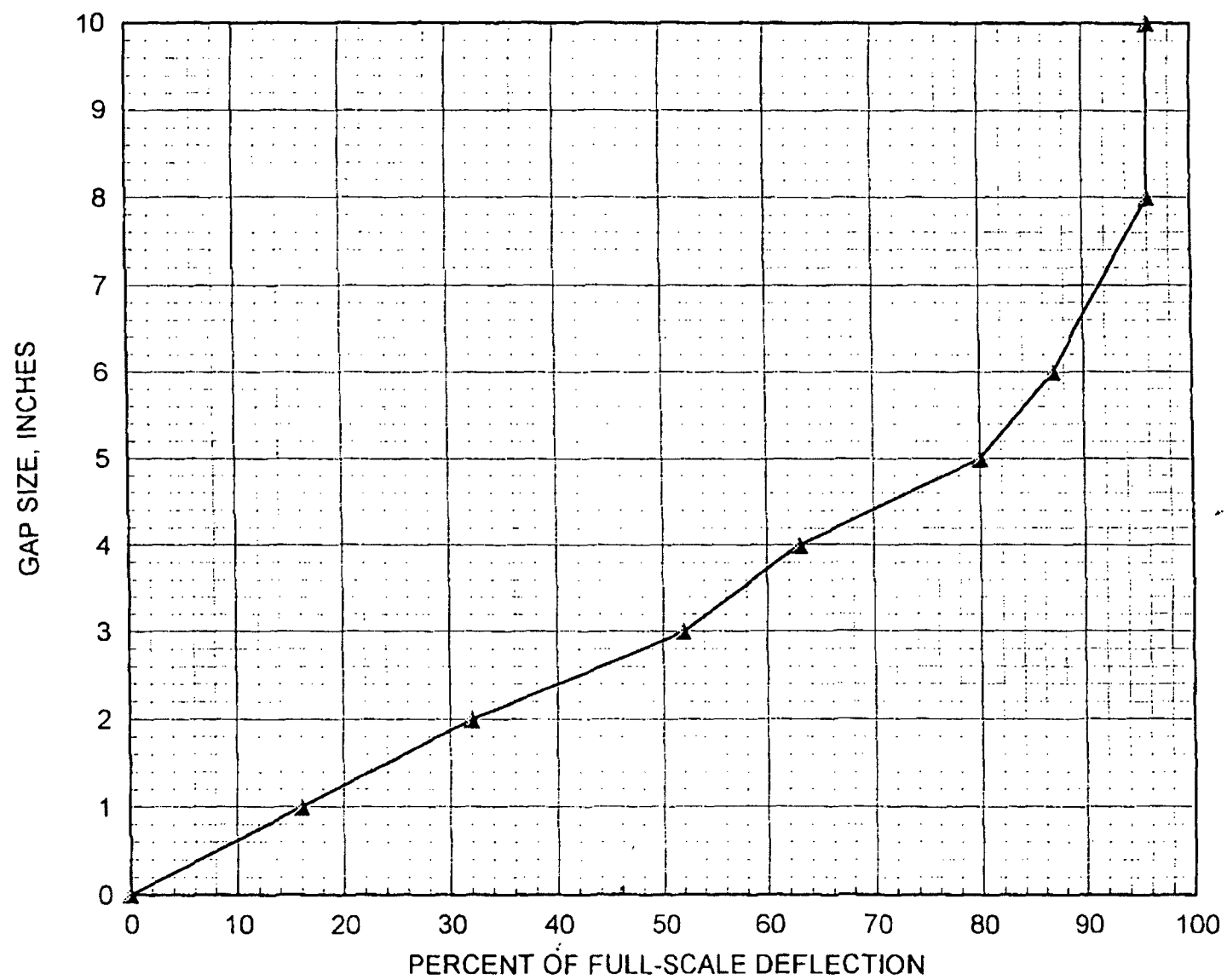


Fig. 2 Correlation curve for gap sizes

**Attachment 2**

**GNRO-2011/00025**

**Grand Gulf Nuclear Station Extended Power Uprate**

**Proposed Technical Specification Changes (Markup)**

#### 4.0 DESIGN FEATURES

---

##### 4.1 Site Location

The site for Grand Gulf Nuclear Station is located in Claiborne County, Mississippi on the east bank of the Mississippi River, approximately 25 miles south of Vicksburg and 37 miles north-northeast of Natchez. The exclusion area boundary shall have a radius of 696 meters from the centerline of the reactor.

---

##### 4.2 Reactor Core

###### 4.2.1 Fuel Assemblies

The reactor shall contain 800 fuel assemblies. Each assembly shall consist of a matrix of Zircaloy or ZIRLO clad fuel rods with an initial composition of natural or slightly enriched uranium dioxide ( $UO_2$ ) as fuel material, and water rods. Limited substitutions of zirconium alloy or stainless steel filler rods for fuel rods, in accordance with approved applications of fuel rod configurations, may be used. Fuel assemblies shall be limited to those fuel designs that have been analyzed with applicable NRC staff approved codes and methods and shown by tests or analyses to comply with all safety design bases. A limited number of lead test assemblies that have not completed representative testing may be placed in nonlimiting core regions.

###### 4.2.2 Control Rod Assemblies

The reactor core shall contain 193 cruciform shaped control rod assemblies. The control material shall be boron carbide or hafnium metal, or both.

---

##### 4.3 Fuel Storage

###### 4.3.1 Criticality

4.3.1.1 The spent fuel storage racks are designed and shall be maintained with:

- a.  $k_{eff} \leq 0.95$  if fully flooded with unborated water, which includes an allowance for uncertainties as described in Section 9.1.2 of the UFSAR;
- b. A nominal fuel assembly center to center storage spacing of 6.26 inches in the storage racks.

Insert 1



---

(continued)

#### 4.0 DESIGN FEATURES (continued)

---

4.3.1.2 The new fuel storage racks are designed and shall be maintained with:

- a.  $k_{off} \leq 0.95$  if fully flooded with unborated water, which includes an allowance for uncertainties as described in Section 9.1.1 of the UFSAR;
- b. A nominal fuel assembly center to center storage spacing of 6.535 inches within rows and 11.875 inches between rows in the new fuel storage racks.

Insert 2



#### 4.3.2 Drainage

The spent fuel storage pool is designed and shall be maintained to prevent inadvertent draining of the pool below elevation 202 ft 5.25 inches.

#### 4.3.3 Capacity

- 4.3.3.1 The spent fuel storage pool shall be maintained with a storage capacity limited to no more than 4348 fuel assemblies.
  - 4.3.3.2 No more than 800 fuel assemblies may be stored in the upper containment pool.
-

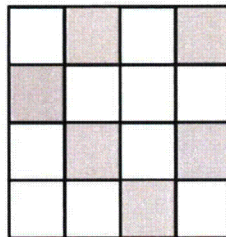
## Inserts

### **Insert 1**

#### 4.3.1.1 ...

- c. Fuel assemblies having a maximum k-infinity of 1.26 in the normal reactor core configuration at cold conditions;
- d. Fuel assemblies having a maximum nominal U-235 enrichment of 4.9 weight percent;
- e. Region II racks are controlled as follows:
  1. Storage cells with any Boraflex panel which has received a gamma dose in excess of  $2.3E10$  rads or which has a Boron-10 areal density less than 0.0133 minus the tolerance allowance associated with the RACKLIFE monitoring criteria, which is designated within the Spent Fuel Pool Rack Boraflex Monitoring Program, are treated as Region II panels.
  2. Storage cells face-adjacent to Region II panels are either restricted from fuel storage by physically blocking the isolated cells or are configured to meet, as a minimum (i.e., additional cells may be blocked), the Region II fuel storage configuration requirements in Figure 4.3-1.
  3. When a 4x4 array of cells is classified as Region II and face-adjacent to another Region II 4x4 storage array, the new Region II 4x4 array is required to be blocked in the same 6 of 16 pattern and at the same orientation as the adjacent Region II 4x4 storage configuration.

Figure 4.3-1  
Region II 4X4 Storage Configuration



Fuel Assembly Storage Location



Location Physically Blocked to Prevent Storage

### **Insert 2**

#### 4.3.1.2 ...

- c. Fuel assemblies having a maximum k-infinity of 1.26 in the normal reactor core configuration at cold conditions;
- d. Fuel assemblies having a maximum nominal U-235 enrichment of 4.9 weight percent.

**Attachment 3**

**GNRO-2011/00025**

**Grand Gulf Nuclear Station Extended Power Uprate**

**Response to Request for Additional Information**

**Reactor Systems Branch**

**Non-Proprietary**

This is a non-proprietary version of Attachment 1 from which the proprietary information has been removed. The proprietary portions that have been removed are indicated by double square brackets as shown here: [[ ]].

**Non-Proprietary**

**Response to Request for Additional Information  
Reactor Systems Branch**

By letter dated September 8, 2010, Entergy Operations, Inc. (Entergy) submitted a license amendment request (LAR) for an Extended Power Uprate (EPU) for Grand Gulf Nuclear Station, Unit 1 (GGNS) (Accession Number ML102660403). The U.S. Nuclear Regulatory Commission (NRC) staff has determined that the following additional information (Accession Number ML110820227) requested by the Reactor Systems Branch is needed for the NRC staff to complete their review of the amendment. Entergy's response to each item is also provided below.

**RAI # 1**

**RAIs related to NEDC-33173P**

The NRC staff has reviewed the PRIME T-M methodology and documented its approval in its safety evaluation (SE) dated January 22, 2010 (ML102600259). The GNF2 fuel system design evaluation for GGNS EPU application has been performed using the updated PRIME T-M methods. Footnote 3 to Appendix A of the PUSAR states that the GSTRM thermal-mechanical properties will be used in the downstream codes until the changes have been implemented and the NRC has performed an audit of that process and published their SE. This is consistent with the NRC staff approval of IMLTR Supplement 4 describing the plan to implement PRIME models and inputs into downstream safety analysis codes. However, the licensee should justify the continued use of GSTRM methods consistent with the "Interim Process Thermal Overpower Condition" specified in Appendix A to the NRC staff safety evaluation that approved the PRIME T-M methodology (ML102600259).

Provide information demonstrating compliance with the "Interim Process Thermal Overpower Condition" specified in the NRC staff SE for PRIME T-M methods.

**Response**

This footnote refers to the Thermal Overpower (TOP) screening criteria. If the GSTRM TOP screening criteria is exceeded, the PRIME Overpower limits are used. These GSTRM based limits are conservative due to being based on Gadolinia alone. When more detailed calculations are necessary, the UO<sub>2</sub> and Gadolinia rods are then compared to their respective limits. Therefore, the use of the GSTRM screening criterion is conservative with respect to PRIME. For the transient evaluation supporting the PUSAR, the RWE TOP evaluation passed this conservative GSTRM screening criterion. The LFWH RWE TOP evaluation result, however, did exceed this conservative GSTRM screening criterion, and therefore UO<sub>2</sub> and Gadolinia results were analyzed individually using the PRIME T-M UO<sub>2</sub> limit. This result was 34.8% TOP for a limiting cycle exposure and pressurization condition, which meets the exposure dependent

**Non-Proprietary**

PRIME  $\text{UO}_2$  limit of 44% TOP. Therefore, these results are compliant with the "Interim Process Thermal Overpower Condition" specified in the NRC staff safety evaluation for PRIME T-M methods.

**RAI # 2**

Footnote 4 to Appendix A of the PUSAR states, "As a consequence of the NRC staff review of the GE Part 21 report, a modified GNF2 T-M basis using GESTR-M was established by the GNF2 Compliance Report (Reference A-6)." Clarify whether this implies that GNF2 thermal-mechanical operating limit (TMOL) is based on GESTR-M.

Also, confirm that the GE14 LHGR is based on the revised TMOL provided in Appendix C of the GE14 GESTAR II Compliance Report, NEDC-32868P Revision 3.

**Response**

The GNF2 TMOL was based on PRIME. This footnote refers to the implementation of an improved fuel temperature calculation (PRIME), which was modified as compared to GESTR-M.

The GGNS EPU representative equilibrium core consists only of the GNF2 fuel type. For the cycle-specific reload analysis, the revised GE14 LHGR TMOLs from Appendix C of the GE14 GESTAR II Compliance Report, NEDC-32868P, Revision 3 will be used.

**RAI # 3**

**Fuel and Core Design**

The average bundle power increases from the current licensed thermal power (CLTP) by 13.1% from 4.87 MW/bundle to 5.51 MW/bundle, which corresponds to the same percent increase of total core power from CLTP to EPU. It is assumed in the constant pressure EPU for BWRs that the additional core power is obtained by raising the average bundle power, and that the peak bundle power should remain the same. However, past EPU operations have shown that peak bundle power can increase by a limited amount. Please provide the current peak bundle power and compare it with the expected value of peak bundle power for EPU operation in GGNS.

**Response**

The current peak bundle power for CLTP (previous Cycle 17 and current Cycle 18) is approximately 7.4 MW and expected peak bundle power for EPU is projected to be approximately 7.8 MW.



**Non-Proprietary**

**RAI # 4**

As stated in the PUSAR, GGNS EPU analyses assumed an “equilibrium” core comprised of GNF2 fuel. Describe the GGNS core design for the first EPU cycle. If the EPU core design is comprised of any other fuel types (including other GE fuels), then justify how using a GNF2 equilibrium core provides bounding results for EPU.

**Response**

The power uprate evaluation process as outlined in the CLTR is based on a representative equilibrium core design. This is specified in Section 1.3 of the NEDC-33173-P-A as well: “An equilibrium cycle core design is the generic approach applied in each of these methods for reactor core and fuel performance related evaluations supporting license change requests.” Therefore, a GGNS EPU 24-month representative equilibrium core has been applied for all applicable evaluations (several evaluations are dispositioned to the cycle-specific analysis). In addition, the equilibrium GNF2 core was used for the accident and dose consequence evaluations where the higher batch fractions make it conservative. However, there are some evaluations performed for both GE14 and GNF (e.g., Reactor Internal Pressure Difference (RIPDs)) and it is acknowledged that GE14 is bounding.

The initial EPU core will contain both GE14 and GNF2 fuel types. Since the initial EPU core will contain two batches of GNF2 and one twice burned batch of GE14, GNF2 will dominate the core response. The transition core, including any remaining GE14, is evaluated at the time of the reload analysis.

**RAI # 5**

Pellet clad interaction (PCI) and stress corrosion cracking (SCC) phenomena can cause clad perforation resulting in leaking fuel bundles and resultant increased reactor coolant activity. Therefore, the staff requests the licensee to provide the following additional information regarding PCI/SCC for GGNS at EPU conditions:

- a. Describe whether GNF2 fuel design has barrier cladding which have built-in PCI resistance.
- b. Describe any differences in operating procedures associated with PCI/SCC at EPU conditions versus pre-EPU operations.
- c. From the standpoint of PCI/SCC, discuss which of the Anticipated Operational Occurrences (AOOs), if not mitigated, would most affect operational limitations associated with PCI/SCC.

**Non-Proprietary**

- d. For the AOOs in part c), discuss the differences between the type of required operator action, if any, and the time to take mitigating actions between pre-EPU and EPU operations.
- e. If the EPU core will include fuel designs with non-barrier cladding which have less built-in PCI resistance, then demonstrate by plant-specific analyses that the peak clad stresses at EPU conditions will be comparable to those calculated for the current operating conditions.
- f. Describe operator training on PCI/SCC operating guidelines.

**Response**

- a. At the startup from the upcoming EPU outage, the GGNS core is expected to consist of GE14 and GNF2 fuel types, both of which have barrier cladding.
- b. The fuel vendor, Global Nuclear Fuel (GNF), provides operating recommendations associated with PCI/SCC. These operating recommendations are the same for pre-EPU and post-EPU conditions. Basically, these operating recommendations (soft duty guidelines) allow unrestricted operation below a threshold linear heat rate, which is a function of nodal exposure. The threshold value does not change with EPU. Power level rate restrictions are imposed above the threshold until a 'conditioned envelope' is obtained. The effect of EPU would be that some bundle nodes would be ramped to a slightly higher power level, and therefore would have a slightly higher conditioned envelope at rated power. Supporting evidence that these operating recommendations are effective with EPU operation is provided by the successful use of the recommendations in operation of many plants and cycles already at EPU conditions (or at uprates between 105 and 120% or original rated power) without a PCI/SCC failure to date.
- c. From the standpoint of PCI/SCC, the AOO that would most affect operating limitations associated with PCI/SCC is the Loss of Feed Water Heater AOO. This is a relatively slow transient, however the power increases associated with this event might exceed the ramp rate increases recommended by the 'soft duty guidelines.' This could reduce the margin to fuel failures associated with PCI/SCC. However, with barrier fuel, no fuel failures associated with PCI/SCC for this AOO are expected; no fuel failures in GNF barrier fuel have occurred to date in any plants from a Loss of Feedwater Heating AOO. Furthermore, operating procedures specify a reduction in core recirculation flow early in the event, which reduces the increases in nodal powers, so that failures, even with non-barrier fuel, are not likely or expected.
- d. As discussed in response to "c," no PCI fuel failures associated with this AOO with barrier cladding fuel are expected and no operator actions are required. However, to improve

**Non-Proprietary**

**Non-Proprietary**

margin to PCI failures and to be in alignment with GNF's operational guidelines associated with PCI/SCC, a mitigating action in this event is for operations to reduce the increases in nodal powers by reducing core recirculation flow early after the initiation of the event. There is no difference in the type or time to take this mitigation action of reducing core flow, especially with barrier cladding fuel.

- e. At the startup from the upcoming EPU outage, the GGNS core is expected to consist of GE14 and GNF2 fuel types, both of which have barrier cladding.
- f. The GGNS operators are trained on the need for fuel pre-conditioning limits to mitigate the potential for fuel damage due to PCI/SCC. This training includes learning objectives regarding the causes of PCI/SCC, the primary factors affecting PCI/SCC, the purpose of fuel pre-conditioning, and the benefits of barrier fuel designs. The concepts of fuel preconditioning envelopes, xenon transients, ramp rate restraints, and deconditioning are addressed.

**RAI # 6**

**Control Rod Drive (CRD) Scram Time**

It was stated in Section 2.8.4.1.1 of the PUSAR, "To address the expected increase in scram times, GGNS is implementing Option B scram times to maintain operating margin." Please provide the following additional information:

- a. Clarify the usage "Option B" scram times and their effects on transient and accident analysis.
- b. Explain how they maintain operating margin as well as ensure safe operation.
- c. Discuss the scram times assumed to perform AOO analyses for EPU, as presented in the PUSAR, and justify that it was conservative.

**Response**

- a. The use of Option B scram times is one of the Minimum Critical Power Ratio (MCPR) margin improvement options described in GESTAR II (NEDE-24011P-A-17-US, "General Electric Standard Application for Reactor Fuel," Revision 17, dated September 2010, United States Supplement, Section S5.1.5). Usage of Option B scram times refers to the establishment of a less restrictive Operating Limit Minimum Critical Power Ratio (OLMCPR) based on a conservative demonstration of AOO analysis results considering actual scram time performance. This option (and the relaxed operating limit) can be utilized when actual scram time performance is better than the scram times assumed in the transient analyses supporting the Technical Specification requirements for scram time performance.

**Non-Proprietary**

**Non-Proprietary**

The operating limits for both Option A and Option B scram times are controlled in the Core Operating Limits Report (COLR).

- b. As described above, the MCPR operating limits for the Option B scram times will provide additional operating margin.

The higher steam flow associated with EPU increases the pressurization rate during transients. Since scram speed is dependent on the reactor pressure response, this can result in slower scram times, which in turn, can contribute to a more restrictive operating limit. The relaxed operating limit under the Option B serves to maintain operating margin by crediting actual scram time performance that is better than that assumed in the transient analyses.

- c. Only the Technical Specification basis scram speeds were used in the EPU AOO analyses, which account for the effects of pressurization during the transient. Specifically, the analyses incorporate event specific scram speeds, which bound the Technical Specifications pressure dependent scram fraction versus time values. There was no credit for Option B scram speed for the EPU LAR Attachment 5 (i.e., PUSAR) analyses. The use of Option B scram times is requested in Section 4.1.8 of Attachment 1 to the GGNS EPU LAR (Accession Number ML102660403).

**RAI # 7**

**Reactor Core Isolation Cooling (RCIC)**

In Section 2.8.4.3.2 of the PUSAR it was stated, "GGNS plant procedures caution operators that damage may occur if the SP temperature exceeds 140°F with the RCIC suction aligned to the SP." As the SP temperature is expected to increase for EPU, discuss how this requirement is satisfied for EPU operation.

**Response**

The Reactor Core Isolation Cooling (RCIC) operating instruction provides a precaution that, except in an emergency, the RCIC suction temperature is not allowed to exceed 140°F to prevent equipment damage. This operator guidance precludes RCIC operation above this pool temperature. The RCIC system has been evaluated for short-term operation with suction temperatures as high as 170°F. The preferred and initial suction source for RCIC pump is from the Condensate Storage Tank (CST), which contains water at temperatures less than 140°F. Although the suppression pool peak temperature has been determined to increase for EPU, the RCIC system is not credited to take suction from the suppression pool in any accident in which the pool temperature is greater than 140°F.

**Non-Proprietary**

**Non-Proprietary**

**RAI # 8**

**Transient and Accident Analyses**

Please provide the following additional information regarding the Loss of One Feedwater Pump analysis performed in support of EPU operation at GGNS:

- a. Provide plant-specific result for Loss of One Feedwater Pump event showing water level vs. time. (Similar to Fig. 2.8-21 of PUSAR.)
- b. It was stated in Section 2.8.5.2.3.2 of PUSAR that the Loss of One Feedwater Pump event only addresses operational considerations to avoid reactor scram on low reactor water level (Level 3). This requirement is intended to avoid unnecessary reactor shutdowns. Clarify whether Level 3 scram was avoided for this event at EPU condition; and if not, explain how this requirement was addressed.

**Response**

- a. Figure 8-1 provides a plant-specific plot of level vs. time along with the Level 3 setpoint for the Loss of One Feedwater Pump event. This simulation is based on an installed capacity of 70.5% of EPU feedwater flow for the feedwater system after the pump trip. This result is conservative, as the installed capacity has been evaluated to be greater than 80%; providing even greater margin to the Level 3 setpoint.
- b. Analyses at EPU conditions have been performed and show that the Level 3 scram is avoided. Figure 8-1 shows margin to the Level 3 scram for the Loss of One Feedwater Pump event.

Non-Proprietary

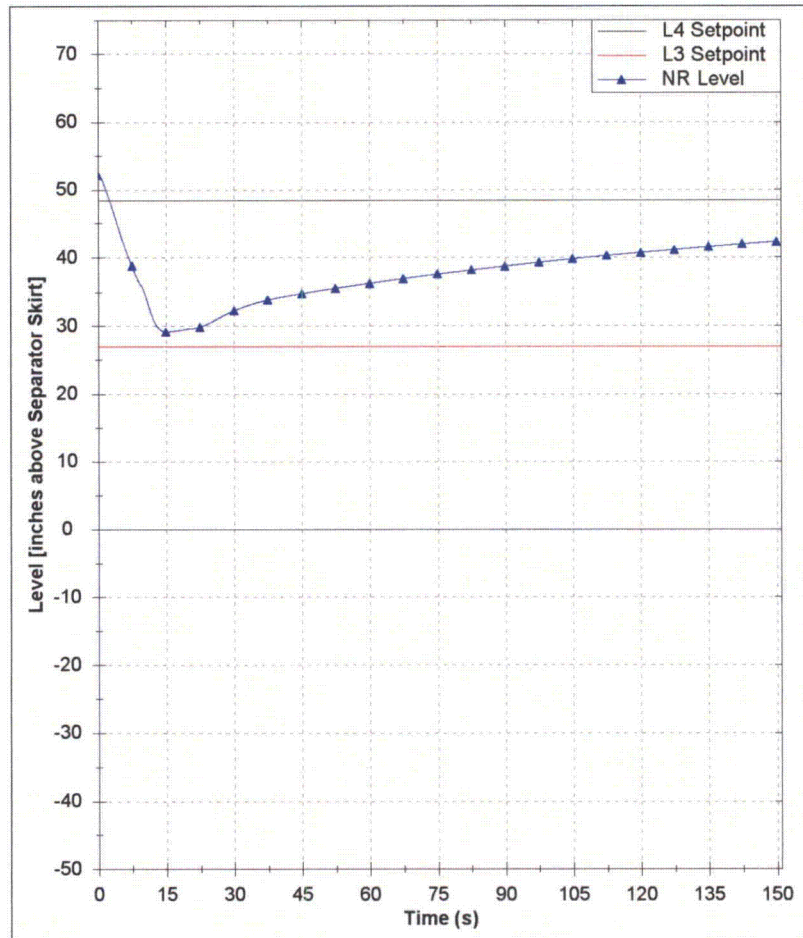


Figure 8-1 - Single Feedwater Pump Trip Level Response

#### **RAI # 9**

In Section 2.8.4.2 of the PUSAR, it was stated, “....based on both plant initial core analyses and subsequent power uprate evaluations, the MSIVF is more limiting than the TT event with respect to reactor overpressure. The EPU evaluations show a 40 to 50 psi difference between these two events.” If an analysis was performed for the Turbine Trip with Bypass Failure and Scram on High Flux (TTNBPF), as it is required in Table E-1 of ELTR-1, please provide a plot comparing the pressure transients for the Main Steam Isolation Valve Closure with Scram on High Flux (MSIVF) and the TTNBPF events. If a TTNBPF analysis was not performed for EPU, then justify why not.

Non-Proprietary

Non-Proprietary

**Response**

A TTNBPF analysis was performed for EPU and the peak reactor pressure as measured in the steam dome was confirmed to be approximately 40 psi lower than the MSIVF event. Figure 9-1 below is the system response for the TTNBPF and the MSIVF events.

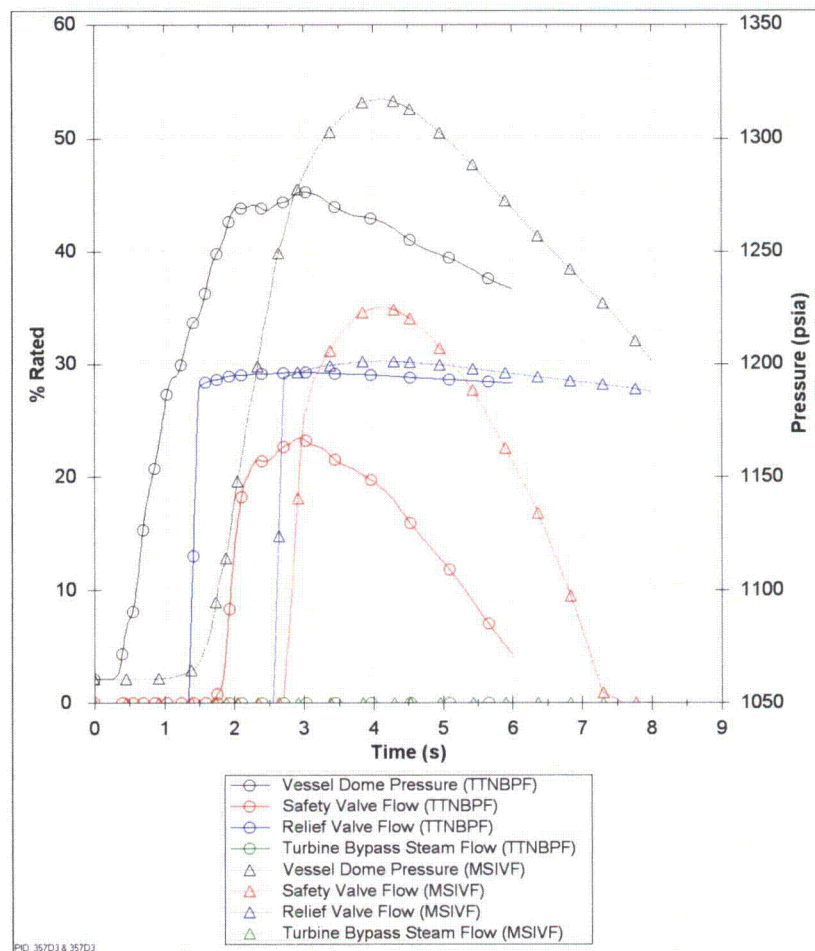


Figure 9-1 – Compare Plot of TTNBPF and MSIVF Events

**Non-Proprietary**

**RAI # 10**

In Table 2.8-5 of the PUSAR, the most limiting fuel thermal margin event was listed as the Generator Load Rejection with Steam Bypass Failure (LRNBP) event having delta-CPR equal to 0.23. What are the delta-CPR values for the MSIVF event and for the Turbine Trip with Bypass Failure and Scram on High Flux (TTNBPF) event? If the delta-CPR value is higher than 0.23 for either of these events, then discuss why the event was not considered as the limiting fuel thermal margin event?

**Response**

The MSIVF and TTNBPF events are special events performed for ASME overpressure compliance. Section S.3 of "General Electric Standard Application for Reactor Fuel (Supplement for United States)," NEDE-24011-P-A-17-US, Revision 17, dated September 2010, describes the background for the ASME overpressure compliance. These events have an additional failure and are not normal AOOs for consideration in determining the Operating Limit MCPR. Therefore, a  $\Delta$ CPR calculation is not applicable for these events.

**RAI # 11**

Please provide the following additional information regarding the LOCA analysis performed in support of EPU operation at GGNS:

- a. Discuss the reasons, supported by analytical results, at what flow rate, i.e., minimum flow, rated flow, or increased core flow (shown as state-points C, D or E in the Power-Flow (P/F) map for EPU in Fig. 1-1 of the PUSAR) the most conservative PCT occurs. Confirm that the GGNS licensing Basis PCT for EPU and CLTP were calculated at the most conservative state-point in the P/F map, and identify those state-points for EPU and CLTP. If the state-points are different for pre-EPU and EPU condition, explain why.
- b. Discuss the limiting single-failures for EPU and CLTP for Large-Break (LB) and Small-Break (SB) LOCA analyses. If the limiting single-failure changed from pre-EPU to EPU, then explain why.
- c. What are the limiting break sizes for the worst SB-LOCA for EPU and CLTP conditions?
- d. Provide the vendor (GEH) prepared report on the ECCS-LOCA analyses for GGNS at EPU power using SAFER/GESTER methodology.



**Non-Proprietary**

**Response**

- a. The ECCS-LOCA analysis was performed in keeping with the provisions of "Licensing Topical Report Generic Guidelines for General Electric Boiling Water Reactor Extended Power Uprate," NEDC-32424P-A, dated February 1999. To show acceptability of the EPU, the ECCS-LOCA analysis is performed for a representative break spectrum, or a reference to an applicable break spectrum analysis provided. Given the limiting break location and sizes of the current licensing basis analysis, the EPU analysis is performed to address the extension of the operating domain represented by the EPU. Table 11-1 below shows peak clad temperature (PCT) results under Appendix K assumptions for Power/Flow Points C and D, with reference to Figure 1-1 of Attachment 5 to the GGNS EPU LAR. The fact that the state points at which the limiting PCT for the large break scenario occurs at a different state point at CLTP than at EPU is attributed to the level in the core beginning to recover during core reflood and the effectiveness of the secondary heat transfer mechanisms such as steam cooling in overcoming the temperature excursion at the respective state points. The limiting condition for the small break occurs at EPU and is attributed to the increased decay heat associated with EPU, which results in a longer ADS blowdown and a higher PCT.

Table 11-1

[[			
			]]

[[ ]]

Increased core flow conditions shown as Point E on the EPU power flow map in Figure 1-1 of Attachment 5 of the GGNS EPU LAR are characterized by [[

]] Therefore, increased core flow conditions were qualitatively addressed in both the GGNS CLTP Analysis of Record as well as the EPU SAFER/GESTR-LOCA analysis and not specifically analyzed.

**Non-Proprietary**

The limiting power and core flow condition for the PCT of [[

]] it is used as the basis to assess the licensing basis PCT of 1690°F, used to demonstrate compliance to Acceptance Criteria of 10CFR50.46.

- b. As noted above, the EPU analysis references the previously licensed analysis for GGNS and extends the analysis to accommodate the expanded power/flow domain. No feature about the EPU would cause a change to the limiting single failures previously determined and analyzed for the current licensing basis. By methodology, if substantial margin is not demonstrated in the current analysis, confirmatory cases would be analyzed to assure identification of the limiting single failure. This was not the case with GGNS as ample PCT margin was demonstrated previously for alternate assumed single failures compared with the [[ ]] failure as analyzed for the CLTP basis. Therefore, only the [[ ]] failure is analyzed for EPU conditions to account for the change for the power uprate.
- c. The analysis PCT results presented above (Table 11-1) have been annotated to indicate the limiting small break sizes, both for CLTP and EPU, each at rated core flow and similar single failure. Confirmatory calculations have been performed to assure identification of the worst break size.
- d. A GEH prepared report with proprietary markups on the ECCS-LOCA analyses for GGNS at EPU power using the SAFER/GESTER methodology was not generated. As indicated above, the approach of LTR NEDC-32424P-A is to extend the base SAFER/GESTR analysis, which has previously determined a limiting case for ECCS-LOCA Acceptance Criteria compliance, and to expand the operating range to show acceptability of the EPU.

**RAI # 12**

It is stated in Section 2.8.5.7.1 of the PUSAR that the limiting ATWS event with respect to RPV overpressure for GGNS is ATWS-MSIVC event and that the ATWS-PRFO event produces the highest peak upper plenum pressure at SLCS initiation (1205 psia). Please provide the following additional information:

- a. What core flow was assumed for these analyses? The staff believes that in order to maximize the pressure, the Increased Core Flow (ICF) condition of 105% core flow should have been assumed. Confirm that it was; otherwise explain.
- b. Compare the highest peak upper plenum pressure at SLCS initiation for CLTP and EPU conditions, and justify that sufficient margin remain available in the setpoint for the SLCS pump discharge relief valve at EPU condition.

**Non-Proprietary**

**Non-Proprietary**

**Response**

- a. The Maximum Extended Load Line Limit Analysis (MELLLA) initial condition was used for this analysis, which is at 92.8% core flow. The highest peak upper plenum pressure after Standby Liquid Control System (SLCS) injection occurs well after the recirculation pumps have coasted down such that the difference in driving head between initial MELLLA and ICF conditions is not relevant. The MELLLA condition starts from a higher rod line than ICF and produces the maximum integrated power and demand for the safety relief valves. The peak upper plenum pressure is primarily driven by the safety relief valve opening setpoints and the pressure drop from the SRVs to the upper plenum.
- b. The peak Anticipated Transient Without Scram (ATWS) upper plenum pressure during SLCS operation is 1136 psig for CLTP conditions and 1190.3 psig (1205 psia) for EPU conditions. These pressures result in an SLCS pump discharge pressure of 1283 psig for CLTP conditions and 1337.3 psig for EPU conditions. The relief valve margin for EPU, as identified in Attachment 5, Section 2.8.4.5.2 of the GGNS EPU LAR is 305.9 psi, based on a pump relief valve minimum setpoint of 1643.2 (cold differential set pressure of 1694 psig minus 3% tolerance). A margin of 30 psi from the minimum relief valve setpoint is considered sufficient.

**RAI # 13**

In Table 2.8-9 of PUSAR, the results for ATWS analysis were presented. Please provide the following additional information:

- a. Confirm that the peak SP temperature of 165 F for EPU was obtained for the ATWS-PRFO event, and compare this result with the GGNS design limit for peak SP temperature for ATWS.
- b. The higher core power and decay heat for EPU should have resulted in higher SP temperature for EPU. Explain why the peak SP temperature remains same (165 F) for both CLTP and EPU.

**Response**

- a. It is confirmed that the peak suppression pool temperature was obtained from the ATWS-PRFO (Pressure Regulator Failure Open) event. The ATWS-PRFO event bounds the ATWS-MSIVC (Main Steam Isolation Valve Closure) event by less than 1°F. The peak value of 165°F (EPU LAR Attachment 5, Table 2.8-11) is less than the design limit of 210°F, which is stated under the Technical Evaluation reflected in Section 2.8.5.7 of Attachment 5 of the EPU LAR.

**Non-Proprietary**

- b. The decay heat is not a large component of the load for the ATWS analysis. In an ATWS event, power is first reduced by the ATWS recirculation pump trip, followed by level reduction and SLCS injection (See Figures 13-1 and 13-2 below). As the core flow is reduced, both the EPU power level and CLTP level reach a very similar absolute power as both conditions initiate from the MELLLA boundary. The level reduction and SLCS injection both have a similar power reduction effect independent of the initial power level. For GGNS, hot shutdown is achieved in approximately 11 minutes, and in this time frame, it is the elevated core power that is produced prior to hot shutdown that is the primary heat load, not the decay heat.

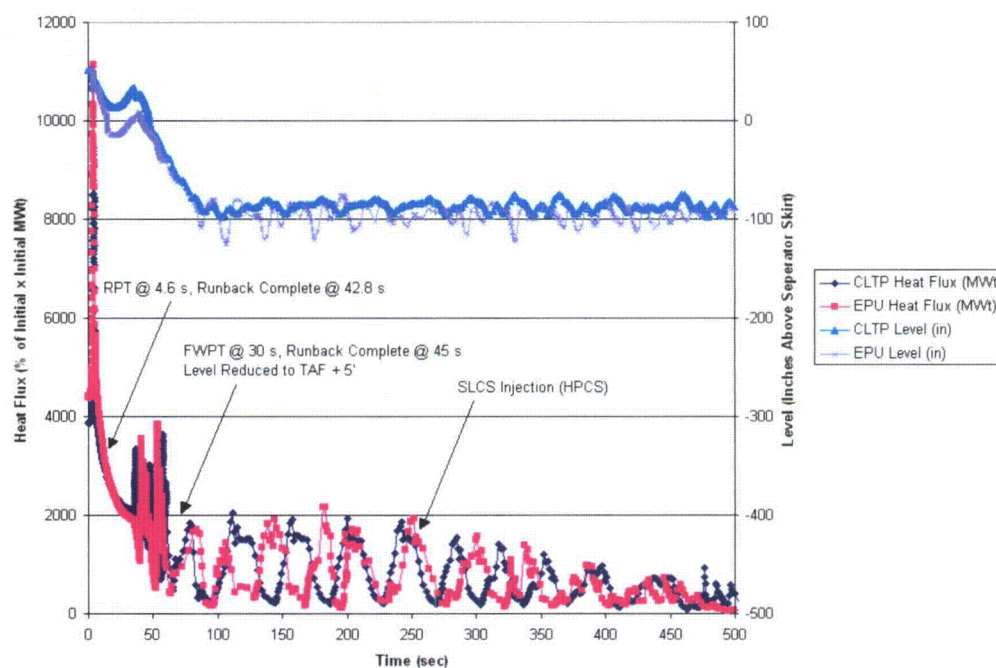


**Figure 13-1 – EOC MSIVC Heat Flux, Level vs. Time**

Non-Proprietary

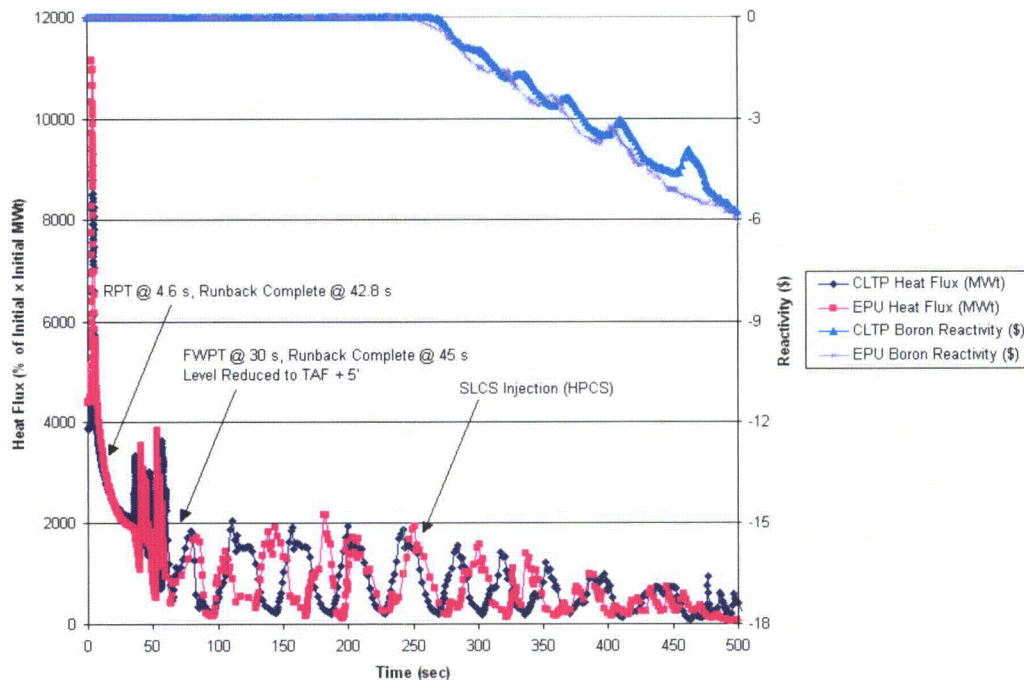


Figure 13-2: EOC MSIVC Heat Flux, Reactivity vs Time

#### RAI # 14

In Table 2.8-8 of PUSAR, the key inputs for ATWS analysis were provided. Please provide the following additional information:

- With higher core power, increased steam flow and higher vessel peak pressure for EPU, explain why five (5) SRVs can be out-of-service (OOS) during EPU, vs. only one (1) SRV can be OOS during CLTP in order to meet the safety limits.
- Which decay heat model was used for EPU ATWS analysis; and are all the inputs for ATWS analysis consistent with ELTR1 guidelines for ATWS input parameters? If not, justify.

#### Response

- The CLTP reference values provided in Attachment 5 of the EPU LAR were based on the latest ATWS analysis of record for GGNS; however, additional analyses have shown that the CLTP power level also produces acceptable peak pressure results for five SRV OOS.
- The May-Witt decay heat model is used in the ATWS analysis. The May-Witt correlation bounds the ANSI/ANS-5.1-1979 + 2 $\sigma$  decay heat model. It is confirmed that the inputs for

Non-Proprietary

**Non-Proprietary**

the ATWS analysis are consistent or are more conservative than the guidelines specified in Section L.3.4 of Appendix L to ELTR-1.

**RAI # 15**

**Bypass Voiding**

Characterize the expected amount of bypass voiding under CPPU conditions. Provide the expected bypass void level at points A, C, and D of Figure 1.1 of NEDC-33477P, Rev 0, using a methodology equivalent to that used by ISCOR for both hot and average channel.

**Response**

Points D, C, and A of Figure 1-1 are at the following Power/Flow Statepoints:

Point	Power (% Rated)	Flow (% Rated)	Core Average D-Level Bypass Voids (%)	Hot Channel D-Level Bypass Voids (%)	Core Average TAF Bypass Voids (%)	Hot Channel TAF Bypass Voids (%)
D	100	100	0	0	0	1.2
C	100	92.8	0	0	0	1.6
A	46.9	25.9	14.9	24.1	16.1	25.3

For Points D and C, the Core Average and Hot Channel D-Level Bypass Voiding is shown to be less than 5% when operating at steady state conditions within the MELLLA boundary (note that this is the MELLLA+ boundary in the requirement of Limitation 9.17).

For Point A, the Core Average and Hot Channel Bypass Voiding values at the D-level are shown above. The Core Average and Hot Channel Bypass Voiding values are also shown at the Top of Active Fuel (TAF) location and confirmed to be less than 17% and 29%, respectively. These values are not specific criteria, but ranges for bypass voiding for the MELLLA operating domain as shown in Sections 5.4, 6.1.1.1, and 6.2 of NEDC-33173-P-A, Revision 1, "Applicability of GE Methods to Expanded Operating Domains," September 2010. Note also that ISCOR conservatively calculates the hot channel bypass voiding using its direct moderator-heating model and providing no credit for cross flow while applying conservative hot channel bypass heating. The core average bypass void fraction calculated by ISCOR has also been shown to have additional conservatism.

**RAI # 16**

**Effect of bypass voids on instrumentation during normal operation**

Reliability of the local power range monitor (LPRM) instrumentation and accurate prediction of in-bundle pin powers typically requires operation with bypass voids lower than 5% at nominal conditions (e.g. point D of Fig 1.1 of NEDC-33477P, Rev 0). If the expected bypass void

**Non-Proprietary**

conditions at Constant Pressure Power Uprate (CPPU) are greater than 5%, evaluate the impact on (1) reliability of LPRM instrumentation, (2) accuracy of LPRM instrumentation, and (3) in-bundle pin powers.

**Response**

Per results noted in Section 2.8.2.4.1 of Attachment 5 of the EPU LAR (and in response to RAI 15), bypass void conditions at EPU are not expected to be greater than 5% at Point D of the power/flow map.

**RAI # 17**

**Effect of bypass voids on instrumentation to detect and suppress (D&S) unstable oscillations**

The presence of bypass voids affects the LPRM calibration. Evaluate the expected calibration error on OPRM and APRM cells induced by the expected level of bypass voids. Document the impact of this error on the D&S Option III scram setpoint.

**Response**

The effect of LPRM calibration errors on the Oscillation Power Range Monitor (OPRM) system scram amplitude due to bypass voiding would be less than 5% (see Section 6.2 of the Safety Evaluation in GE Energy Nuclear, "Applicability of GE Methods to Expanded Operating Domains," NEDC-33173P-A Revision 1, Class III (Proprietary), September 2010). This translates to 0.01 difference in OPRM amplitude setpoint.

In accordance with the Stability Setpoints Adjustment Limitation in Section 6.2 of the Safety Evaluation in NEDC-33173P-A, a 5% penalty was applied to the calculated OPRM amplitude setpoint, which translates to a 0.01 decrease. The OPRM amplitude setpoints presented in Section 2.8.3 of Attachment 5 of the EPU LAR includes the 0.01 setpoint penalty due to LPRM calibration errors.

The APRM system is not used for detect and suppress of thermal-hydraulic oscillations, therefore there is no effect of APRM calibration errors on the D&S Option III scram setpoint.

**RAI # 18**

**D&S Setpoint calculations**

Table 2.8-2 only shows Option III Setpoint Demonstration. Please provide an example setpoint calculation for Cycle 19 including an uncertainty term reflecting the possible LPRM miss-calibration under bypass void conditions.

**Non-Proprietary**

**Response**

Table 2.8-2 of Attachment 5 to the EPU LAR shows the Option III setpoint for the EPU equilibrium core.

The following is an example of the calculational method used to determine the OPRM setpoint for the two-pump trip event, which is the more limiting of the two bounding stability events for the EPU equilibrium core.

For an OPRM setpoint of 1.09, the hot channel oscillation magnitude was calculated as  $\Delta h = [ ]$  for GGNS based on the statistical methodology described in NEDO-32465-A, *Reactor Stability Detect and Suppress Solutions Licensing Basis Methodology for Reload Applications*, dated August 1996. The Delta Critical Power Ratio (CPR) over Initial CPR (ICPR) Versus Oscillation Magnitude (DIVOM) slope was calculated as  $[ ]$  for the GGNS EPU equilibrium core. In order to protect the Safety Limit Minimum Critical Power Ratio (SLMCPR), the initial Minimum Critical Power Ratio (IMCPR) is determined using the following relationship (Section 4.5.1 of NEDO-32465-A):

$$IMCPR > SLMCPR / (1 - \Delta CPR/ICPR)$$

$\Delta CPR/ICPR$  in the above equation is the product of  $\Delta h$  and DIVOM slope. For the EPU equilibrium core, SLMCPR is 1.10 including the steady-state uncertainties resulting from LPRM calibration. Therefore, MCPR at the start of the oscillations is calculated as follows:

$$IMCPR > [ ]$$

It was determined from a PANAC11 analysis that this IMCPR after the pump trip will be attained if the MCPR at rated conditions prior to the pump trip, OLMCPR(2PT), is 1.364.

This OLMCPR(2PT) is to be compared to the transient-based OLMCPR. Per Limitation and Condition 9.19 of NEDC-33173P-A Revision 1, *Applicability of GE Methods to Expanded Operating Domains*, dated September 2010, 0.01 is added to OLMCPR(2PT):

$$OLMCPR(2PT) = 1.364 + 0.01 = 1.374$$

The OLMCPR(2PT) value of 1.374 was calculated for an OPRM setpoint of 1.09. In order to account for impact of the setpoint uncertainties resulting from bypass voiding discussed in the response to RAI 17, 0.01 is subtracted from the setpoint and the result is conservatively reported as applying to the reduced setpoint (as reported in Table 2.8-2 of Attachment 5 of the EPU LAR). Hence, the minimum OLMCPR that can be supported based on a two recirculation pump trip event is 1.374 for an OPRM setpoint of 1.08.

Thus, this OLMCPR value accounts for the LPRM calibration uncertainty due to bypass voiding.



**Non-Proprietary**

The above methodology will be applied to the Cycle 19 core design to determine the cycle-specific OPRM setpoint, which will be reported in the Cycle 19 Supplemental Reload Licensing Report.

**RAI # 19**

**DIVOM slope for Cycle 19 under CPPU conditions**

The DIVOM slope does not include in Table 2.8-2 under CPPU conditions. Please provide DIVOM slope for Cycle 19.

**Response**

The DIVOM slope calculated for the EPU equilibrium core is [[        ]]. The DIVOM slope for Cycle 19 is calculated as part of the cycle-specific reload licensing analysis, and will be available prior to startup from the Spring 2012 refueling outage.

**RAI # 20**

**Interface between GE Methods and existing Solution EI-A hardware**

Provide a short summary of the stability-related hardware currently installed in GGNS (Solution EI-A, III, and or DSS-CD)). Provide a plan for transition between methods. Are there any issues related to the interface between the existing hardware and GE methods?

**Response**

GGNS currently operates with the Option E1A stability solution, which is described in NEDO-32339-A, Revision 1, *Reactor Stability Long-Term Solution: Enhanced Option I-A*, dated April 1998.

The transition from Option E1A to Option III is to take place during the Spring 2012 refueling outage with the removal of the GGNS Neutron Monitoring System hardware used for Option E1A and the installation of the new Power Range Neutron Monitoring (PRNM) system, which is required for Option III. Since Option E1A hardware and the PRNM hardware will not co-exist, there are no interface issues.

An LAR, *Grand Gulf Unit 1, License Amendment Request Regarding Power Range Neutron Monitoring System Upgrade*, (Accession Number ML093140463), dated November 3, 2009, has been submitted separately for the installation of the PRNM hardware and implementation of Option III stability solution at GGNS. Following PRNM System installation and startup from the 2012 refueling outage, Entergy will conduct a 90-day monitoring period in which Option III

**Non-Proprietary**

hardware will be operated in an "indicate only" mode. This monitoring period is discussed in Section 3.3 of the PRNM LAR.

The Detect and Suppress Solution – Confirmation Density (DSS-CD) stability solution has not yet been installed at GGNS. Its future installation and use at GGNS was addressed in the response to RAI #3 of Entergy Letter GNRO-2010-00035 to NRC dated May 18, 2010, *Responses to NRC Requests for Additional Information Pertaining to License Amendment Request for Power Range Monitoring System (TAC No. ME2531)* (Accession Number ML101410094).

**RAI # 21**

**ATWS EPGs**

What version of emergency operating guidelines is currently implemented in GGNS? Provide a short description of the process used to ensure that the EPG variables (e.g. HSBW, HCTL) are adequate under CPPU conditions.

**Response**

GGNS is currently applying emergency operating guidelines based on BWR Owners' Group Emergency Procedure and Severe Accident Guidelines, Revision 2. The Emergency Procedure Guidelines (EPGs) are reviewed for impact as part of the standard plant modification process, which includes the implementation of EPU. This process ensures any impacts are identified, with the applicable calculations and procedures updated, before implementation of the modification. In addition, the operators are trained on any changes in the procedures.

**RAI # 22**

**ATWS/Stability**

Provide a short description of how the Stability Mitigation Actions (e.g. immediate water level reduction and early boron injection) are implemented in GGNS. Does operation at CPPU conditions require modification of any operator instructions?

**Response**

In the event of an ATWS (i.e., where any control rod is not inserted to or beyond position 02 and the reactor will not remain subcritical without boron), the operator is directed by GGNS Emergency Procedures to immediately:

- initiate standby liquid control (SLC) if reactor power is above 4% or the suppression pool temperature is greater than or equal to 110°F; and

**Non-Proprietary**

**Non-Proprietary**

- lower level to reduce subcooling, while ensuring SLC injection, CRD and RCIC flows are maintained, if reactor power is above 4% or unknown. The first target level is -70 inches, with a second target level at approximately the top of active fuel if the suppression pool temperature exceeds 110°F.

The ATWS Core Instability analysis basis supporting EPU is unchanged and is based on the same analyses (EPU LAR Attachment 5, References 77 and 78) as the CLTP basis. Thus, operation at EPU conditions does not require any modifications to the operator instructions for stability mitigating actions.

**RAI # 23**

**Plant-Specific OPRM System**

GGNS will operate under Option III solution. Please provide a clarification for the following areas:

- a. Describe the process that was followed by GGNS to implement Option III L/T Stability Solution and to verify that Option III is still applicable under CPPU operation.
- b. Describe the expected effects of CPPU operation on Option III.
- c. Describe any alternative method to provide detection and suppression of any mode of instability if licensed OPRM scram becomes unavailable.
- e. Provide a summary of the GGNS Technical Specifications affected by the Option III implementation and future CPPU operation.
- f. Provide approved methodologies used to calculate the OPRM setpoint by the current operation and future GGNS CPPU operation.

**Response**

- a. The process followed by GGNS to implement the Option III Long Term Stability Solution is described in the PRNM LAR (*Grand Gulf Unit 1, License Amendment Request Regarding Power Range Neutron Monitoring System Upgrade*, Accession Number ML093140463, dated November 2009). Validity of the Option III solution at EPU conditions has been shown generically in *Constant Pressure Power Uprate*, NEDC-33004P-A, Revision 4, (Proprietary), July 2003; and NEDO-33004-A, Revision 4, (Non-Proprietary), July 2003. The Option III solution has plant and cycle-specific features, such as the OPRM trip-enabled region, OPRM trip setpoint, and Backup Stability Protection region. Section 2.8.3 of Attachment 5 of the EPU LAR established the basis for the plant-specific feature, namely the OPRM trip-enabled region at EPU conditions. A demonstration analysis for the EPU

**Non-Proprietary**

**Non-Proprietary**

conditions is also presented in Attachment 5, Section 2.8.3 of the EPU LAR. The cycle-specific features are to be developed with the reload analysis.

- b. The EPU expands the operating domain beyond in a region of the power to flow map where the plant is not susceptible to thermal-hydraulic instability events. There may be an indirect effect of EPU due to the core design changes. As shown in the response to RAI #24, such effects on the plant stability characteristics are minimal. Furthermore, the OPRM Setpoints and Backup Stability Protection regions are generated, and the OPRM Trip-enabled region boundaries are confirmed each reload. Therefore, EPU does not affect the applicability of the Option III solution.
- c. The Backup Stability Protection at GGNS is discussed in response to RAI#1 for PRNM LAR (Entergy Letter to NRC dated May 18, 2010, *Responses to NRC Requests for Additional Information Pertaining to License Amendment Request for Power Range Monitoring System (TAC No. ME2531)* (Accession Number 101410094)). There is no change to the Backup Stability Protection implementation with EPU.
- d. Not used.
- e. The changes to the Technical Specifications due to the installation of the PRNM System and the implementation of Option III long-term stability solution are listed in the PRNMS LAR (Accession Number ML093140463) for the CLTP conditions. EPU affects LCO 3.3.1.1 Condition K, SR 3.3.1.1.23, and Table 3.3.1.1-1 Function 2.f. The Technical Specification changes to update the PRNMS Technical Specifications to reflect EPU conditions are described in the EPU LAR Attachment 1, Section 4.1.10 and markups of the affected pages are provided in EPU LAR Attachment 2.
- f. There are no differences in the methodology used to determine the OPRM setpoints for CLTP or EPU conditions; both use the approved methodology specified in NEDO-32465-A (*Reactor Stability Detect and Suppress Solutions Licensing Basis Methodology for Reload Applications, Licensing Topical Report*, dated August 1996). However, it should be noted that the setpoint penalties discussed in the response to RAI #18 are applied at EPU conditions. The OPRM setpoints are determined each cycle as a part of the reload analysis.

**RAI # 24**

**Hot Channel and Core-Wide Decay Ratio**

Provide a table of hot channel and core-wide decay ratios at the most limiting state point for the last cycles and the proposed CPPU condition. The purpose is to evaluate the impact of CPPU on relative stability of the plant, and the applicability of Option III to GGNS under these new conditions.

**Non-Proprietary**

**Non-Proprietary**

**Response**

The core decay ratio and hot channel decay ratio was calculated at the intersection of the Natural Circulation Line (NCL) and High Flow Control Line (HFCL) for the same EPU equilibrium core that was used in the demonstration analyses in Attachment 5 of the EPU LAR. The decay ratios were also calculated for the CLTP equilibrium core, at the same absolute power / flow values. The results are summarized in the table below. As can be seen from the table, the difference between the decay ratios calculated for EPU and CLTP conditions is negligible.

Also note that the Backup Stability Protection regions are generated for each reload. Therefore, while a change in decay ratio may affect the size of the scram and controlled entry regions, it does not affect the applicability of Option III.

[[						
						]]

**RAI # 25**

**Suppression Pool Cooling**

Describe any effects or impacts, if any, of EPU on suppression pool cooling during isolation ATWS events and/or EOPs.

**Response**

As noted in the "Constant Pressure Power Uprate" Licensed Topical Report (NEDC 33004P-A, Revision 4 dated July 2003), "An ATWS event under EPU conditions has the same symptoms and requires the same operator actions as under the pre-uprate conditions. These actions are consistent with the BWR EPGs [Emergency Procedure Guidelines]."

As demonstrated in the response to RAI 13, the peak suppression pool temperature response to an ATWS event at GGNS is similar between the CLTP and EPU conditions. Thus, the EPU does not affect the suppression pool cooling or the Emergency Operating Procedures (EOPs) during an ATWS event.

**Non-Proprietary**

**RAI # 26**

**ECCS NPSH Requirements**

Provide the GGNS ECCS net positive suction head (NPSH) requirements. Are these affected by the CPPU upgrade?

**Response**

Required NPSH is a design characteristic associated with a particular pump. It is typically provided by the pump vendor, determined by vendor testing, and provided along with the pump flow-head curve. The required NPSH for the GGNS ECCS pumps are provided below. These values are the required head at a reference datum that is 3 ft above the pump mounting flange. Emergency Core Cooling System (ECCS) pump  $NPSH_R$  is not affected by EPU.

Pump	$NPSH_R$ (ft)
RHR (all 3 pumps)	2.0
LPCS	1.6
HPCS	2.0

Available NPSH has been reduced for EPU due to an increase in the peak suppression pool temperature for the DBA-LOCA event. The effect of higher pool temperatures on available NPSH is summarized in the response to Containment and Ventilation Systems Branch RAI #20 (Accession Number ML110900586).

**RAI # 27**

**GGNS Simulator Update**

Please provide a short description of the simulator neutronic core model. Also, provide the schedule to show when the GGNS simulator is upgraded for EPU conditions.

**Response**

The neutronic core model for the training simulator is S3R, which is a real time version of the Studsvik's Simulate-3. The installed core model is updated at the beginning of each new operating cycle to match the core design for that cycle. The GGNS core is modeled in S3R with 16 axial nodes and one radial node for each of the 800 GGNS fuel assemblies. The core hydraulic inputs into the neutronic model are developed with the THOR model. The S3R model includes reactivity effects of changes in density, fuel temperature, control rod position, boron, and fission products such as xenon and samarium. The cross section model ranges from cold

**Non-Proprietary**

**Non-Proprietary**

to highly voided conditions, and is thus designed to go from startup all the way to transient and accident situations. The GGNS simulator modifications are scheduled for implementation by April 2012, prior to the GGNS planned startup for Cycle 19, which will include power ascension to the EPU power level.

**RAI # 28**

**Approved Methodologies**

Provide a list of approved methodologies used to support the calculation for Section 2.8.3 and 2.8.5.7 of the proposed CPPU LAR.

**Response**

The following approved methodologies were used in Attachment 5, Section 2.8.3 of the EPU LAR.

- NEDC-33173P GE Nuclear Energy, "Applicability of GE Methods to Expanded Operating Domains," NEDC-33173P, (Proprietary); and NEDO-33713, (Non-Proprietary), Revision 0, February 2006 (Reference 7).
- GE Nuclear Energy, "Reactor Stability Detect and Suppress Solutions Licensing Basis Methodology for Reload Applications," NEDO-32465-A, (Non-Proprietary), August 1996 (Reference 72).
- GE Nuclear Energy, "Licensing Topical Report, ODYSY Application for Stability Licensing Calculations Including Option I-D and II Long Term Solutions," NEDE-33213P-A, (Proprietary), April 2009; and NEDO-33213-A, (Non-Proprietary), April 2009 (Reference 76).

The approved methodologies used to support ATWS analyses (Section 2.8.5.7) are listed in Attachment 5, Table 1-1 of the EPU LAR. The applicable information from Table 1-1 is provided below.

Task	Computer Code*	Version or Revision	NRC Approved	Comments
Anticipated Transient Without Scram	ODYN	09	Y	NEDE-24154P-A Supp. 1, Vol. 4
	STEMP	04	(6)	
	PANACEA	11	Y(4)	NEDE-30130P-A
	ISCOR	09	Y(2)	NEDE-24011P Rev. 0 SER
	TASC	03A	Y	NEDC-32084P-A Rev. 2 (11)

\* The application of these codes to the EPU analyses complies with the limitations, restrictions, and conditions specified in the approving NRC SER where applicable for each code. The application of the codes also complies with the SERs for the EPU programs.

**Non-Proprietary**

**Non-Proprietary**

- (2) The ISCOR code is not approved by name. However, the SER supporting approval of NEDE-24011P Rev. 0 by the May 12, 1978 letter from D. G. Eisenhut (NRC) to R. Gridley (GE) finds the models and methods acceptable, and mentions the use of a digital computer code. The referenced digital computer code is ISCOR. The use of ISCOR to provide core thermal-hydraulic information in reactor internal pressure differences, Transient, ATWS, Stability, Reactor Core and Fuel Performance and LOCA applications is consistent with the approved models and methods.
- (4) The physics code PANACEA provides inputs to the transient code ODYN. The improvements to PANACEA that were documented in NEDE-30130P-A were incorporated into ODYN by way of Amendment 11 of GESTAR II (NEDE-24011P-A). The use of TGBLA Version 06 and PANACEA Version 11 in this application was initiated following approval of Amendment 26 of GESTAR II by letter from S.A. Richards (NRC) to G.A. Watford (GE) Subject: "Amendment 26 to GE Licensing Topical Report NEDE-24011-P-A, GESTAR II Implementing Improved GE Steady-State Methods," (TAC NO. MA6481), November 10, 1999.

TGBLA06 with Error Correction 5 was used in the GGNS Core Design analysis and it meets the requirements established by the Safety Evaluation for Licensing Topical Report NEDC-33173P (Reference 7).

- (6) The STEMP code uses fundamental mass and energy conservation laws to calculate the suppression pool heatup. The use of STEMP was noted in NEDE-24222, "Assessment of BWR Mitigation of ATWS, Volume I & II (NUREG-0460 Alternate No. 3) December 1, 1979." The code has been used in ATWS applications since that time. It has also recently been accepted in the NRC review of NEDC-33270, "GNF2 Advantage Generic Compliance with NEDE-24011-P-A (GESTAR II)." There is no formal NRC review and approval of STEMP.
- (11) The NRC approved the TASC-03A code by letter from S. A. Richards, NRC, to J. F. Klapproth, GE Nuclear Energy, Subject: "Review of NEDC-32084P, TASC-03A, A Computer Code for Transient Analysis of a Single Fuel Channel," TAC NO. MB0564, March 13, 2002.

**RAI # 29**

**Fuel Storage (Sections 2.8.6)**

Section 6.5.1 of NEDC-33621P discusses the use of a blocking device to prevent storage of fuel in certain cells. The section appears to conclude that misloading a bundle into a blocked location in Region II is not a credible event. Provide a quantitative analysis that evaluates the probability of occurrence of a fuel misloading event at GGNS, in order to support the licensee's

**Non-Proprietary**



**Non-Proprietary**

position that the event is not credible. Note that the NRC staff requested similar information in a recent application that attempted to use a similar approach to justify that a misloading event was not a credible event (ML091550832).

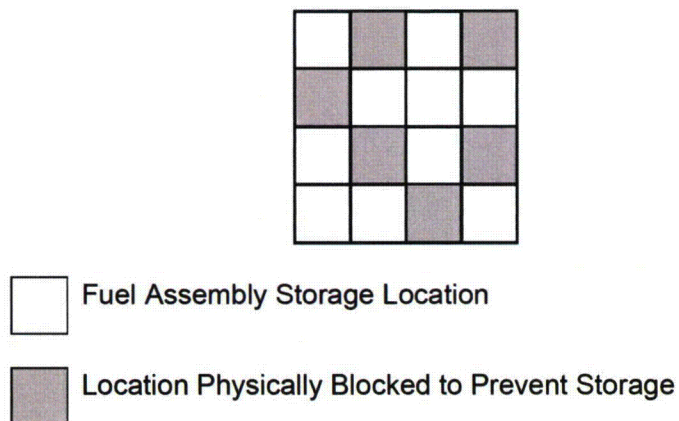
**Response**

**1.0 Introduction**

The following quantitative probability analysis addresses the likelihood of misloading a fuel bundle in a spent fuel pool (SFP) storage location that is restricted from fuel storage. The restrictions are required in order to comply with the requirements of the Region II spent fuel storage criticality analysis. This probability analysis concludes, based on GGNS processes and operating experience, that the probability of such an event is approximately  $2.70\text{E-}7/\text{year}$ . As discussed below, this analysis conservatively does not credit the number of potential misload locations in the SFP. Additionally, this result does not consider the consequences of such a misload event. The number of available fuel assemblies that would be expected to result in a challenge to the criticality safety analysis acceptance criteria is relatively small.

The GGNS criticality storage analysis of fuel storage rack areas where the presence of Boraflex is not credited (Region II), restricts the loading of fuel in the following pattern:

Region II 4X4 Storage Configuration



As illustrated by the figure above the Region II fuel storage configuration restricts 6 fuel storage cells of a 4x4 area. Additionally, isolated cells that meet the Region II Boraflex assumptions are also restricted from storing fuel. The fuel storage restrictions are reinforced with the installation of half-guides ( $\frac{1}{2}$  guide) which prevent the fuel from being inserted into a given storage location.

### **Non-Proprietary**

A ½ guide is an open box whose outside dimensions are similar to a fuel assembly. The ½ guide has a handle that allows the fuel handling mast to move the ½ guide into a spent fuel storage location. The ½ guide is much lighter than a fuel assembly and visually distinct from fuel assemblies.

All fuel movements are carefully planned activities. Fuel movement plans are developed and independently verified by trained and qualified individuals. This process is controlled by site procedures. The *ShuffleWorks* program is used to develop fuel movement plans. The *ShuffleWorks* model includes the Region II fuel loading restrictions which provide various user alerts if a movement plan is developed that attempts to load fuel into a restricted location.

Actual SFP movement activities are performed on the Fuel Handling Platform. Operation of the Fuel Handling Platform is performed by qualified trained personnel. A qualified platform operator and a spotter must be on the platform at all times during movement of the platform and/or any of the platform equipment. The two positions must be filled by separate individuals that are qualified and meet all requirements for their respective position. The operation of the bridge requires 3-way communication by the bridge operator and the spotter for all actions. The spotter independently verifies critical procedure steps.

## **2.0 Assumptions**

1. The likelihood that the initial ½ guide configuration is not known and documented is considered negligible. This is based on the fact that the initial configuration of fuel bundles and ½ guides in the SFP are carefully tracked and maintained by Reactor Engineering. In particular, the GGNS fuel movement procedure requires that the blocked locations must be confirmed to be properly indicated and blocked prior to storing fuel assemblies in the spent fuel racks.
2. The likelihood of making an error in a complex calculation using advanced computer codes is similar to a simple calculation using pen and paper. The code user must be qualified to run this code. However, the analyst can still make errors in input file development similar to the errors in performing simple calculations.
3. The results of the computer code output are reviewed both by the preparer and by an independent reviewer. A step-by-step walk-through of the fuel movement plan is also performed, using spent fuel maps and markers that represent fuel bundles and ½ guides. Based on these reviews, the likelihood of an initial error being detected during the review is taken to be 90%.

### **Non-Proprietary**

**Non-Proprietary**

4. The *ShuffleWorks* program restrictions on moving ½ guides are considered comparable to an annunciated display with a response by a single operator since the peer reviewer would not necessarily have to run *ShuffleWorks* for fuel pool moves.
5. Errors associated with moving a ½ guide instead of a fuel bundle are considered comparable to a check reading display error using an analog meter with easy limit marks. The first indication is the bundle is visually distinct from a ½ guide. The second is the weight differential, which is vastly different and is verified as part of fuel movement.
6. This evaluation does not credit the reactivity of the fuel bundle that is placed in the ½ guide location. The reactivity of many of the bundles is low enough that placing that fuel bundle in the ½ guide location would not challenge criticality. However, it is conservatively assumed that any fuel bundle will impact criticality.
7. This evaluation does not credit the proportion of the rack containing restricted locations. Currently Region II is a relatively small area of the rack but it may increase. Even if the entire rack was converted to Region II, only 38% of the fuel storage locations would be restricted and subject to these types of errors.

**3.0 Analysis**

Misloading a fuel assembly into a restricted storage location would require at least two errors in the fuel movement process to create the condition. The first error is to move a ½ guide from its designated position in the fuel pool. The second error involves moving a spent fuel bundle into that position. In addition, the differences between a ½ guide and a regular fuel bundle provide opportunities for the operator and spotter to detect the error and correct an error before it impacts the fuel storage configuration.

**3.1 Inadvertent ½ Guide Move from Region II**

An inadvertent move of a ½ guide from its designated position would involve either an error in the fuel movement plan or the bridge operator chooses the wrong movement location and the spotter not catching the error.

**3.1.1 Likelihood of an Error in the Fuel Movement Plan (FMP ERROR)**

This event looks at the likelihood of an error in the fuel movement plan that would contain an error that is not caught in the verification process. The fuel movement plan is prepared and independently verified by reactor engineering. The fuel movement plan is developed using a computer code called *ShuffleWorks*. U.S. Nuclear Regulatory Commission Report NUREG/CR-1278 (*Handbook of Human Reliability Analysis with Emphasis on Nuclear*

### Non-Proprietary

*Power Plant Applications*, by Swain, A.D. and H.E. Guttman, dated August 1983), page 3-27, predicts a calculation error rate of "slightly more than 1%." Note that this error rate is associated with simple calculations performed using pen and paper. The likelihood of more complicated calculation performed with a computer code would be expected to be approximately 1%. Self review and independent verification are expected to catch 90% of the errors in the calculation. This action is similar to checking a routine task per NUREG/CR-1278, Table 20-22, which gives a human error probability (HEP) of 0.1 for this action. Therefore, the likelihood of error existing in the fuel movement plan is  $1\% \times (1 - 0.9)$  or  $1E-3$  per fuel move.

#### 3.1.2 Likelihood of an Error in Moving the Wrong Bundle (PICK ERROR)

This event represents an error in moving the wrong bundle. If the fuel movement plan contains an error, then it is assumed that the operators would follow the plan and move the bundle. If there is no error in the fuel movement plan, there is still a probability that a fuel movement error can occur. The probability of a fuel movement error is calculated based on a review of the GGNS fuel movement history since 1999. A review of GGNS Condition Reports associated with fuel handling shows three errors in picking up the wrong bundle. A review of fuel movements in the SFP and the Upper Containment Pool during this time frame determined that approximately 5014 fuel bundles were moved out of a fuel storage location. Therefore, the mean failure probability is  $6E-4$  per fuel move.

#### 3.1.3 Likelihood in Removing a ½ Guide

The probabilities in Sections 3.1.1 and 3.1.2 are developed based on any error in the fuel movement plan or during fuel movement. However, there are significant differences between normal fuel bundles and ½ guides that reduce the likelihood of a ½ guide move compared to a normal fuel bundle. First, the *ShuffleWorks* has two restrictions on the blocked locations:

1. There is a "do not remove" tag on the ½ guide.
2. There is a "do not place an assembly in these locations."

These features can be overridden in *ShuffleWorks* but numerous warnings will be provided to alert the user to potential errors. The user has to acknowledge these errors to continue. The likelihood that the warnings from the computer code would be ignored is similar to a failure to respond to an annunciator with a single operator. From NUREG/CR-1278, Table 11-13, the failure probability is taken to be 0.001.

During fuel movement, there are also indications that a ½ guide is being erroneously moved rather than a normal fuel bundle. The first indication is that the ½ guide is visually

### **Non-Proprietary**

distinct from fuel bundles. The  $\frac{1}{2}$  guide is hollow and does not reflect light in the same manner as a fuel bundle. This difference is clearly visible and would likely be spotted by either the bridge operator or the spotter.

Another major difference in the movement of the  $\frac{1}{2}$  guides is the difference in weight between the fuel bundles and the  $\frac{1}{2}$  guides. A fuel bundle weighs 700 plus pounds compared to around 100 pounds for a  $\frac{1}{2}$  guide. The fact that the load was significantly lower would flag the bridge operator to stop and re-assess the move. The spotter would also require that the move be stopped. One of the primary checks when lifting a fuel bundle is that the crane is properly loaded. Given this load check, the bridge operators do not consider lifting a  $\frac{1}{2}$  guide instead of a fuel assembly a credible event.

Based on a review of these factors, the likelihood that a  $\frac{1}{2}$  guide is inadvertently moved rather than a fuel bundle is considered comparable to an error of commission in reading an analog meter with easily seen limit marks. From NUREG/CR-1278, Table 11-4, the HEP associated with this action is 0.001.

For errors in the fuel movement plan, both the indications from the *ShuffleWorks* code and the operations from the bridge would be applicable. Therefore, the probability would be  $0.001 \times 0.001$  or  $1E-6$  if the errors are completely independent of one another. However, the bridge operators would be expected to follow the fuel movement plan, which would create some dependence between the error in the movement plan and the half-guide movement. On the other hand, the bridge operators rarely move half-guides and thus the operators would tend to question the move of a half-guide if it was not discussed as part of a pre-job brief. Therefore, an error in the fuel movement plan would not be completely dependent with an inadvertent half-guide move. This dependence would reduce the fuel movement error by approximately an order of magnitude, and thus, the probability of not correcting the error through either the computer code or the bridge is taken to be  $1E-4$ . If the fuel movement plan is correct, then only the operations from the bridge would be applicable to indicate an incorrect move is being made and the probability is 0.001.

### **3.2 Moving a Fuel Bundle in the $\frac{1}{2}$ Guide Location**

Given that a  $\frac{1}{2}$  guide has been inadvertently moved to a different location, a spent fuel bundle would have to be moved into this position to create a misload into a restricted storage location. An inadvertent move of a fuel bundle into a  $\frac{1}{2}$  guide location would involve either an error in the fuel movement plan or the bridge operator setting a fuel bundle in a  $\frac{1}{2}$  guide location and the spotter not catching the error.

### **Non-Proprietary**

### Non-Proprietary

#### 3.2.1 Fuel Movement Plan Error – Fuel Bundle in ½ Guide Spot (FMP ERR2)

This error represents a second error in the fuel movement plan that would place a fuel bundle in the location that was previously occupied by the ½ guide. As indicated in Section 3.1.3, the *ShuffleWorks* code should indicate that this SFP location is blocked. However, since this is credited in Section 3.1.3, no credit will be taken for that warning in the event. However, this warning is credited to indicate that the second fuel movement plan error is independent of the first error that moved the ½ guide. Therefore, the probability of the second error is considered to be the same as FMP ERROR in Section 3.1.1. This probability is 0.001.

#### 3.2.2 Place a Fuel Bundle in the ½ Guide Spot (SET ERROR)

This event represents an error in setting the bundle in the wrong location. If the fuel movement plan contains an error, then it is assumed that the operators follow the plan and set the bundle. If there is no error in the fuel movement plan, there is still a probability that a fuel movement error can occur. The probability of a fuel movement error is calculated based on a review of the GGNS fuel movement history since 1999. A review of GGNS Condition Reports associated with fuel handling shows two errors in setting the bundle down in the wrong location. A review of fuel movements in the SFP and the Upper Containment Pool during this time frame determined that approximately 7653 fuel bundles were moved into place. Therefore, the mean failure probability is 2.6E-4 per fuel move.

NOTE: The number of PIC movements from 3.1.2 differs from the number of SET movements from 3.2.2 because fuel movements occur to/from non-SFP locations (e.g., Dry Cask, Fuel Prep Machine, Upender, Reactor).

### 4.0 Results and Conclusions

An event tree was developed for the current configuration based on the information in Section 3.0. Figure 29-1 shows the event tree with the probabilities for each branch. The outcome for these sequences is either OK or Fail. If the outcome is OK, the errors that would result in a fuel bundle being placed in a ½ guide location are caught before the bundle is placed in the wrong position. If the outcome is Fail, then the fuel bundle is allowed to be placed in a half ½ guide location. The results from this evaluation show that the likelihood of loading a fuel bundle in a ½ guide location is 1.56E-10 + 1.0E-10 or 2.56E-10 per fuel move.

#### 4.1 Conversion to Annual Frequency

The probability of a misloaded bundle in a ½ guide location is converted to an annual frequency by determining the number of fuel moves per year. The number of fuel moves



### Non-Proprietary

between 1999 and 2010 (12 years) is 12,667 moves. This averages to 1055 moves per year. Therefore, the frequency of a fuel bundle in a ½ guide location given the current configuration is approximately 2.70E-7/year.

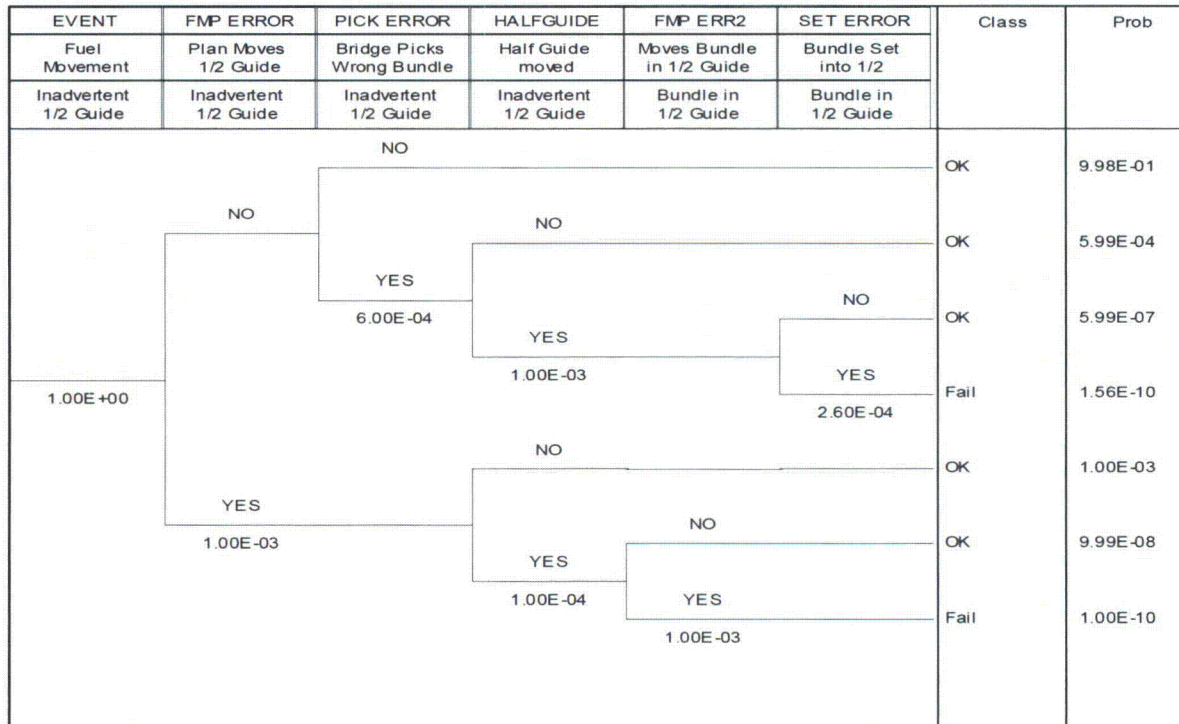


Figure 29-1 – Fuel Bundle in ½ Guide Location

### RAI # 30

Boraflex is known to degrade in a high radiation environment leading to panel cracking, panel gap formation, and boron carbide dissolution. Demonstrate that a stable structural configuration of the poison panels exists under the design basis seismic events to ensure that the stored fuel assemblies remain subcritical. This could be accomplished by either

- (1) demonstrating through seismic and mechanical analysis that the Boraflex panels will not be affected (i.e. the poison panels will not split, shift, and/or dissolve to the extent to which the k-effective of the storage rack may become unacceptable) by the design basis loads or
- (2) demonstrating that the storage rack will continue to meet the k-effective requirements even if the poison panels split, shift, and/or dissolve to the maximum credible extent.

**Non-Proprietary**

**Response**

A detailed mechanical analysis of the Boraflex panels under seismic conditions is not available. During a seismic event, it is reasonable to assume some Boraflex panel cracking and redistribution will occur. Assuming all of the Boraflex shifts downward, closing all the gaps, produces the largest possible unpoisoned area. Other assumptions result in smaller unpoisoned areas and less coupling between gaps. Due to the close tolerances between the Boraflex panels and the rack structural material, the slipping of panel fragments past one another (slumping) is not considered credible.

The criticality safety analysis (CSA) was repeated using the measured Boraflex gap distributions provided in GNRO-2010/00073 (ML103330092, non-proprietary). The use of the measured Boraflex gap distribution is conservative since it corresponds to gamma dose values that exceed the acceptance criteria threshold. The CSA assumed all gaps migrated to the top of the panel. Additionally, the revised analysis included 6-inches of natural uranium in the top of the fuel bundle consistent with GGNS fuel designs. Consistent with the base CSA (NEDC-33621P, Rev. 0), 20 gap configurations were independently modeled. The variation in the results of the 20 gap configurations is less than observed in NEDC-33621P, Rev. 0 and the weighted mean value k-effective is [[            ]] below the NEDC-33621P, Rev. 0 results. This demonstrates that the K-effective acceptance will continue to be met in the unlikely event that a seismic event results in a redistribution of all the Boraflex to the worst case credible configuration.

**RAI # 31**

Section 3.6 of NEDC-33621P, "Assumptions and Conservatisms," states that the Boron-10 content for Region I panels is assumed to be 70% of the 95/95 minimum assayed areal density. Clarify the meaning of "70% of the 95/95 minimum assayed areal density." Is the value based on the minimum certified areal density of the GGNS Boraflex panels? Is it based on the minimum as-fabricated value of the panels?

**Response**

Individual as-built panel data is not available. The Boraflex material was fabricated in batches. Process data from these batches is available for Boraflex density, weight percent (w/o) of  $B_4C$  in the batch, weight percent Boron in  $B_4C$  and weight percent  $B_{10}$  in Boron. Using this data, the  $B_{10}$  areal density is calculated for each of the 82 batches used in the GGNS racks assuming all the panels were at the minimum panel thickness.

That is, the  $B_{10}$  areal density is equal to the batch Boraflex density (gm/cc) x conservative panel thickness (cm) x the batch w/o  $B_4C$  x w/o boron in  $B_4C$  x w/o  $B_{10}$  in boron. For example, the  $B_{10}$  areal density based on the following data is:

**Non-Proprietary**



**Non-Proprietary**

$$1.7576 \text{ gm/cc} \times 0.16002 \text{ cm} \times 0.472 \times 0.787 \times 0.1847 = 0.0193 \text{ gm-B}_{10} / \text{cm}^2$$

This approach is very conservative since the nominal thickness is approximately 10% higher. The 95/95 lower limit of the areal densities determined from the 82 batch results is the "minimum assayed areal density." The resulting 95/95 minimum areal density, 0.0191 gm-B<sub>10</sub> / cm<sup>2</sup> is rounded down to 0.0190 and further reduced by a factor of 0.70 to establish the CSA assumption of 0.0133 gm-B<sub>10</sub> / cm<sup>2</sup>. There is very little variability in the areal density between batches. The primary factor that establishes this areal density is the assumption that all the panels are at the lower limit of the panel thickness fabrication tolerance.

**RAI # 32**

Attachment 1 to GNRO-2010/00073 states that 32 panels were measured in Region I and Region II locations. How many Region I panels were measured? How many panels total are in Region 1? How can we ascertain that the bounding panels in the Region I population have been represented in the measured sample?

**Response**

Eighteen of the 32 measured panels have dose and areal density values that allow them to be considered Region I. A few of these panels are actually in Region II storage cells because of the performance of other panels in the same storage cell or other Region II configuration requirements. There are approximately 9000 Region I panels and approximately 275 Region II panels.

The tested Region I panels were selected based on RACKLIFE predictions of B<sub>4</sub>C loss and dose. The selected panels include some variation in B<sub>4</sub>C loss and dose that are biased to the highest loss and dose values for Region I.

The GGNS Boron-10 Areal Density Gage for Evaluating Racks (BADGER) test was conducted over a 10 day period. This test duration does not include the time to reconfigure the SFP to isolate the test area from other discharged fuel. In order to determine that the bounding panel was in the BADGER test population, a substantial fraction of the Region I panels would need to be measured. Such a test would require many months and is not necessary.

Testing a representative sample is sufficient for the monitoring program to ensure the limiting panels are bounded by the analysis assumptions. This is the basis for the March 9, 2011 response to RAI #2 (ML110680507). RACKLIFE can perform this monitoring function when an appropriate allowance for BADGER/RACKLIFE uncertainty is included. In addition, the Areal Density Criterion described in the response to RAI #2 accounts for the sample size used in development of the 95/95 limit.

**Non-Proprietary**

**Non-Proprietary**

**RAI # 33**

Attachment 1 of GNRO-2010/00073 states that the Region I panels that were tested had accumulated doses up to  $1.77\text{E}10$  rads. What is the highest accumulated dose for a Region I panel in the GGNS spent fuel pool?

**Response**

The highest accumulated dose for a Region I panel on January 1, 2011 was  $1.86\text{E}10$  Rads.

**RAI # 34**

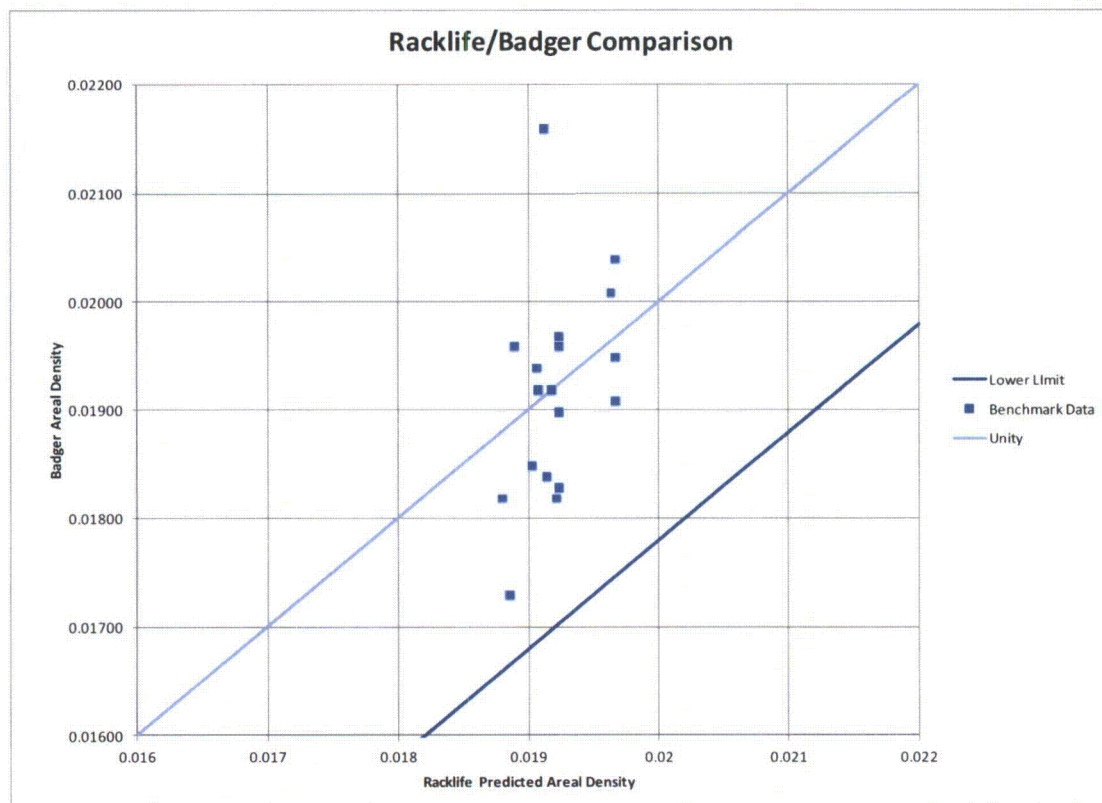
Attachment 1 of GNRO-2010/00073 states that BADGER and RACKLIFE difference is bounded by a 95/95 uncertainty of 0.0022 gram/square centimeter. Explain how BADGER and RACKLIFE comparisons were made. Also, what is the basis for the 0.0022 gram/square centimeter uncertainty?

**Response**

The RACKLIFE results reported in the 2007 BADGER report were scoping calculations used to select the test locations. The RACKLIFE results have been updated to account for the actual BADGER test date and to include any fuel movements during the interim period. Additionally, the RACKLIFE loss coefficient was increased to remove a small areal density bias ( $\sim 0.0003$ ) observed in the Region I BADGER/RACKLIFE results.

BADGER test results for panels that are below the dose criteria of  $2.3\text{E}10$  Rads were compared to RACKLIFE predictions. The RACKLIFE panel loss results were converted to areal density based on the nominal design areal density, consistent with the BADGER reference panel. The difference distribution determined from the BADGER/RACKLIFE areal density results was determined to be normally distributed based on Shapiro-Wilk test results and a visual comparison to the normal cumulative probability distribution. The uncertainty in the difference distribution was multiplied by a one-sided 95/95 k-factor from Owen, "Factors for One-Sided Tolerance Limits and for Variables Sampling Plans," which results in the 95/95 BADGER/RACKLIFE uncertainty. The RACKLIFE/BADGER data along with the lower limit are illustrated in the figure below.

Non-Proprietary



**RAI # 35**

According to your predictions, when will the most degraded panel in Region I exceed the assumptions in the criticality analysis? RACKLIFE is not intended for precise prediction of local degradation. How does just monitoring for areal density capture the other possible degradation modes such as gapping and scalloping?

**Response**

As a note of clarification, this response is based on when the next Region I panel is projected to exceed the Region I dose or areal density criteria.

RACKLIFE predictions of future rack performance are based on the most limiting discharge bundle. This bundle is assumed to be simultaneously loaded into every fuel storage location, which is conservative for the next cycle. This discharged bundle is assumed to remain in this storage location for future cycles (~10 years). While a given storage location could be loaded with multiple discharge fuel assemblies over several cycles, a single discharge assumption is

**Non-Proprietary**

reasonable since 10 years of discharge fuel is less than half of the SFP storage capacity and the actual discharge fuel is distributed to manage the Boraflex impact.

RACKLIFE areal density predictions show that several panels will be near but none will exceed the Region II loss criterion prior to 2021.

RACKLIFE dose predictions show no Region I panels exceeding the dose limit prior to February 19, 2012 (i.e., in the current cycle). As noted in the response to RAI #3 of the March 9, 2011 submittal (ML110680507), an additional 3% of the Region I panels will exceed the dose criteria prior to January 1, 2013 (i.e., during the next cycle). As noted above, active management of the fuel storage is expected to significantly reduce this number. Significant increases in the number of Region II storage cells are expected by January 1, 2015.

**RAI # 36**

Table 1 of Attachment 1 to GNRO – 2010/00073 provides the results of the BADGER test in terms of “Panel Loss (%)” Define “Panel Loss (%)” Describe how the “Panel Loss (%)” provides a measure that includes the effects of the different degradation modes (e.g., uniform thinning, shrinkage, localized dissolution, etc.). With respect to each BADGER campaign provide the following information:

- a. What was the actual areal density of the reference panel used during the BADGER campaign?
- b. How did GGNS verify the actual areal density of the reference panel?
- c. Provide the distribution of the as-built areal densities of the Boraflex panels installed in the GGNS SFP.
- d. Explain how the as-built areal densities are distributed in the SFP.

**Response**

The “Panel Loss (%)” provided in Table 1 of Attachment 1 to GNRO – 2010/00073 is only related to gap losses. Table 1 was developed to support the selection of the dose limit that is used in the monitoring program to ensure the applicability of the Region I criticality analysis gap assumptions. The Table 1 “Panel Loss (%)” is the total size of the gaps in a given panel divided by the initial panel length x 100. The BADGER areal density measurements are provided in response to RAI #37. The BADGER results include the impact of uniform thinning, local dissolution, and shrinkage in the panel areal density. The graphs of the neutron transmission, provided in the BADGER report, show low levels of local dissolution for the Region I panels.

**Non-Proprietary**

- a., c., d. As noted in response to RAI #31, individual as-built panel data is not available. There is no information available to GGNS which relates the batch data described in RAI #31 to specific racks or individual rack storage locations.
- b. The reference panel areal density is based on the nominal design value of 0.0204 gm/cm. Inclusion of the design areal density uncertainty in the acceptance criterion for the Region I monitoring program addresses the potential for the reference panel to be below the nominal design value.

The batch data evaluation noted in the response to RAI #31 was performed assuming all panels were at the minimum thickness. When the thickness assumption is revised to the nominal value, the batch average areal density increases to 0.0213 with a 95/95 lower limit of 0.0212. This shows that there is very little uncertainty associated with the Boraflex material composition across the batches. Most of the uncertainty in areal density is associated with the thickness of the panels. The panel thickness is a readily observed value that is monitored during the fabrication of the Boraflex panels. GGNS installed a set of Boraflex monitoring coupons that are periodically removed and were subject to neutron transmission testing. The first 6 coupons were removed and tested prior to accumulating any significant dose. The transmission measurements of these coupons are consistent with a  $B_{10}$  loading of 0.020 gm/cm<sup>2</sup> or slightly greater. This data supports the appropriateness of the areal density design nominal and tolerance values for the development of the areal density acceptance criteria.

**RAI # 37**

Supply the BADGER campaign report to all the NRC staff to confirm the basis for the Boraflex assumed in the criticality analysis.

**Response**

The BADGER campaign report is provided as Enclosure 1. Note this is Revision 1 of the report issued in October 2010 to correct a data processing error that was found after the original version of the report. Additionally, excerpts from the Blackness test report that support the gap measurement campaign are also provided as Enclosure 2. Summary tables and figures from the Blackness tests were not included since they are not used as the bases for the gap assumptions used in the criticality safety analysis. The data from Table 1 is the basis for the gap measurements used to establish the CSA gap assumptions.

**Non-Proprietary**

**RAI # 38**

What is the BADGER measurement uncertainty associated with measuring shrinkage-induced gaps? Does BADGER miss detecting certain gaps? How are these considerations addressed in the criticality model?

**Response**

The BADGER measurement uncertainty is determined for each panel measurement based on counting statistics and other panel specific results. Figure 4-5 of the BADGER test report (Enclosure 1) illustrates the BADGER measurement uncertainty for several panels. The lower limit of detectability for gaps is 1/3 inch. Gaps of this size or smaller cannot be distinguished from small areas of local dissolution. The criticality analysis uses an assumed gap distribution that is significantly more conservative than that observed at GGNS. Additionally, the dose limit was established for Region II to bound formation of large gaps. The criticality safety analysis does not specifically account for these small gaps. Gaps that are too small to be detected by neutron radiography are not considered to have a material impact on the criticality analysis results and are negligible considering the significant conservatisms in the assumed gap distribution.

**RAI # 39**

Provide a sample MCNP model that graphically shows the axial modeling of the Boraflex degradation.

**Response**

Images of the base case, Region I MCNP model were generated. These images (Figures 1 and 2) show the axial modeling of the Boraflex degradation. [[

]]

The gap size distributions correspond to the base case (Configuration 1 of Table 16) of NEDC-33621P. The gap sizes and locations were derived using the methodology in Section 6.2.1 of NEDC-33621P.

**Non-Proprietary**

[[

[[

]]

]]

**Non-Proprietary**

**Non-Proprietary**

[[

]]

[[

]]

**RAI # 40**

Table 17 of NEDC-33621P provides the lattice information at zero void condition. Show that other void conditions have been considered and are bounded by the selected lattice.

**Response**

Lattice depletions to support the bounding nature of the values in Table 17 of NEDC-33621P have been performed at three in-channel void fractions to simulate variation in in-core operating conditions. The three in-channel conditions used to deplete the lattice are [[

]] void fractions. These three void histories were used to create three sets of isotopic content as a function of lattice exposure (depletion). The isotopic content was then evaluated in the cold (20°C), uncontrolled (control blade withdrawn) in-core configuration to determine the

**Non-Proprietary**



**Non-Proprietary**

peak in-core cold reactivity as a function of exposure. For high reactivity, high enrichment lattices, which are shown to be the most limiting from a rack efficiency standpoint, the gadolinium depletion rate is the dominant factor in determining the point of maximum cold reactivity. For lattices with gadolinium present, the peak in-core cold reactivity generally occurs in the 0% void history condition. This is a direct result of the rate of gadolinium depletion being maximized in the 0% in-channel void fraction condition.

To demonstrate the conservatism of using a 0% in-channel void condition for depletion calculations, peak in-core and Region-I in-rack reactivity values as a function of void fraction are provided in Table 40-1. The cases presented correspond to the highest rack efficiency fuel loadings for each lattice design listed in Table 17 of NEDC-33621P. [[

]]

**Table 40-1 – Void History Sensitivity Study Results**

Case	Lattice Type	Void Fraction (%)	Average Lattice Enrichment (U235 wt%)	Number of Gad Rods*	Gad Enrichment (Gd wt %)*	Peak Reactivity Exposure (GWd/ST)	TGBLA06 Defined In-Core k <sub>∞</sub>	MCNP-05P Defined In-Rack k <sub>∞</sub>
[[								
								]]

[[

]]

**Non-Proprietary**

]]

**RAI # 41**

10 CFR 50.36(c)(4) states:

Design features to be included are those features of the facility such as materials of construction and geometric arrangements, which, if altered or modified, would have a significant effect on safety and are not covered in categories described in paragraphs (c) (1), (2), and (3) of this section.

In a separate applicant request, the NRC staff has taken a position that U-235 enrichment and in-core k-infinity limits should be specified in the Technical Specifications. The licensee is requested to specify these limits in the GGNS Technical Specifications in accordance with 10CFR 50.36.

In addition, the proposed Region I and Region II storage configuration requirements are normally required in the Technical Specification. The licensee is requested to specify these requirements in the GGNS Technical Specifications in accordance with 10CFR 50.36.

**Response**

A proposed markup of GGNS Technical Specification (TS) 4.3.1, *Criticality* is included in Attachment 2. The proposed change adds requirements for two parameters for both the spent fuel storage racks (TS 4.3.1.1) and the new fuel storage racks (TS 4.3.1.2):

- Fuel assembly maximum k-infinity (1.26) in the normal reactor core configuration at cold conditions.
- Maximum nominal U-235 enrichment (4.9 weight percent).

The values for these parameters are consistent with NEDC-33621P, Revision 0, *Grand Gulf Nuclear Station Fuel Storage Criticality Safety Analysis of Spent and New Fuel Storage Racks*, submitted by letter dated November 23, 2010 to the NRC (Accession Number ML103330093).

In addition to the above parameters, the spent fuel pool storage configuration requirements to account for potential degradation of Boraflex are specified in TS 4.3.1.1. The storage cells with degraded Boraflex are designated as Region II cells and are those cells that have at least one

**Non-Proprietary**

**Non-Proprietary**

panel that has either a lower areal density or a higher accumulated dose than assumed in the Region I analysis. As demonstrated in the responses to questions from the Steam Generator and Chemical Engineering Branch (Accession Number ML110680507), the dose threshold in the analysis is a significant indicator associated with transition to high Boraflex loss.

The current actual gamma dose and areal density values were determined using a combination of RACKLIFE, Blackness testing, and BADGER assessment tools and are monitored in the Spent Fuel Pool Rack Boraflex Monitoring Program. Changes to the monitoring program may be made in accordance with 10 CFR 50.59, *Changes, tests, and experiments*.

The proposed figure ensures at least 6 of 16 Region II fuel assembly storage locations are physically blocked in the designated configuration. Since the Boraflex in Region II is not credited, additional locations within the 4 x 4 Region II storage array may be conservatively blocked without compromising the minimum 6 x 16 configuration. The orientation of any adjacent Region II 4x4 array is required to be consistent with the existing Region II 4x4 array. Cells face-adjacent to isolated panels that meet the Region II threshold are physically blocked from storing any fuel assemblies. The Region II storage configurations designated in the Technical Specifications are consistent with the Spent Fuel Pool Criticality Safety Analysis.